

The QANTAS/CROYDON Total Solar Eclipse Flight

23 November 2003 UT

Mission Planning & Definition Overview

REQUIREMENTS for Assisted Real-Time Computation and Navigation

Dr. Glenn Schneider, Ph. D.
Associate Astronomer & NICMOS Project Instrument Scientist
Steward Observatory, The University of Arizona
Tucson, Arizona 85750 USA

Contact email: gschneider@as.arizona.edu, gschneider@mac.com
URL: <http://nicmosis.as.arizona.edu:8000>

Abstract

No total solar eclipse has ever been observed from Antarctica both because of the infrequency of occurrence and the logistical complexities associated with Antarctic operations. This paradigm of elusivity regarding Antarctic eclipses in the historical record of science and exploration is about to be broken. The next total solar eclipse, which occurs on 23 November 2003 U.T., the first in the Antarctic since 12 November 1985, will be very largely unobserved due to the geographic remoteness of the path of totality. Yet, interest in securing phenomenological observations of, and associated with, the eclipse by members of the scientific research communities engaged in solar physics, astrodynamics, aeronomy and upper atmospheric physics, as well as educators and amateur astronomers has been extremely high. The development of a flight concept to enable airborne observations, with a dedicated aircraft chartered from QANTAS Airlines, will permit the previously unobtainable to be accomplished. To do so successfully requires detailed preparatory planning for the execution of such a flight. The technical groundwork to achieving this goal has been pursued with diligence over the past four years and is predicated on a legacy and computational infrastructure capability founded on more than three decades of eclipse planning for ground, sea, and airborne venues. Here, given the geometrical circumstances of the eclipse, the uncertainties associated with weather, and the constraints of operations of the Boeing 747-400 aircraft, the requirements for the successful execution an intercept flight with the base of the Moon's shadow over the Antarctic are reviewed. The *unequivocal need for real-time, in-situ re-computation of an executable flight plan in response to in-flight conditions* is discussed. The mechanism for fulfilling that need, through the expert operation of EFLIGHT, a well-tested highly specialized software package of unique pedigree designed specifically for this purpose by the author of this report, working in concert with the flight crew on the flight deck is elaborated upon in the specific context of the requirements of this flight.

The 23 November 2003 Antarctic Total Solar Eclipse

On the long-term average, a total solar eclipse is visible somewhere in the world about once every sixteen months. However, the overlap between the "cycles" of solar eclipses is complex. The next total solar eclipse occurs on 23 November 2003 and its immediate predecessor, the 4 December 2002 total solar eclipse, occurred only 354 days earlier. The next one (which has a maximum total phase duration of only 42 seconds) will not happen until 08 April 2005. Also on average, any given spot on the Earth will see a total solar eclipse about once every 360 years. However, eclipse paths can cross specific locations more frequently (e.g., the 2001 and 2002 eclipse paths crossed in South Africa, and those living in the right location saw both of them). The last total solar eclipse in the Antarctic occurred on 12 November 1985, but was unobserved.

The 23 November 2003 total solar eclipse (TSE2003) will be visible only from a small portion of the Eastern Antarctic. The "path of totality", the region on the Earth's surface which will be swept by the Moon's umbral shadow, and where the total phase of the eclipse can be seen, begins off the coast in the Antarctic (Great Southern) Ocean. The umbral shadow will "touch down" on the Earth at 22h 24m Universal Time (U.T.). At that time, the total phase of the eclipse becomes visible at sunrise at a latitude of 52.5°S, southeast of Heard Island and the Kerguelen archipelago. The lunar shadow then moves southward toward Antarctica, and traverses an arc-like sector of the continent from approximately longitudes 95E to 15E where it will "lift off" into space only 51 minutes later at 23h 15m U.T.

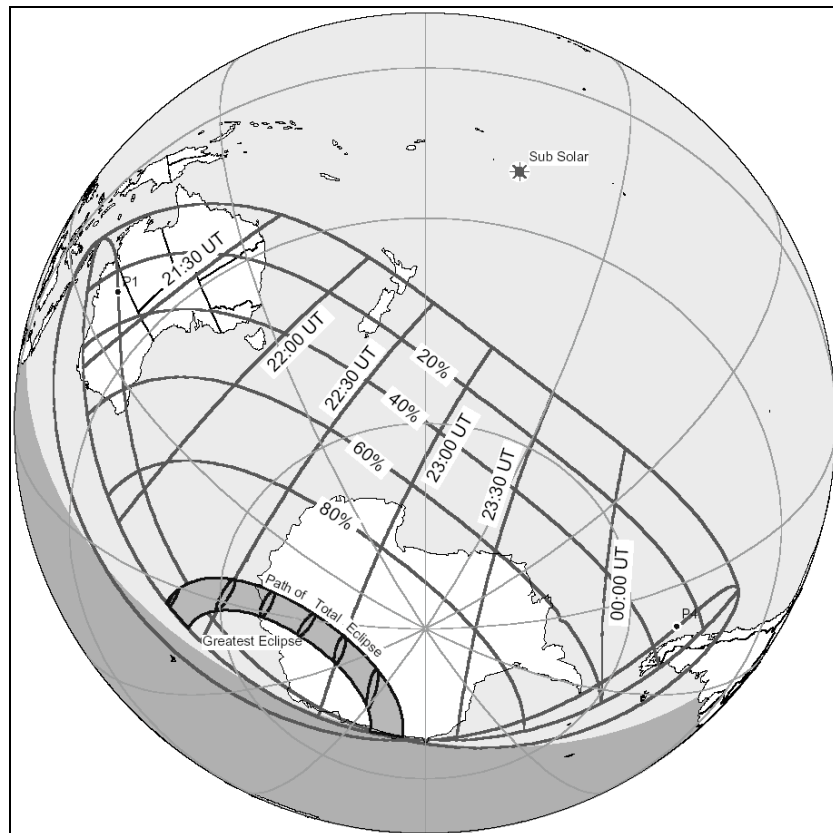


Fig. 1 – TSE2003 visibility. Partial eclipse seen in the region of the overlaid grid. Total eclipse seen within gray arc over Antarctica (path of totality). Ellipses indicate instantaneous surface projection of umbral shadow.

Total solar eclipses in the Polar Regions can have unusual geometries, and TSE2003 is no exception. In this case, the Moon's shadow passes "over the pole" before reaching the Earth. So the path of totality advances across Antarctica opposite the common direction of the Earth's rotation and the lunar orbit. The eclipse occurs in the hemisphere of the Earth which, except at southern polar latitudes, is experiencing nighttime. Hence mid-totality occurs very close to local midnight. Antarctic total solar eclipses are infrequent, but not particularly rare, the last occurring (but unobserved) eighteen years earlier in 1985 (the Saros predecessor to TSE2003).

Accessibility to, and mobility in, the path of totality on the Antarctic continent is severely limited and generally inaccessible inland. A Russian icebreaker will be making way to the coast with eclipse observers, but the coastal weather at the location and time of year of the eclipse is often cloudy, accompanied by high winds and ice fog. A ground-based expedition to the Russian Antarctic station at Novolazarevskaya, very close to the end of the eclipse path and sunset, is planned, but the Sun will be very close (only a degree) above the horizon and obscuration by blowing snow or white-out conditions is a strong possibility. Until this juncture in time and technology Antarctic total solar eclipses have been elusive targets, and never before has one been observed. If ever there was a clear-cut case for the necessity of using an airborne platform to observe a total solar eclipse, however, TSE2003 is it.

The QANTAS/Croydon Boeing 747-400 Total Solar Eclipse Flight

The upcoming opportunity to conduct high-altitude airborne observations of the 23 November 2003 (UT) total solar eclipse over Antarctica is unique in the history of science, and indeed of humanity. To this day no total solar eclipse has ever been witnessed from the Antarctic. To fill this void in the experience base of humankind, while enabling compelling and otherwise unobtainable observations furthering a wide variety of astronomical, solar dynamical, and aeronomic studies, a truly unique Qantas B747-400 flight will depart Melbourne, Australia on 23 November 2003 (Universal Time). After a poleward journey to a latitude of $\sim 70S$, the flight will rendezvous with the base of the Moon's shadow, nominally at 22:44:00 UT at an altitude of 11 km above the Earth's surface, as the shadow rapidly and obliquely sweeps over the eastern end of the White Continent.

Sightseeing flights over the Antarctic have been implemented over the past decade on a fairly regular basis by Croydon Travel, an Australian based company, in concert with QANTAS Airlines. Croydon periodically charters a B747-400 aircraft from QANTAS for this purpose, and has done so with great success 40 times over the past decade. Given this experience base, the concept of developing an eclipse observation flight was a natural "variant", but with many special needs and requirements, which are absent on Antarctic sightseeing flights.

Additional general information on the 23 November 2003 eclipse and the QANTAS B747-400 flight concept may be found in *Appendix A* of this document.

Shadow Dynamics and the Duration of Totality

The dynamics of the eclipse are driven by the inexorable laws of Newtonian celestial mechanics, as naturally applied to the orbital configurations of the Earth/Moon/Sun system. The long slender

conic of the TSE2003 lunar umbral shadow, $1/2^\circ$ in angular extent at the distance of the moon, is only 34 nautical miles in radius at 11 km above the Earth's surface and tapers to a geometrical point below. The umbral shadow slices through the Earth's atmosphere at very high speed with a non-linear acceleration profile (see Figure 2), decelerating to its slowest instantaneous velocity of 2109 Nm/hr with respect to the rotating surface of the Earth at 22:49:17 UT. At that instant, the instant of "greatest eclipse", a ground-based observer concentrically located along the shadow axis would experience 1m 59s of totality, the maximum possible for this eclipse. Elsewhere within the path of totality the achievable ground-based duration is reduced. Time in totality is a highly precious commodity. Given the intrinsically short maximum duration of TSE2003, and the very limited opportunities to position observers within the path of totality, extreme care must be taken in the planning and execution of an airborne shadow intercept to avoid unnecessarily shortening the achievable duration due to targeting and/or navigation errors.

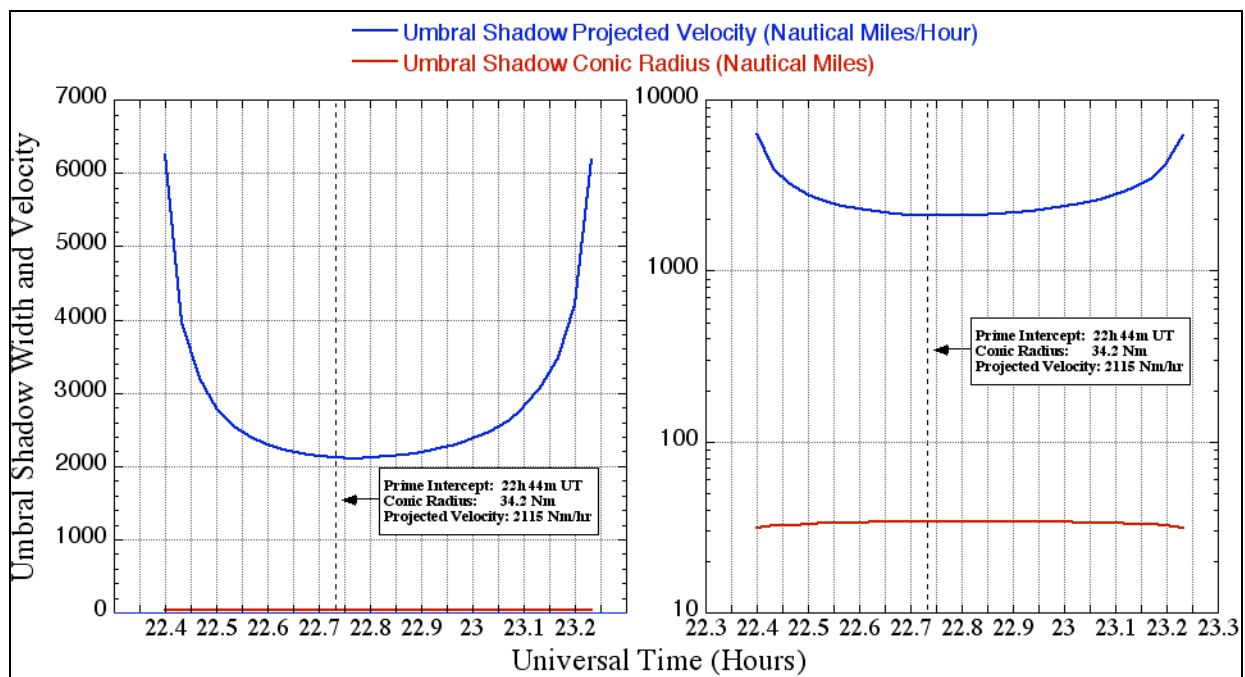


Fig. 2 – Instantaneous speed (blue) and radius (red) of the umbral shadow as a function of time.

The maximum duration *along* centerline declines very slowly (except near the points of sunrise and sunset) but reduces significantly and non-linearly (to zero) *across* the direction of the shadow's velocity vector at the extrema of the shadow. For a ground-based observer, the duration of the total phase as seen at some particular location within the umbral shadow declines, to first order, as $(1 - [1 - \text{abs}\{x/R\}]^2)^{1/2} / D$; where R is the radius of the umbral shadow where it intersects a *surface of constant elevation*, x is distance of the observer from the shadow axis perpendicular to its instantaneous direction of motion, and D is the duration of totality on centerline at the same Universal Time of mid-eclipse. The duration of totality for an airborne observer, with three degrees of positioning freedom (X, Y and Z [or longitude, latitude and altitude]), is shown in Figure 3 as a function of the $(X^2 + Y^2 + Z^2)^{1/2}$ displacement of the aircraft from the shadow axis in a plane perpendicular to the axis.

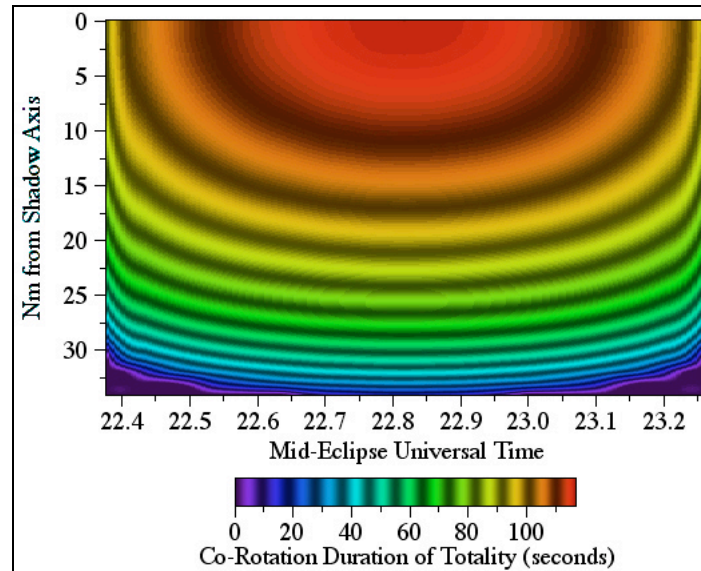


Fig. 3 – Duration of totality for perpendicular off-axis position displacements along the path of totality.

The Modifying Effects of the Aircraft Velocity Vector

For simplicity, Figure 3 does not consider the effect of the aircraft's velocity vector on the absolute achievable duration of totality and is directly applicable for a stationary (Earth co-rotating) observer. For *any* aircraft trajectory the duration of totality will decline with an aircraft/shadow axis centration error as illustrated in Figure 3, but the duration will additionally be modified by the aircraft's motion relative to the lunar shadow.

The nominal at-altitude cruise speed of the B747-400 (with a no-wind condition) is 470 Nm/hr. The lunar shadow, then, moves across the Earth with a minimum speed (near the point of greatest eclipse) approximately 4-1/2 times faster than the aircraft's speed. Hence, with the aircraft properly positioned at the critical time the lunar shadow will overtake the aircraft, but, depending upon the aircraft heading, more slowly than for a stationary observer. An *increase* in the duration of totality is realized for an aircraft with a net velocity component in the direction of motion of the lunar shadow axis. Without the necessary consideration of other constraining factors, a maximum theoretical gain of 37s may be realized for an aircraft with a *ground* speed of 470 Nm/hr following the trajectory of the lunar shadow axis and precisely co-aligned with axis at the instant of greatest eclipse. Such an optimal trajectory for the aircraft may not be sustainable, or even desirable, as the goal of maximizing the duration of totality cannot be taken in isolation.

Primary Factors for Simultaneous Optimization

A) AXIAL CONCENTRICITY: At the selected instant of mid-eclipse, the aircraft must be concentrically located along the lunar shadow axis. To the requisite degree of targeting precision, (discussed below) this is complicated because the photocentric location (i.e., the "center of figure") of the Moon's shadow is not coincident with its dynamical center (i.e., its "center of mass") due to irregularities along the lunar limb (selenographic features such as mountains, ridges, and valleys). It is these features that give rise to the "diamond ring" and "Baily's Beads" phenomenon at second and third contacts). The "lunar limb profile" (for example see Figure 4),

changes with topocentric physical and optical librations and will differ with an observer's latitude, longitude, and altitude along and across the path of totality, and hence, must be applied dynamically (and differentially) with changes in aircraft position and targeting.

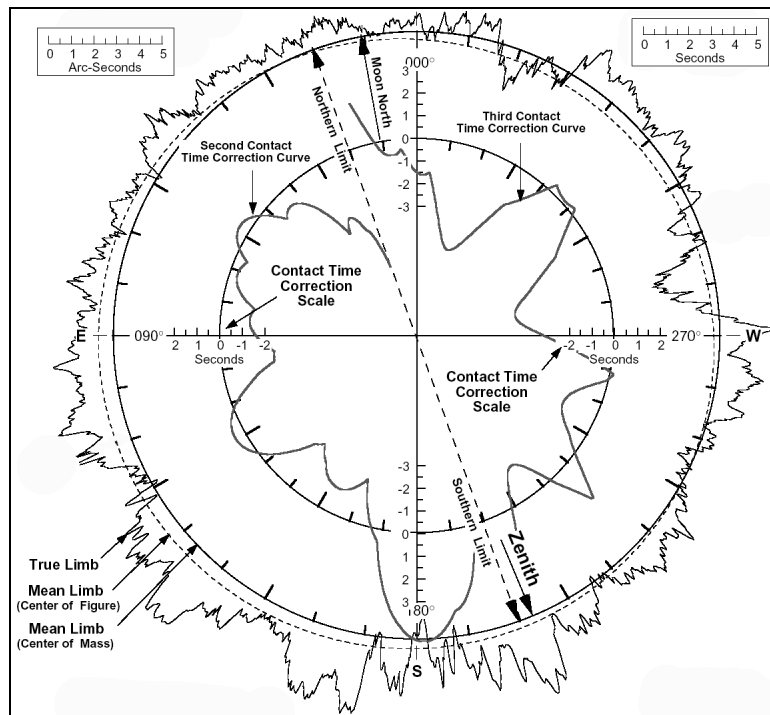


Fig. 4 – Representative lunar limb profile for mid-eclipse at 22:40 UT for an observer at sea level on centerline. The scale-height of the features along the lunar limb as seen at this location has been vertically amplified for illustrative purposes. Note that one arcsecond at the distance of the moon is approximately 1.8 kilometers.

B) MID-ECLIPSE APPROACH/DEPARTURE SYMMETRY: Observation and analyses of the spectrally decomposed brightness and “color” gradients of the sky, illuminated by light scattered into the umbral shadow by upper atmospheric particulates, will provide unique insights into the bulk aerosol content over the Antarctic. In-situ measures by Antarctic ground stations rely on back-scattered LIDARs, whereas aerosol scattering of sunlight *into* the lunar shadow is uniquely front-scattered and can be used to break the degeneracies in particle scattering models applied to the upper atmosphere. Quantitative calibration of aeronometric studies of the bulk physical properties of the upper atmosphere, particularly due to airborne contaminants, require sampling the scattering properties of the atmosphere in a symmetrical manner with respect to concentric shadow illumination, and hence immersion and emersion of the aircraft’s penetration through the umbral shadow.

(A) and (B), above, define a temporal shadow concentricity/symmetry requirement for the aircraft trajectory, i.e., how close to the geometrical shadow axis the aircraft must be at the instant of mid-eclipse, and where it must be positioned as it transitions through the umbral boundary at second and third contacts. An offset in time would produce a time and position error not only reducing the duration of totality but causing a temporal shift in the expected contact times of the eclipse which is counter to the needs of planned imaging and photographic experiments to be conducted.

C) **MID-ECLIPSE HEADING ALIGNMENT:** For the purpose of observing, photographing, and providing a proper field-of-view for those on-board the aircraft observing the eclipse, the line-of-sight to the Sun through the cabin windows should be in a plane very close to perpendicular to the aircraft heading. I.e., to provide an unimpeded, and near optimal viewing opportunity through the cabin windows. Such orientations will generally yield crossing-geometries with respect to centerline, and thus will preclude a full maximization of the duration of totality. The heading alignment and duration must be simultaneously optimized.

D) **MINIMIZE INTER-TOTALITY RUN HEADING RE-ALIGNMENTS.** The azimuth of the Sun varies continuously depending upon the time and aircraft position. To fully optimize (C) would require near-continuous differential course corrections, which cannot be accommodated at high temporal cadence due to CDU/FMS granularity and operational procedures constraints. Large discrete corrections during totality would cause a sudden displacement in the positioning of the Sun with respect to the line-of-sight, which should be avoided.

Derived Navigation Requirements and Error Tolerance

Taken together, and applied to the topocentric circumstances of the eclipse, the following navigational precision requirements to meet the goals of (A) – (D), above, emerge:

TABLE 1
REAL-TIME NAVIGATION/TARGETING REQUIREMENTS

- 1) **Absolute Position Error Tolerance:**
 - a) Maximum Aircraft lateral (cross track) position error ± 1 km at mid-eclipse, contact II, and contact III.
 - b) Maximum Aircraft vertical position error ± 100 meters.
- 2) **Absolute Timing Error Tolerance :** ± 6 s in time w.r.t. U.T. predictions* at CII and CIII.
- 3) **Heading Constraint: Portside Orthogonality:**

Absolute: $\pm 1.5^\circ$ from mid-eclipse ± 5 minutes.
Differential: $\pm 0.5^\circ$ from mid-eclipse ± 5 minutes.
- 4) **CDU/FMS Way Point Input Updates During Totality Run:**
 - a) Precluded within 2 minutes of mid-eclipse, except for mid-eclipse update.
 - b) Avoided if possible within 5 minutes of mid-eclipse.
 - c) Desired Granularity: 5 minute intervals at relative mid-eclipse times of -15, -10, -5, (0), +5 minutes.
- 5) **Aircraft Altitude:** Maximum possible altitude for least air-mass along line of sight to Sun.

* Exclusive of delta-T correction based upon pre-eclipse IERS updates (see: <http://www.iers.org/iers/>)

The Boeing 747-400 is exceptionally well suited to this task given the operational capabilities and characteristics of the aircraft. The experience base of the QANTAS flight crews conducting previous Antarctic overflights, though less demanding in navigational specificity and compliance than the 23 November 2003 flight, is unparalleled in commercial aviation. Hence, the choice of QANTAS B747-400 platform for this purpose was unequivocally clear.

External Influences and Parametric Variation

The requirements for previous QANTAS Antarctic flights, carried out with great success, were driven by the more casual needs to provide a suitable downward looking venue for sightseeing. These flights were unconcerned with the specific and highly demanding external constraints imposed by the unique needs of a solar eclipse intercept. For the 23 November 2003 eclipse flight the necessary responsiveness to uncontrollable, but anticipated, atmospheric variables (Table 2A) will be fettered and constrained by defining astrodynamical geometry of the eclipse (Table 2C) and coupled to the performance restrictions of the B747-400 aircraft (Table 2B/D).

TABLE 2

PRIMARY FLIGHT DEFINITION VARIABLES, CONSTRAINTS & RESTRICTIONS

A ATMOSPHERICS: METEOROLOGICAL CONDITIONS

Local obscuration by cloud: monolithic and multi-layer along the line-of-sight to the Sun.
 Wind speed and direction and vector gradients.
 Atmospheric turbidity along the line-of-sight to the Sun.
 Flight-level turbulence (platform stability).

B AIRCRAFT PERFORMANCE CONSIDERATIONS

Take-off or In-flight delay.
 Maximum service ceiling for gross weight at eclipse intercept.

C ASTRO-DYNAMICS: TIME/POSITION DEPENDENT FUNDAMENTAL GEOMETRY

Non-linear motions (absolute & relative) of Earth, Moon, and Sun.
 Shadow Velocity and instantaneous acceleration profile.
 Shadow axis (X,Y,Z) position loci as functions of altitude above geoidal surface (MSL), differentially corrected through atmospheric refraction models based upon Temperature/Pressure scale-height profiles.
 Shadow boundary loci as a functions topocentric lunar limb profile and atmospheric refraction corrections.
 Conic shadow projection on the elevated oblate geoidal surface.

D AIRCRAFT OPERATIONS CONSIDERATIONS

Minimum/Maximum Airspeed.
 FMS Targeting Compliance (input granularity and precision).

A “Baseline” Flight Concept for Plan Evaluation

Maintaining flexibility in the execution of the shadow intercept, within the previously delineated constraints, is paramount to permit the critical optimization of the spatial and temporal positioning of the aircraft to allow an unprecedented set of observations to be conducted to the greatest possible advantage that the circumstances of the eclipse will allow. In a decoupled sense, the outer envelopes of the flight definition parameter spaces can (and has) been evaluated and were used to define “baseline” or “nominal” flight intercept profiles for evaluation and early planning purposes. The “baseline” totality run intercept calls for a mid-eclipse intercept at 22:44:00 U.T, flight altitude of 35,000 ft, direction of flight to orient the sun orthogonal to the port-side windows, and waypoint pre-loads into the 747 CDU/FMS requiring no more frequent than 5 minute updates. This “baseline” plan, *which was developed for planning purposes*, is shown graphically in Figure 5 and tabulated in Table 3.

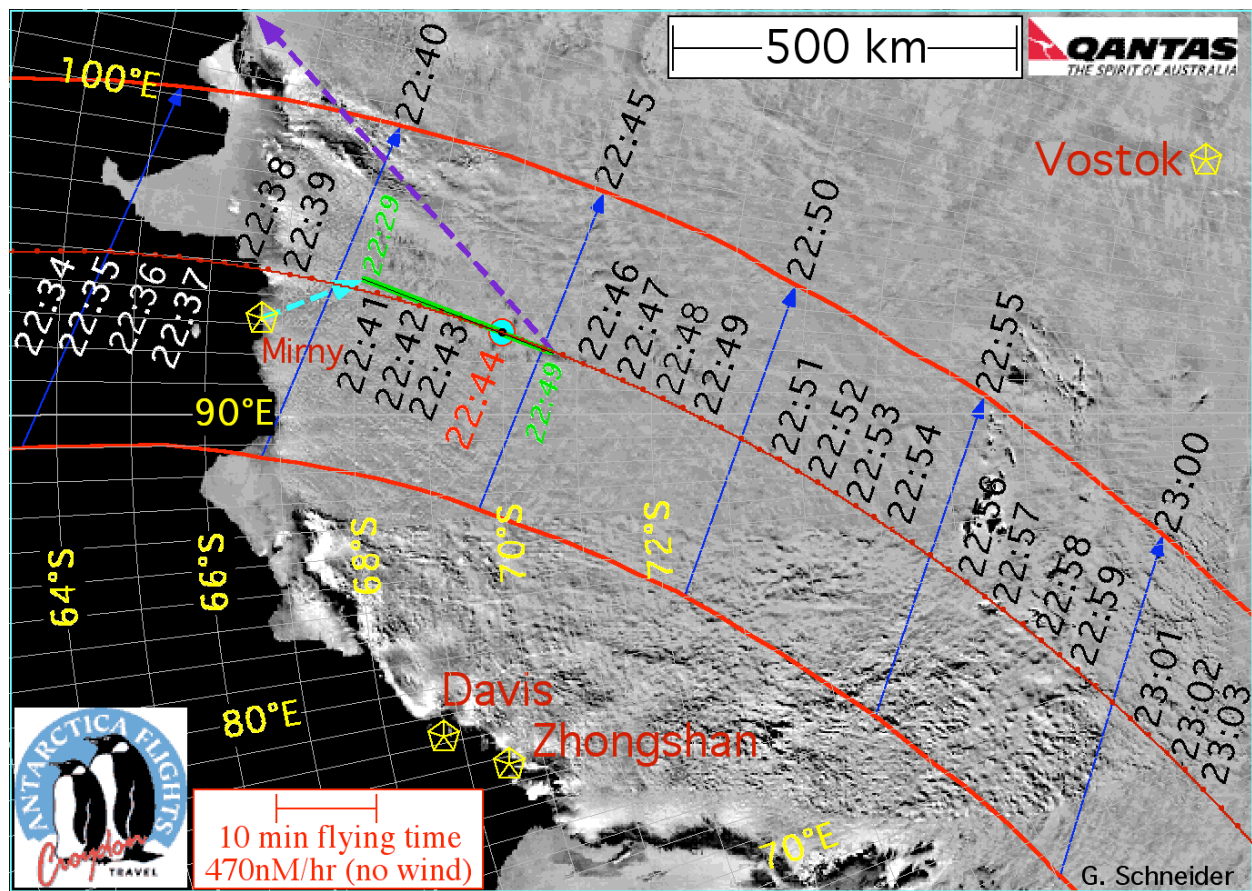


Fig. 5 – Schematic representation of the “baseline” flight used for planning purposes. Dotted red line: Centerline at 35,000 ft in 30-second intervals (1 minute annotation). Solid red lines: PROJECTION of the shadow conic major axis extrema onto a geoidal surface of 11 km constant elevation. Blue arrows: Lines of sight to Sun.

This particular point of mid-eclipse intercept and its corresponding baseline flight trajectory of approach and recession simultaneously satisfy the optimization criteria previously discussed. In particular, this scenario if executed in this form would achieve: (a) a 2m 34.7s extended duration totality, 36s longer than on the ground at the same mid-eclipse U.T. and only 0.6s shorter than the theoretical maximum for this eclipse, (b) a LOS viewing angle deviating by only (+0.3°, -0.1°)

throughout the totality run, and (c) a solar elevation at mid-eclipse only 0.2° lower than theoretically possible. Additionally, at this point the lunar shadow velocity (2115 nM/hr) is very nearly at its minimum for this eclipse (2109 nM/hr) providing a greater temporal margin for tolerable positioning error than most other locations along the path of totality.

TABLE 3
BASELINE INTERCEPT PROFILE FOR PLAN EVALUATION

```

=====
U.T. Intercept: 22:44:00          TOTALITY DURATION = 2m 34.7s
Flight Altitude: 35000ft
Heading:          198.80°
Air Speed:       470.0nm/h
Wind Speed:      0.0nm/h
Wind Direction:  0.0°

          Cnt  hh:mm:ss.f  Alt°  Az°  P°  Cnt  Cnt  hh:mm:ss.f  Alt°  Az°  P°
          2ND 22:42:42.7 +14.8 109.0 109.3  3RD 22:45:17.4 +15.0 108.6 289.7
          LATITUDE: -069° 49' 09.4''
          LONGITUDE: +093° 09' 59.0''
          LATITUDE: -070° 08' 17.2''
          LONGITUDE: +092° 51' 6.8''
=====
HMMSS  Umbra Lon Umbra Lat  WidKM  Uaz°  Ual°  AC Long  AC Lat  MidAT  MidAD  LOS  Bearng  ACaz  Acal
222900  9321.788E 6031.704S  541.8  113.7 10.2  9442.029E 6807.104S -900s  117.5nm +0.3  197.22 108.5 14.6
222930  9334.818E 6053.937S  540.9  113.4 10.5  9438.915E 6810.838S -870s  113.6nm +0.3  197.27 108.5 14.6
223000  9346.587E 6115.758S  539.9  113.1 10.8  9435.783E 6814.571S -840s  109.7nm +0.3  197.32 108.5 14.6
223030  9357.178E 6137.205S  538.8  112.7 11.0  9432.635E 6818.303S -810s  105.8nm +0.3  197.37 108.5 14.7
223100  9406.659E 6158.313S  537.6  112.4 11.3  9429.470E 6822.034S -780s  101.8nm +0.3  197.42 108.5 14.7
223130  9415.088E 6219.109S  536.3  112.2 11.5  9426.287E 6825.764S -750s  -97.9nm +0.3  197.47 108.5 14.7
223200  9422.514E 6239.618S  535.1  111.9 11.8  9423.086E 6829.493S -720s  -94.0nm +0.3  197.52 108.5 14.7
223230  9428.976E 6259.863S  533.7  111.6 12.0  9419.868E 6833.221S -690s  -90.1nm +0.3  197.56 108.5 14.7
223300  9434.508E 6319.862S  532.4  111.4 12.2  9416.632E 6836.947S -660s  -86.2nm +0.2  197.62 108.6 14.7
223330  9439.140E 6339.632S  531.0  111.1 12.4  9413.378E 6840.673S -630s  -82.3nm +0.2  197.67 108.6 14.7
223400  9442.892E 6359.188S  529.6  110.9 12.6  9410.106E 6844.398S -600s  -78.3nm +0.2  197.72 108.6 14.7
223430  9445.786E 6418.544S  528.1  110.7 12.8  9406.815E 6848.122S -570s  -74.4nm +0.2  197.77 108.6 14.7
223500  9447.834E 6437.712S  526.7  110.5 13.0  9403.507E 6851.845S -540s  -70.5nm +0.2  197.82 108.6 14.8
223530  9449.051E 6456.701S  525.3  110.3 13.1  9400.179E 6855.567S -510s  -66.6nm +0.2  197.87 108.6 14.8
223600  9449.442E 6515.523S  523.8  110.1 13.3  9356.833E 6859.287S -480s  -62.7nm +0.2  197.92 108.6 14.8
223630  9449.013E 6534.185S  522.4  109.9 13.4  9353.468E 6903.007S -450s  -58.8nm +0.2  197.98 108.6 14.8
223700  9447.769E 6552.695S  521.0  109.8 13.6  9350.084E 6906.725S -420s  -54.8nm +0.2  198.03 108.6 14.8
223730  9445.707E 6611.060S  519.6  109.6 13.7  9346.681E 6910.442S -390s  -50.9nm +0.2  198.08 108.6 14.8
223800  9442.827E 6629.286S  518.2  109.5 13.9  9343.258E 6914.158S -360s  -47.0nm +0.2  198.13 108.6 14.8
223830  9439.124E 6647.379S  516.8  109.3 14.0  9339.816E 6917.873S -330s  -43.1nm +0.1  198.19 108.7 14.8
223900  9434.591E 6705.344S  515.4  109.2 14.1  9336.354E 6921.587S -300s  -39.2nm +0.1  198.24 108.7 14.8
223930  9429.218E 6723.185S  514.0  109.1 14.2  9332.872E 6925.300S -270s  -35.3nm +0.1  198.30 108.7 14.8
224000  9422.996E 6740.906S  512.7  109.0 14.3  9329.370E 6929.011S -240s  -31.3nm +0.1  198.35 108.7 14.9
224030  9415.910E 6758.510S  511.4  109.0 14.4  9325.847E 6932.722S -210s  -27.4nm +0.1  198.41 108.7 14.9
224100  9407.947E 6816.000S  510.1  108.9 14.5  9322.305E 6936.430S -180s  -23.5nm +0.1  198.46 108.7 14.9
224130  9359.087E 6833.379S  508.8  108.8 14.6  9318.742E 6940.138S -150s  -19.6nm +0.1  198.52 108.7 14.9
224200  9349.314E 6850.648S  507.5  108.8 14.7  9315.157E 6943.845S -120s  -15.7nm +0.1  198.57 108.7 14.9
224230  9338.603E 6907.811S  506.3  108.8 14.7  9311.552E 6947.551S -90s  -11.8nm +0.0  198.63 108.8 14.9
224300  9326.933E 6924.866S  505.1  108.8 14.8  9307.926E 6951.255S -60s  -7.8nm -0.0  198.69 108.8 14.9
224330  9314.278E 6941.816S  503.9  108.8 14.9  9304.278E 6954.958S -30s  -3.9nm -0.0  198.73 108.8 14.9
224400  9300.609E 6958.660S  502.7 108.8 14.9  9300.609E 6958.663S +0s +0.0nm -0.0 198.71 108.8 14.9
224430  9245.896E 7015.398S  501.6  108.8 15.0  9256.939E 7002.362S +30s +3.9nm -0.0 198.53 108.8 14.9
224500  9230.106E 7032.030S  500.5  108.9 15.0  9253.292E 7006.064S +60s +7.8nm -0.0 198.37 108.8 14.9
224530  9213.204E 7048.556S  499.4  109.0 15.1  9249.666E 7009.769S +90s +11.8nm -0.0 198.22 108.8 15.0
224600  9155.152E 7104.972S  498.4  109.1 15.1  9246.061E 7013.474S +120s +15.7nm -0.1 198.06 108.9 15.0
224630  9135.910E 7121.279S  497.4  109.2 15.1  9242.476E 7017.181S +150s +19.6nm -0.1 197.91 108.9 15.0
224700  9115.435E 7137.472S  496.4  109.3 15.2  9238.913E 7020.889S +180s +23.5nm -0.1 197.75 108.9 15.0
224730  9053.680E 7153.551S  495.4  109.5 15.2  9235.371E 7024.598S +210s +27.4nm -0.1 197.60 108.9 15.0
224800  9030.598E 7209.511S  494.5  109.6 15.2  9231.848E 7028.309S +240s +31.3nm -0.1 197.45 108.9 15.0
224830  9006.134E 7225.348S  493.6  109.8 15.2  9228.346E 7032.020S +270s +35.3nm -0.1 197.30 108.9 15.0
224900  8940.235E 7241.057S  492.7  110.0 15.2  9224.864E 7035.732S +300s +39.2nm -0.1 197.16 108.9 15.0
=====

```

Notes: See Appendix B for definition of terms, bold line is instant of mid-eclipse.

The possibility of the execution of the “baseline” plan in the form shown in Table 3 is wholly dependent upon the imponderable in-flight state of the multi-parametric set of input variables noted in sections A/B of Table 2, which then drive those in section C/D of Table 2. The likelihood that the speculative set of (optimized) conditions postulated for planning purposes will actually arise in flight is small. Deviations and variations are unquestionably expected. “Solution sets” for alternate scenarios have been considered (see Appendix C) but by the sheer nature of the number of dynamical variables is far from exhaustive and *the need for in-flight recomputation should be anticipated.*

Real-Time Responsivity: A Necessary Pathway to Success

The experience base of the QANTAS flight crew is unquestionable in aircraft operations and “conventional” navigation. The demands of the computation and evaluation of real-time astrodynamical differential calculations, essential to the success of the flight mission objectives however, is outside of the scope of that experience base and augmentation to their essential expertise will be required. Such augmentation can only be provided by real-time collaborative interaction and consultation on the flight deck with an expert in astrodynamical navigation and the planning and executing airborne eclipse intercept flights.

The dynamical variables, which ultimately define both the characteristics of the intercept and the resulting executable flight plan, are not independent. The analytic forms they assume are correlated and the trade spaces to be evaluated are complex. The actual execution of a detailed, multi-variate and dynamic flight plan, *amenable to in situ modification* as required by meteorological and other conditions encountered in flight, *is absolutely essential* to assure the success of the eclipse intercept and the requisite differentially corrected flight vector through the totality run. Ultimately, this translates into computing and defining highly constrained sets of time-correlated target “way points” *which must be determined iteratively in real-time*, and with convergence toward mid-eclipse, based upon actual changing conditions in flight.

The differential numerical processes and algorithmic procedures required to yield an optimized solution to satisfy the simultaneous criteria required for a successful eclipse intercept expressed as an executable flight plan have been codified in a highly specialized software package called EFLIGHT. EFLIGHT was designed specifically for this purpose. EFLIGHT has a long and significant pedigree and has been put to the test in flight, with great success, during previous total solar eclipse intercept missions. EFLIGHT has matured into a fully integrated interactive eclipse flight planning and navigation S/W package, and is fully described in *Appendix B* of this report and to which the reader is referred for further understanding and detail.

Inherent in EFLIGHT’s operation and utilization, particularly under the stress and pressure of real-time demands in flight, is an intimate familiarity with its underpinnings. Such familiarity is essential in order to effectively and rapidly supply parametric inputs most germane to and best representing evolving conditions in flight and to evaluate EFLIGHT’s computational astrodynamical results. This is a task fully demanding of uninterrupted attention and is inappropriate for a member of the flight crew whose responsibilities (and necessary expertise) lay elsewhere and whose attention cannot be so diverted and consumed. It is strongly suggested here that the real-time analyses and transformation of EFLIGHT results into flight plan updates, directly and subsequently implemented by the QANTAS B747-400 flight crew, would be carried out with the greatest degree of effectiveness and highest efficiency by the program’s creator, Dr. Glenn Schneider. Unimpeded multi-directional communication and information flow in the in situ operational environment of the B747-400 flight deck between the pilot in command, the flight officer, and Dr. Schneider serving as an astrodynamics navigator, is essential to the successful realization of the primary goals of this historic, and unique flight opportunity.

Dr. Glenn Schneider

Dr. Glenn Schneider, Ph. D., is an Associate Astronomer at the University of Arizona's Steward Observatory with thirty-three years of experience in solar eclipse expeditionary logistics planning, instrumentation design, observation, and data analysis and interpretation. Dr. Schneider is uniquely qualified and positioned to provide the necessary scientific and technical expertise to work and interface with the flight crew to successfully achieve the real-time critical and highly specialized navigational requirements of the QANTAS 23 November 2003 eclipse flight.

Dr. Schneider is the Project scientist for the NICMOS (Near-Infrared Camera and Multi-Object Spectrometer) instrument on the Hubble Space Telescope (HST). He has worked extensively for eighteen years in conjunction with HST mission and flight operations personnel at NASA's Goddard Space Flight and other Centers on a variety of mission definition and execution issues. His curriculum vitae (*Appendix D*) and publication list (*Appendix E*) bespeak his relevant technical and scientific expertise, and should be consulted for more information and details. A more general familiarity with his research interests may be gained through his web site: <http://nicmosis.as.arizona.edu:8000/>.

More immediately germane, Dr. Schneider is a member of the International Astronomical Union's Working Group on Solar Eclipses. He is recognized in the international astronomical community as a leading expert in the high-precision numerical calculation of eclipse circumstances and the application of those computations in planning and carrying out observations of total solar eclipses. For more than three decades, Dr. Schneider has lead expeditionary groups and conducted such observations on land, sea and air of twenty-three (of the twenty-four) total solar eclipses occurring since 7 March 1970 from remote locations across the globe. He has previously executed two, and planned four, high-altitude eclipse intercepts with jet aircraft:

(a) Planned and Executed: A 44,000 ft very highly technically challenging and navigationally critical intercept using a Citation II over the North Atlantic on 03 October 1986.

See: http://nicmosis.as.arizona.edu:8000/ECLIPSE_WEB/ECLIPSE_86/ECLIPSE_86.html

(b) Planned and Executed: A 41,000 ft intercept over the South Atlantic, working in situ on the flight deck of a VASP airlines DC-10, extending the duration of totality to 6m 15s.

See: http://nicmosis.as.arizona.edu:8000/ECLIPSE_WEB/ECLIPSE_92/ECLIPSE92_REPORT.html

(c) Planned: A supersonic one-hour totality at 60,000 ft intercept over the South Atlantic using an Air France Concorde. Very sadly, this was cancelled due to the grounding of the Concorde fleet following the horrific crash of AF 4590 outside of Paris on 25 July 2000.

See: http://nicmosis.as.arizona.edu:8000/ECLIPSE_WEB/ECLIPSE_01/CONCORDE_ECLIPSE.html and http://nicmosis.as.arizona.edu:8000/ECLIPSE_WEB/ECLIPSE_01/ECLIPSE_2001_REPORT.html#MEMORIUM

(d) Planned: The QANTAS 23 November 2003 Antarctic eclipse flight, the subject of this document. Also see: http://nicmosis.as.arizona.edu:8000/ECLIPSE_WEB/ECLIPSE_03/ECLIPSE_03.html

The planning of each of the above flights was rooted in the use of EFLIGHT (*Appendix B*), created by Dr. Schneider, specifically to address the problem and optimization of intercepting the

moon's shadow from a moving aircraft. The core algorithms developed for the 1986 eclipse were augmented for the 1992 eclipse flight to provide greater flexibility for real-time use on the DC-10 flight deck. The S/W was modified in preparation for the 2001 Concorde eclipse flight, for consideration of an intercept in the supersonic regime where the instantaneous speed of the aircraft was greater than that of the lunar umbra given the geometrical circumstances of that eclipse. Most recently EFLIGHT was again modified specifically for the "over the pole" approach geometry of the lunar shadow which will occur for the 23 Nov 2003 eclipse and tailored for real-time use given the manual input requirements of the Boeing 747-400 FMS.

Summary

The successful airborne observation of the 23 November 2003 Antarctic total solar eclipse will be a milestone in the annals not only of astronomy, but also of human endeavor. Success, however, cannot be assured by reliance on pre-planned flight trajectories. Such "baseline" plans are necessary to the planning effort. They are, however, built inherently upon the unrealistic simplification of presumptively static, but in actuality highly dynamic, input variables. While the likely states of those variables can be probabilistically bounded, their values cannot be a priori ascertained. Such foreknowledge with the requisite degree of specificity is in fact unobtainable.

The real-time development of an executable flight plan, built in situ upon evolving in-flight conditions, is absolutely essential. The path toward successfully accomplishing the primary flight objectives is computationally extensive and algorithmically complex. Developed and tested over many years, EFLIGHT, a highly specialized software application has evolved specifically for this purpose. EFLIGHT provides the requisite computational resources, codified and integrated into its infrastructure, to solve the highly complex and multiply constrained optimization problem at hand. Yet, EFLIGHT it is merely a tool that can only be used effectively by a skilled practitioner of the highly specialized art (and science) of astrodynamics navigation.

The skill set required to guarantee success of the QANTAS TSE2003 flight does not rest in a single individual but rather through the confluence and synthesis of the specialized experience bases afforded by Capt. John Dennis, pilot in command, and Dr. Glenn Schneider, in the role of on-board astrodynamics and celestial navigator. Implicit in the successful co-joining of experience toward the common goal to which they will work, is the equally necessary unimpeded real-time flow of specific flight status and navigation information available on the flight deck, presented through the CDU/FMS, jointly interpreted for the specific demands of achieving a high-precision time-critical intercept with the axis of the lunar umbral shadow.

Acknowledgements

The degree of maturity which has been reached in the technical planning of the QANTAS eclipse flight could not have been achieved without the most welcome assistance and collaborative efforts of Capt. John Dennis. The author is also most grateful for the insights provided by other members of the QANTAS family, Capts. Black, Elston and Hunter. Figures 1 and 4 in this document have been adapted from NASA Technical Publication 2002-211618 (Espenak & Anderson 2002).

APPENDIX A

Frequently Asked Questions on TSE2003 and the QANTAS Eclipse Flight Concept

(embedded links resolved in): http://nicmosis.as.arizona.edu:8000/ECLIPSE_WEB/ECLIPSE_03/FAQ_747.html

Q. When is the next total solar eclipse?

A. The next total solar eclipse will occur on 23 November 2003. The Moon's umbral shadow will "touch down" on the Earth at 22h 24m Universal Time (U.T.) and "lift off" at 23h 15m U.T.

Q. How often do total solar eclipses occur?

A. On the long-term average, a total solar eclipse is visible somewhere in the world about once every sixteen months. However, the overlap between the "cycles" of solar eclipses is complex. The total solar eclipse before the 23 November 2003 eclipse occurred 11 months earlier, the next one (which has a maximum duration of the total phase of 42 seconds) will not happen until 08 April 2005. Also, on average, any given spot on the Earth will see a total solar eclipse about once every 360 years. However, eclipse paths can cross specific locations much more frequently (for example the 2001 and 2002 eclipse paths crossed in South Africa and those living in the right location saw both of them).

Q. Where will the 23 November 2003 total solar eclipse be visible?

A. Only in the Antarctic. The "path of totality", the region on the Earth's surface which will be swept by the Moon's umbral shadow and where the total phase of the eclipse can be seen, begins in the Antarctic (Great Southern) Ocean and traverses over part of the Antarctic. The eclipse will not be visible from land anywhere except over a small portion of Antarctica.

Q. Has a total solar eclipse ever previously been observed from (or over) the Antarctic?

A. No.

Q. Are eclipses in the Polar Regions rare?

A. No, but accessibility is difficult. Until this juncture in time (and technology) Antarctic eclipses have been elusive targets.

Q. Do polar eclipses have unusual characteristics?

A. The eclipse geometries can be "unusual". For example, with this eclipse, the Moon's shadow passes "over the pole" before reaching the Earth. So, the eclipse occurs in the hemisphere of the Earth which is experiencing nighttime (except in the Antarctic region), and the path of totality advances across Antarctica opposite the direction of the Earth's rotation.

Q. When will we see totality?

A. Our planned mid-eclipse intercept, when our Boeing 747-400 will be co-located in the center of the Moon's shadow, is at 22h 44m Universal Time. We remain flexible, and can intercept the shadow earlier in time (closer to the coast) or later (further inland) in the event of any obscuring

cloud or turbulent air.

Q. How long will totality last?

A. In the absence of any winds, totality, as seen from our aircraft with mid-eclipse at 22h 44m UT, will last 2m 35s.

Q. Does the aircraft's speed prolong the duration of totality compared to a ground-based observer?

A. It does. From the ground totality (at the location where mid-eclipse occurs at 22h 44m U.T.) will last only 01m 59s, thirty-six seconds shorter than we will experience in our aircraft. Note that the *difference* is longer than the maximum duration of totality experienced during the last total solar eclipse from Australia on 04 December 2002, and is only 8 seconds shorter than the maximum duration of totality of the next, 08 April 2005 total solar eclipse, in the middle of the South Pacific Ocean.

Q. How fast will the aircraft be moving?

A. Our true airspeed will be 470 nautical miles (870.5 kilometers per hour).

Q. How fast will the Moon's shadow be moving?

A. At the 22h 44m UT instant of mid-Eclipse the Moons' shadow will be moving at 3917 kilometers per hour (2115 nautical miles per hour) projected onto a surface of constant elevation at 35,000 ft above mean sea level.

Q. How does the aircraft's speed help us?

A. The aircraft will be moving with a speed of app. 22.4% of the lunar shadow (along its direction of motion at 22h 44m U.T.). Our aircraft will be moving almost in the same direction as the moon's shadow. Hence the shadow will overtake and pass us more slowly than a stationary observer on the ground.

Q. In detail, what are the "local" circumstances of the eclipse as seen from the aircraft, where will we see the eclipse?

A: For the following "baseline" flight parameters:

□U.T. Intercept:□ 22:44:00
 □Flight Altitude:□ 35000ft
 □Heading:□□□□□□□□□□ 198.80°
 □Air Speed:□□□□□□ 470.0nm/h
 □Wind Speed:□□□□□□ 0.0nm/h
 □Wind Direction:□□□□□□ 0.0°

the circumstances of the total phase of the eclipse are as follows:

□TOTALITY DURATION = 2m 34.7s
 □MID-ECLIPSE INTERCEPT:
 □□ LATITUDE□ = -69° 58' 39.8"S
 □□ LONGITUDE = +93° 00' 36.5"E
 □□ Solar Altitude = 14.9°
 □□ Solar Azimuth□ = 108.8°

□ SECOND CONTACT (START OF TOTALITY)
 □□ UNIVERSAL TIME□□□□ = □ 22:42:42.7
 □□ AIRCRAFT LATITUDE□ = □ -069° 49' 09.4''
 □□ AIRCRAFT LONGITUDE = +093° 09' □ 59.0''
 □□ Solar Altitude = +14.8°
 □□ Solar Azimuth□ = 109.0°
 □□ Position Angle of Contact = 109.3°

□ THIRD CONTACT (END OF TOTALITY)
 □□ UNIVERSAL TIME□□□□ = 22:45:17.4
 □□ AIRCRAFT LATITUDE□ = -070° 08' 17.2''
 □□ AIRCRAFT LONGITUDE = +092° 51' 06.8''
 □□ Solar Altitude = +15.0°
 □□ Solar Azimuth□ = 108.6°
 □□ Position Angle of Contact = 289.7°

Conditions in flight may call for a mid-eclipse intercept at a different altitude or Universal Time. At 22h 44m UT, the path of totality shifts anti-sunward toward an azimuth of 288.7° by approximately 4000 ft (2/3 nautical mile) for every 1000 ft of declining altitude, or toward the solar azimuth of 108.8° for commensurately higher altitudes (see Figure A1)

Q. Is our intercept at the point of the longest possible duration of the total phase of the eclipse?

A. Strictly speaking, no, this occurs at a location corresponding to a mid-eclipse of 22h 49.2m U.T.

Q. Why aren't we planning to fly to that (the maximum) point?

A. The maximum centerline duration changes very little over this portion of the path of totality. Indeed the maximum duration of totality we could experience from our aircraft (at 22h 49.2m U.T.) is only 0.6 seconds longer than we will experience (at 22h 44m U.T.). To reach that point (and return to Melbourne) would require flying an extra 650 km, or 45 minutes. We intend to hold that flight time (and fuel) in reserve, to be "used" prior to the eclipse if needed to compensate for any possible in-flight contingency or delay. If there are none, that time will be used for the Antarctic sightseeing part of the flight.

Q. At what altitude will we view totality?

A. We will observe the eclipse at the maximum altitude which can be supported at this phase of the flight, without necessitating using any fuel margins. This will depend somewhat on the actual pre-eclipse (low-level Antarctic overflight) flight plan as well as weather en route and winds. The "baseline" plan for the eclipse observation described here is for 35,000 feet above mean sea level. However, a different altitude (most likely in the range 32,000 to 38,000 ft) may be required. This possibility is anticipated and is easily accommodated in real-time with no significant change in the duration or viewing aspect of the total eclipse.

Q. At that altitude what sort of winds are we likely to encounter?

A. Our intercept position at 22h 44m U.T. was also chosen to locate the aircraft sufficiently far inland to mitigate normal coastal buffer zone (ice/sea interface) wind effects. The dominant wind pattern over the Antarctic plateau (far inland from the coastal regions) is katabatic. That is, the winds are primarily driven by a gravity gradient over the relatively isothermal ice sheet, and there is a strong tendency for the winds to have low velocity laminar flows. At our chosen latitude for the eclipse flight (-70S) the high-altitude wind pattern is very strongly circular, flowing clockwise at low velocity around the pole. We might expect winds of only 10-20 knots,

though of course anomalous conditions can arise ("climate is what you expect, weather is what you get"). See Figure A2 for an extraction from an Antarctic polar jet stream animation showing the winds over the continent for a week's period of time centered on 23 November (for 2001).

Q. How would such winds (or "abnormal" winds) affect the duration of totality?

A. Because the Moon's shadow is moving much faster than the aircraft, the change in *relative* speed, even with high winds, does not have a big effect on the duration of totality. For example, a headwind of 100 nautical miles per hour (much more than is expected) would reduce the duration of totality to 2m 25.8s, whereas a tailwind would increase it to 2m 44.9s.

Q. How high will the Sun be above the horizon during totality?

A. The Sun will be 14.9° above the astronomical horizon at mid-eclipse. At 35,000 ft, the apparent horizon is at a distance of 368 km, and depressed by 3.3°, so the Sun will appear to be 18.2° above the apparent horizon (in the absence of any topographic features).

Q. What is the "viewing angle" of the Sun during totality?

A. The eclipse intercept is planned such that the Sun will be "straight out" the port (left) side cabin windows, i.e., 90° to our direction of flight. This will maximize the ease of visibility out the cabin windows.

Q. Is there a penalty, in the duration of totality, for adopting a "straight out the window" viewing geometry and flight plan?

A. Technically, yes, as the duration of totality would be maximized by flying an arc following the instantaneous velocity vector of the Moon's shadow. In practice, however, the aircraft's mid-eclipse trajectory is such that and the "loss" to the duration of totality is only about 0.1 seconds.

Q. How clear/dark will the skies be at 35,000 feet?

A. Where weather is concerned one can never be completely assured. However, at 35,000 feet the aircraft will be above 4/5th of the Earth's atmosphere, and at these polar latitudes airborne particulates are extremely low. In the absence of high cloud - which is uncommon but not impossible - the sky transparency along the line-of-sight to the sun should be spectacular, and turbidity should be very low. The sky, during totality, at 35,000 feet should be quite dark. For a comparative example, see Figure A3 of totality at 41,000 feet (similar altitude), which shows the lunar shadow/sky brightness taken from an aircraft window of the 20 June 1992 total solar eclipse over the South Atlantic. High-altitude particulates, which cause light scattering from the illuminated regions outside of the shadow, over the Antarctic interior, are significantly more sparse than at lower latitudes.

Q. Do we have a contingency option in the event of obscuring cloud cover?

A. By design, the eclipse observation is planned after the Antarctic sightseeing portion of the flight. If weather conditions dictate an intercept later in U.T. (further inland), or (though much less likely) earlier in time, i.e., over the Ocean, can be accommodated within the planned flight margins.

Q. What if the flight take-off is delayed or we encounter strong head winds from Melbourne to the Antarctic? Isn't the eclipse intercept time critical?

A. We remain highly flexible. The eclipse-observation portion of the flight is nominally planned

to be conducted after about two and a half hours of low-altitude sightseeing along the Antarctic coast. That time can be used in contingency. If we are delayed we can observe the eclipse first and the sightseeing portion of the flight can be carried out after totality.

Q. If unforeseen contingencies arise can we re-plan the eclipse observation in "real time"?

A. The flight pre-planning, including baseline and contingency (alternate) scenarios have been carried out using a highly specialized software package called EFLIGHT which symbiotically synthesizes dynamical ephemerides generation for an eclipse viewed from a moving platform with aircraft navigation information. EFLIGHT, which is fully described in *Appendix B*, was designed for in situ on the aircraft flight deck and real-time airborne eclipse navigation. It will be used in this manner on the Croydon/QANTAS flight to "guide" the aircraft to an optimal "totality run" and eclipse intercept.

Q. Will the eclipse be observed from any other aircraft?

A. At this time, a second Antarctic eclipse flight is planned, using an Airbus A340 operated by Lan Chile.

Q. Is there any chance of "interference" by the second aircraft?

A. The QANTAS/CROYDON and LanChile/Sky&Telescope flight plans, were co-operatively and contemporaneously designed for non-interference, and the two aircraft will not be operating in the same airspace. On a personal note, I have been privileged to have worked on (and continue to work on) the definition and planning of both flights, and the level of co-ordination between the two flights, to assure their mutual success, has been very high.

Q. Will we see the partial phases of the eclipse from the aircraft?

A. We have made no special plans, nor levied any requirements on the flight profile for viewing first/fourth contacts or most of the ingress and egress phase of the partial eclipse, as this nominally will occur during the "sightseeing" phase of the flight. The orientation of the aircraft, as it maneuvers for viewing along the Antarctic coastline, will likely allow some serendipitous viewing of ingress. About a half an hour before totality (the exact time dependent upon the position of the aircraft) we will break off the site-seeing portion of the flight and head to a pre-determined "hold" point just ahead of the start of the flight path for the "totality run". At 15 minutes before mid-eclipse (app. 13m 40s before Contact II) we will complete a heading alignment maneuver to put the aircraft on a nearly "straight line" course for a mid-eclipse intercept with the center of the umbral cone at 22h 44m. During the run up to totality the Sun will be essentially perpendicular to the direction of flight, "straight out" the left side cabin windows. This will provide an opportunity to view (and prepare photographic equipment during) the latest stages of the partial ingress phase of the eclipse, including the approach of the umbral shadow and the onset of second contact. After third contact the aircraft will continue on the totality run track for an additional approximately 4 minutes to view the first stages of the partial egress phase of the eclipse and the recession of the lunar shadow.

Q. I still have more questions of a "technical" nature regarding this eclipse and the planned flight. How can I get answers?

A. Send email to: [Glenn Schneider \(gschneider@mac.com\)](mailto:gschneider@mac.com)

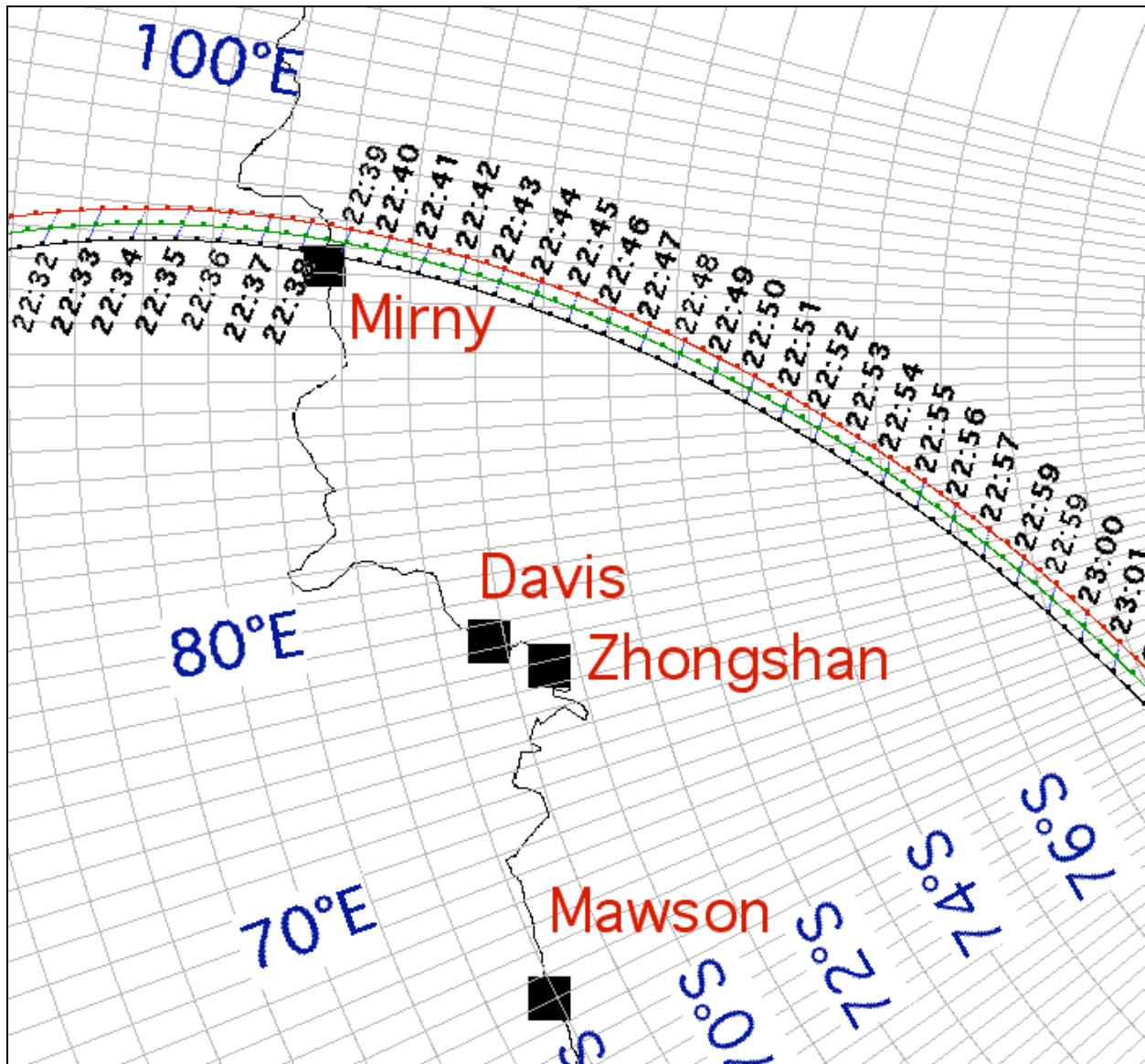


Fig. A1 – The obliquity of the conic axis of the umbral shadow to surfaces of constant elevation above mean sea level causes a “shift” in the location of centerline with altitude and along constant time lines. The centerline of the path of totality over the region of the Antarctic where the QANTAS flight will be operating is shown for sea level (black), 20,000 ft (green) and 40,000 ft (red). The instants of mid-eclipse along the altitude-dependent centerlines are marked in 30s increments (annotated every minute). The isotemporal lines “connecting” the three tracks are instantaneous segmental projections of the lunar shadow axis onto the surface of the Earth and point, in the direction of higher elevation, toward the azimuth of the Sun.

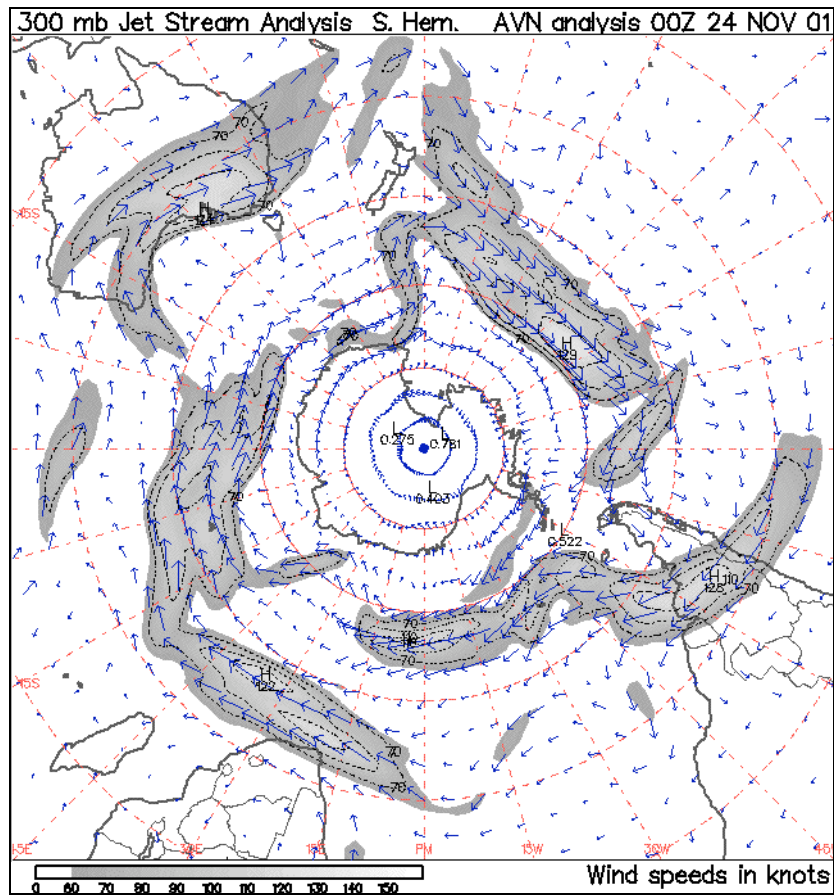


Fig. A2 - Antarctic 300 mb wind field at 24 Nov 2001 0h UT, note the inland low velocity circumpolar flow.
See: http://nicmosis.as.arizona.edu:8000/ECLIPSE_WEB/ECLIPSE_03/wind_pattern.gif



Fig. A3 - 30 June 2003 TSE sky brightness and color gradients at 41,000 ft. Solar elevation = 30°

APPENDIX B



EFLIGHT 2003 X - Eclipse Flight Planning & Navigation S/W



Updated: 04 Apr 2003 for [MacOS X](#)

(embedded links resolved in) http://nicmosis.as.arizona.edu:8000/ECLIPSE_WEB/EFLIGHT/EFLIGHT.html

[Glenn Schneider](#)

Steward Observatory
933 N. Cherry Avenue
University of Arizona
Tucson, Arizona 85750

gschneider@as.arizona.edu or gschneider@mac.com

Prelude on the Art of Eclipse Chasing

The "art" of eclipse chasing sometimes poses difficult and complex logistical, technical (and financial) problems. Unless you are one of the very fortunate < 1% of the world's population which, by pure luck, has a Total Solar Eclipse fall in your backyard sometime during your life, then getting to the path of totality often becomes a challenge, if not an obsession. I suppose I am one of the obsessed. At the risk of redundancy, but for necessary background, elsewhere I had previously written: *"Glenn Schneider is an UMBRAPHILE. Literally a "shadow lover", but properly applied, one who is addicted to the glory and majesty of total solar eclipses. Those who have basked in the moon's shadow will know what I mean without further explanation. Those who have not may have difficulty in understanding that umbraphillia is not only an addiction, but an affliction, and a way of life. The real raison d' etre for many of us. The more common and prolific term "solar eclipse chaser" is nearly synonymous, but somehow does not convey the depth of commitment to this lifelong endeavor. Once every 16 months, or so, (on average) umbraphiles will drop whatever they are doing and trek by plane, ship, train, foot, and camel-back to gather along a narrow strip in some remote God- forsaken corner of the globe defined by the inexorable laws of celestial mechanics. Newtonian physics heeds no national boundaries, and neither do umbraphiles. Wherever the solar photosphere will be extinguished, enshrouded by the ashen lunar disk, umbraphiles will revel in the quasi-twilight darkness."*

Why EFLIGHT?

Occasionally, the path of totality (i.e., the region on or above Earth's surface where a total eclipse may be viewed) is so elusive that an airborne observation of such an eclipse is by far the preferable, if not the only, viable alternative. Such was the case on [03 October 1986](#), and again on [30 June 1992](#). And, the very fortuitous geometrical circumstances associated with the [21 June 2001](#) total solar eclipse could have given rise to an [hour long totality](#) if fate had not [tragically intervened](#). Hitting a moving target (the moon's shadow) from a moving platform (a high speed aircraft) may not intrinsically seem like too complex a problem, though it certainly is non-trivial. To do this successfully, while optimizing a flight intercept to strike a desired balance between duration, observability (i.e., line-of-sight requirements due to aircraft windows), other dynamical and programmatic constraints and restrictions, and cost, must be approached with both care and rigor. The circumstances of the 03 October 1986 eclipse were so constrained (see the above linked page), that virtually no deviation from a very laboriously pre-constructed flight intercept could be tolerated. By 1992, however, the availability and capabilities of portable (aka "laptop") computers had so rapidly evolved, that eclipse flight *re*-planning in reaction to situ conditions became possible. As a result, [EFLIGHT 92](#) - an integrated eclipse flight planning and navigation S/W package - was engineered for the then fledgling Macintosh PowerBook 100 series laptop computers, and then successfully used to navigate a DC-10 through the path of the 30 June 1992 eclipse. (As it begs the question... No. I did not have to "turn off and put away" my Powerbook 170 during take-off for that flight, though I suppose it helped that I was occupying the navigator's seat in the cockpit).

The 23 November 2003 total Solar Eclipse

With the advent of the [23 November 2003](#) total solar eclipse, a prime candidate for an airborne eclipse observation, I have dusted off **EFLIGHT** after the tragic accident on 25 July 2000 canceling its planned use, in its [2001 incarnation](#), on the Concorde for the 21 June 2001 eclipse. Given the large degree of "inaccessibility" to nearly all of the 23 November 2003 eclipse path, such a flight was crying to be flown. This eclipse has met with considerable interest, likely due to the added enticement of its remoteness, and planning for such a flight has actually been underway for some time. Two Antarctic over-flights have evolved which have (and continue) to use **EFLIGHT** to develop their flight concepts, requirements, specifications, and plans:

- 1) [Croydon Travel](#)/QANTAS: Using a Boeing 747-400 from Melbourne, Australia.
- 2) [TravelQuest](#) (Sky & Telescope)/LanChile: Using an Airbus A340 from Punta Arenas, Chile.

The baseline Eclipse Flight Centerline Intercepts and Totality Runs for these flights are illustrated and summarized [HERE](#).

EFLIGHT 2003 X (and UMBRAPHILE) and their predecessors

On the "technical" side, many have queried me about **EFLIGHT** (which I have recently ported to run under MacOS X and is now a native Jaguar/Aqua application). So, here I provide an overview of what it is, and what it can (and will) do. But first...

HISTORY: The core algorithms for **EFLIGHT** have a long history. The computations of the astronomical ephemerides and eclipse circumstances performed by **EFLIGHT** were originally implemented in 1974 in APL on a Xerox Sigma 9 computer under the UTS (and later CP-V) operating system. These core algorithms have been used for planning ground-based and/or airborne observations every total solar eclipse since. Early in its history, the software was migrated to other mainframe computers and operating systems (including the IBM/360, Ahmdahl/470VM and Harris 500). By 1979 the software had also been implemented in a combination of BASIC and 6502 assembly code and "packaged" for use on an APPLE II computer. The eclipse predication and planning software was integrated into a end user oriented system called **CENTERLINE** and migrated to the microAPL desktop environment (in the Waterloo language system) on the Commodore SuperPet SP9000 in 1982. By 1985 **CENTERLINE** had again moved, to a VAX/VMS environment, implemented in APL11 under RSX. **CENTERLINE** was then augmented with some rather special purpose algorithms to aid in the planning of the airborne eclipse observation of the October, 1986 eclipse in the north Atlantic near Iceland. By 1988, **CENTERLINE** was transformed to the paradigm of the graphical user interface under (Mac) OS 6, implemented first on a Macintosh SE in APL/68000. Contemporaneously, following the 1988 eclipse, a real-time automated camera controller called **ROSE** (the Reprogrammable Observer for Solar Eclipses) was developed for the Rockwell AIM-65 (6502) environment as a machine/assembly language program, which relied on computationally derived inputs from **CENTERLINE**. **ROSE**, supported computationally by **CENTERLINE**, was used successfully during the exceptionally long total solar eclipse of 1991. With the advent of the Macintosh Powerbook, in 1992, **ROSE** and **CENTERLINE** were symbiotically merged into a single APL/68000 application running under (Mac) OS 7, the first prototype of **UMBRAPHILE**. But **UMBRAPHILE** would not be field-tested (quite successfully) until the total solar eclipse of 1995 in Ghanoli, India.

Contemporaneous with the early development of **UMBRAPHILE**, a separate (Mac) OS APL/68000 application, **EFLIGHT** predicated on the same core algorithms, was born to plan and assist in the real-time navigation of a VASP airlines DC-10 to observe the total solar eclipse of June 1992 over the South Atlantic. **UMBRAPHILE** evolved in the late 1990's to a user friendly MacOS application and was subsequently used for the 1997 (Siberian) 1999 (Black Sea), total solar eclipses. **EFLIGHT** was upgraded and modified for MacOS 9 nativity as an APL Level II for Power Macintosh application in 2000, in preparation for a planned nearly one-hour airborne observation of the June 2001 eclipse with an Air France Concorde. The tragic event of 25 June 2000, which lead to the subsequent grounding of the Concorde fleet, resulted in the upgraded **EFLIGHT** being put "on the shelf". Observing instead from the ground, the June 2001 eclipse in Zambia was photographed with **UMBRAPHILE**, for the first time by multiple eclipse photographers and at different locations along the path of totality (e.g., see results from

D. McGlaun). And, **UMBRAPHILE** was used again for the 4 December 2002 eclipse, with an three Macintosh Powerbooks spanning 10 years of technology (68K Series 100 by J. Friedland, to G4 by J. Moskowitz and myself) within 5 meters of each other in the middle of the Australian outback.

In preparation for the 23 November 2003 eclipse, which will be viewed by two aircraft over Antarctica, **EFLIGHT** underwent additional modifications and a port to run natively under MacOS X. The current version of **EFLIGHT** (2003 X version 2.0.0), described here, is written in APLX for Macintosh (version 1.1.5) from mcicroAPL Ltd. (UK). Though designed for MacOS X it will run in "Classic" mode under MacOS X, and a release can be prepared to run "native" under MacOS 9.

An Umbraphillic Derivative

EFLIGHT is an eclipse circumstance calculator - but one specifically designed to address the problem of intercepting the moon's shadow from a moving aircraft. The core algorithms for the computation of at-altitude local and centerline eclipse circumstances are the same as those employed in [UMBRAPHILE](#). What? You aren't familiar with [UMBRAPHILE](#)? Then please read about that freeware application to fill in the necessary background details, which I won't repeat here. **EFLIGHT** actually co-evolved with **UMBRAPHILE**, so much so that it uses the same input data file structure, and both shares many common "user" interface elements. However, **UMBRAPHILE** was designed as a more generic application for unrestricted distribution (and hence, "user proofed"). **EFLIGHT** requires a bit more hand-holding and intimate familiarization with embedded concepts, so you won't find a down-loadable application here. For those seriously interested please [contact me](#), but I suggest a likely necessary sentient accessory to have with it on your airplane if you plan to use it there. At least, some think I am sentient. Indeed, I will be using **EFLIGHT** in situ on 23 November 2003 QANTAS/Croydon (Boeing 747-400) eclipse flight over the Antarctic to help guide the aircraft to a seamless and optimized high precision time-critical intercept with the conic axis of the lunar umbral shadow.

Starting up and Running EFLIGHT 2003 X

To start up **EFLIGHT** just double-click the **EFLIGHT** ICON: . **EFLIGHT** will then :

1) Bring up an introductory message in a dismissible dialog (Figure 1), indicating the software version release number. Ephemeris data is pre-loaded with the application for a specific total solar eclipse, though ephemeris data may be imported (as described later) for other eclipses. The eclipse for which eclipse ephemeris data is provided by default as part of the application is also noted at startup in the introductory dialog.

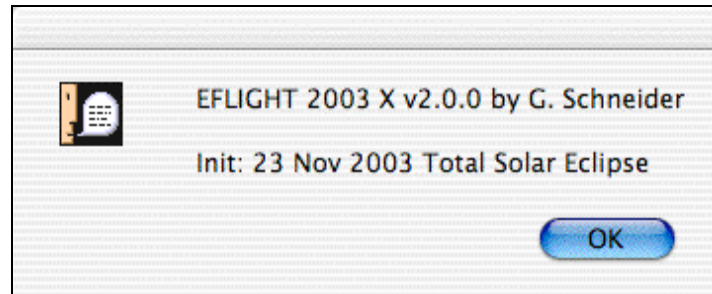


Figure 1. EFLIGHT Introductory Dialog.

2) Pop up an "Info Window" (Figure 2) providing contact information and where to obtain the latest **EFLIGHT** documentation. By design, this window cannot be closed or minimized while running EFLIGHT, but it can be moved "out of the way", or behind other windows.

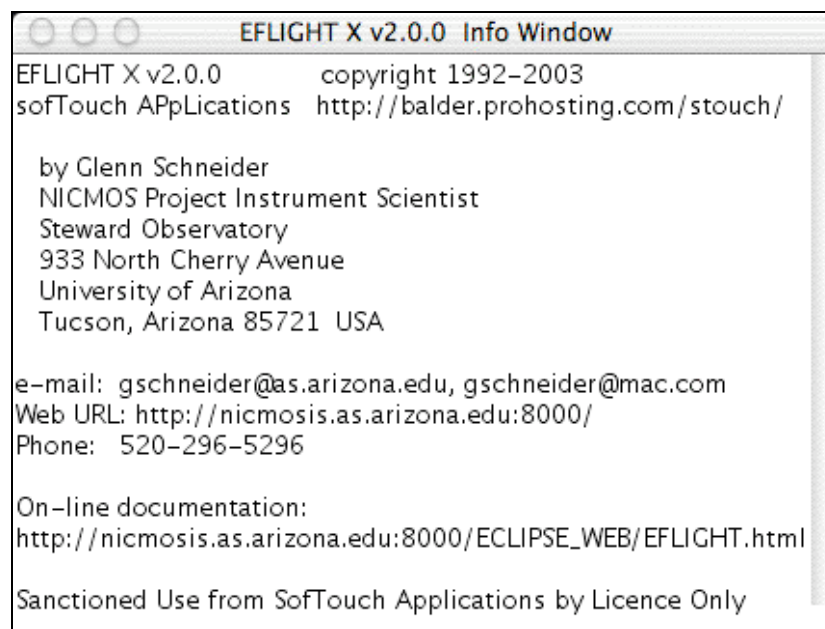


Figure 2. EFLIGHT Info Window

3) Create a text "Output Window" (Figure 3), which **EFLIGHT** will use for displaying textual information and data generated by **EFLIGHT**. The text output window will initially display basic information germane to the operation of the current **EFLIGHT** release:

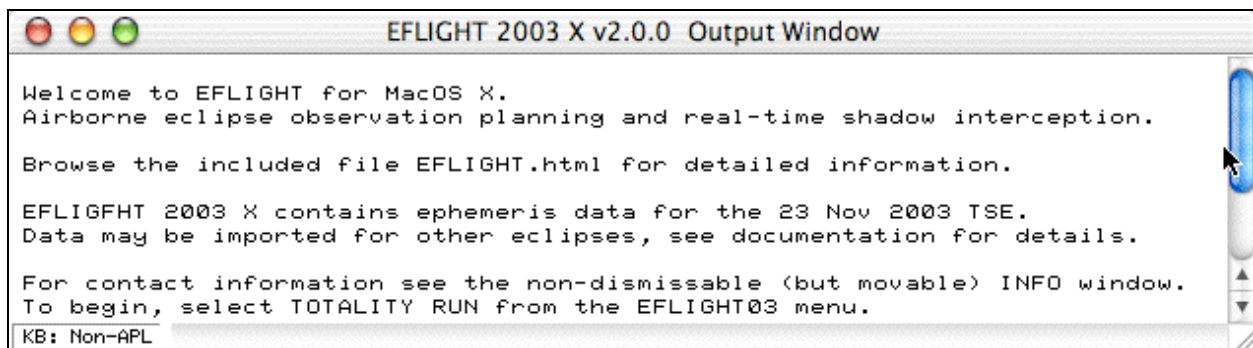


Figure 3. EFLIGHT Output Window

The introductory notes (which may be release dependent) will be cleared when **EFLIGHT** subsequently produces a text display in the output window, but these messages may be refreshed by selecting **HELP** from the **EFLIGHT** menu.

The text output window is scrollable, as the tabular output produced by **EFLIGHT** can be quite lengthy (depending upon the input parameters supplied by the user). The output window, initially, may be smaller than the width of the **TABULATE TOTALITY RUN** table (describe later), but it may be maximized to the full screen size or resized, as usual, by clicking and dragging the lower right edge of the window.

The title bar of the text output window will change name to reflect the current window content, and to display computational status messages for computationally intensive operations in progress.

EFLIGHT 2003 X Menus

The following menus and associated menu items will appear to the right of the Apple menu after starting up **EFLIGHT**:

<u>EFLIGHT</u> {release #}	(MacOS system servicesmenu)
Note: The About... and Preferences... menu items are not used by EFLIGHT	
<u>FILE</u>	(Active only for the text output window)
Save Window Content...	(Export entire window context to ASCII file)
Page Setup...	[to specify printing parameters as usual]
Print...	[to print the content of the output window]
<u>EDIT</u>	(Active only for the text output window)
Provides usual Copy, Paste, Find, etc.	
<u>OPTIONS</u>	(Active only for the text output window)
Font Size	[Select font size for text output window]
<u>EFLIGHT##</u> {## indicates year of TSE ephemeris data included}	
HELP	[Refreshes/provides EFLIGHT start-up advisory messages]
COMPUTE TOTALITY RUN	[Input flight parameters, compute circumstances]
TABULATE TOTALITY RUN	[Tabular (text) display of flight profile & circumstances]
SELECT WAYPOINTS	[Waypoints for FMS entry, track info & local circumstances]
DISPLAY TOTALITY RUN	[Real-time synchronized or time compressed graphical simulation]
COMPUTE COURSE	[Generate pre/post totality run flight profile]
INTERRUPT	[Terminate Totality Run in progress]
QUIT	[Exit from EFLIGHT]

The EFLIGHT Menu

The items under the **EFLIGHT** menu perform the computational and display tasks for planning, optimizing, and executing an eclipse flight totality run. Those items, are described in detail below. The other menus provide standard system services, and so, are not discussed here.

1) COMPUTE TOTALITY RUN

An **EFLIGHT** "totality run" is fundamentally parametrized by specifying a Universal Time (U.T.) at which the aircraft is to be co-axially located in the umbral shadow (i.e., the instant of mid-eclipse). This is combined with the flight altitude, aircraft speed, and several other parameters to develop a set of time-ordered and time-dependent way points (latitude and longitude tuples) which can, for example, be loaded into an aircraft's navigation/autopilot and/or CDU/FMS systems. Importantly, **EFLIGHT** can re-compute a "corrected" flight plan *in situ* given changing wind conditions en route to the eclipse intercept. The set of parameters and selectable options which control the computation, and later tabulation and display of the totality run, is entered through the **EFLIGHT** "flight definition dialog" (Figure 4) which is presented when the **COMPUTE TOTALITY RUN** item is selected from the **EFLIGHT** menu.

Concepts:

1) For planning purposes, **EFLIGHT** can be run in a U.T. synchronous, or asynchronous time-compressed manner. I.e., a flight plan can be developed and "simulated" without regard to the actual U.T. (system) clock time or rate of time-flow. The flight plan can be tested at a sped up (or slowed down) pace, and enabled for real-time use on-board the aircraft (via the **RT SIMULATION** check box). In that case, **EFLIGHT** will synchronize to the computer's internal clock (with a fixed time offset, if desired), and provide position/navigation information in real-time.

2) **EFLIGHT** develops a set of time-correlated way points, in 1, 5, 10, or 30 second intervals, to be targeted within a specified range of times before and after the instant of mid-eclipse. At each instant of time along the flight path, **EFLIGHT** reports on the circumstances of the eclipse, the aircraft position, its flight vector, and related information.

3) Currently **EFLIGHT** builds the "totality run" in one of three ways by specifying/selecting:

a) A user-input fixed aircraft heading to be flown fly through the point of mid-eclipse.

b) A fixed aircraft heading to put the sun perpendicular to the aircraft heading at the instant of mid-eclipse (to put the Sun "straight out the cabin windows" at mid-eclipse) as determined by **EFLIGHT** based upon the circumstances of the eclipse.

c) A flight path parallel to the direction of the velocity vector of the moon's umbral shadow.

U. T. Mid-Eclipse =	hhmmss		
	224400		
Intercept CL	0	<input type="radio"/> km <input type="radio"/> mi toward Sun <input checked="" type="radio"/> nm	
Time Window =	5	3	Min.
True Air Speed =	470	/hr	
<input type="radio"/> Fly Aircraft Heading = 200 Deg. <input checked="" type="radio"/> Fly Perpendicular to Sun <input type="radio"/> Fly Parallel to Shadow			
Altitude in feet AMSL =	35000		
WIND from	0	Deg., Speed =	0
Autoscale +	2	Deg	
Display Time Resolution:	<input type="radio"/> 1s <input checked="" type="radio"/> 5s <input type="radio"/> 10s <input type="radio"/> 30s	Output Format:	<input type="radio"/> DDD.xxxxx <input type="radio"/> DDDMMSS.x <input checked="" type="radio"/> DDDMM.xxx
Display Frame Delay =	.1	s	
<input type="checkbox"/> Export Waypoint Table <input type="checkbox"/> RT SIMULATION			
Graphics Scale =	100	°/°	
			CANCEL
			OK

Figure 4. A centerline-intercept flight profile is created in compliance with a set parameters specified through the EFLIGHT flight definition dialog.

Inputs:

U.T. Mid-Eclipse: Specifies the Universal Time (with one second granularity) at which the aircraft is to be concentrically located in the moon's shadow.

Time Window: Specifies how many minutes before and after mid-eclipse the aircraft is to fly on the to-be-computed "totality run".

INTERCEPT CL: For some eclipses a non-central intercept through the umbra might be desirable, and such an offset can be specified through the INTERCEPT CL option. *This option has been disabled for the 23 November 2003 total solar eclipse.*

(True) AIRcraft Speed: This is the true AIR speed (not the GROUND speed, which EFLIGHT will compute based upon windage and course). The true AIRcraft speed may be entered in kilometers/hour, (statute) miles/hour or nautical miles/hour.

(True) Aircraft Heading: True Heading (not magnetic*) may be entered (in degrees) - but is used only if "Use Entered Heading" is selected.

Choice of Flight Vectors: As defined in (3) a, b, and c, above. Flying perpendicular to the Sun will present an optimized view of the eclipse out the aircraft cabin windows, and will typically be necessary anywhere along the path except relatively near the points of local noon or midnight. Flying parallel to the shadow will maximize the duration of totality - but would likely not be practical near the beginning or end of the path (as the aircraft would then fly "across the shadow" and the sun would not be visible through the cabin windows, or would be a real neck-craner).

Altitude in feet: Fixed altitude of the aircraft above MSL.

Wind Speed/Direction: Specify direction wind is FROM in degrees, and the Wind Speed. Note: Wind Speed is taken to be in same units selected for AIRcraft speed.

Autoscale: The EFLIGHT graphical output (discussed below) is scaled to exactly fit the most constrained end-points along the path of totality at the boundaries of the graphics window. In setting up the output display an optional "buffer" to move the endpoints from the closer end of the window (in degrees of latitude, or longitude) may be entered.

Time Resolution: Specifies the temporal granularity (in seconds) for the computation of eclipse circumstance and navigation data. (see Tabulate and presented graphically, but also affects the [precision of the times of contacts](#) as seen from the moving aircraft. For computation speed, use coarse time intervals, for initial flight planning and evaluation. For high precision contact times and circumstances use 1s granularity.

Export Way point Table: Check this box to automatically also write the information presented in the output window to an ASCII file.

RT SIMULATION: Check this box display a Real Time (i.e., system clock time synchronous) graphical simulation when the **DISPLAY TOTALITY RUN** item is subsequently selected from the EFLIGHT03 menu. .

OUTPUT FORMAT: Three output formats are available for aircraft and umbral shadow coordinates (latitude and longitude) as displayed in the text window (but not in the graphics window) and/or exporting the content of the text output window to an ASCII file. Select from: decimal degrees; degrees, minutes, seconds (and fractional seconds to the nearest 0.1"); or degrees and minutes (and fractional minutes to the nearest 0.001').

* **EFLIGHT** uses true, not magnetic headings. For most locations on the Earth the difference can be computed by a magnetic field model such as the [NGDC/NOAA](#) model. Near the magnetic poles both the magnetic declination and gradient of the declination can be very large. The South magnetic pole is at 66°S latitude, 139°E longitude. For the intercept location given in the Figure 1 example the magnetic declination is -64° 57', and would be -93° 44' for an intercept near maximum eclipse at 22h 49m U.T.

After entering the desired parametric values and selectable options in the Flight Definition Dialog, clicking **[OK]** will prepare **EFLIGHT** to pre-compute the local circumstances and navigational information along flight path of the totality run.

Note on Coordinate Systems and Geodetic Reference:

Many different geodetic reference systems are in use around the world. Thus, for high precision position determinations it is important to know which system is being used, and how to transform topocentric coordinates from one to another. **EFLIGHT** adopts the aspherical definition of the geoid suggested by the International Astronomical Union (see [UMBRAFILE](#) documentation) and adds a fixed constant to the topocentrically dependent radius vector when determining the (X,Y, Z) instantaneous positions of the aircraft. The International Terrestrial Reference System is defined by the [Earth Orientation Rotation Service](#). There are many resources available for transforming between commonly used, but different, map reference data (such as WGS 84, NAD 27, etc.). For more information let me refer a [comprehensive introductory summary](#) prepared by Pete Dana at the University of Texas Dept. of Geography.

☐When you click [OK] in the Flight Definition Dialog:

Before the computation proceeds, **EFLIGHT** will bring up a confirmatory dialog (figure 5) indicating the UT start, end, and increment times and flight altitude (converted to meters) for the totality run. The actual computation spans an interval which is one time step longer, at the start and end of the run, then the time window specification for which the totality run is developed. This dialog is presented to allow you to **[CANCEL]** the computation before it begins in the event an input error is made in the flight definition dialog. Click **[OK]** to proceed. Unless you are intimately familiar with **EFLIGHT**, **DO NOT** alter the information in the confirmatory dialog. (You may adjust the start, and end times and increment - but this **MUST** be done with care. The **ONLY** allowable increments are 1, 5, 10, and 30s, and the start and end times **MUST** differ by an integral number of increments.) It is suggested that if you wish to make any adjustments at this point you **[CANCEL]** the confirmatory dialog, and re-enter any changes in the Flight Definition dialog, otherwise click **[OK]**.

Start Time	HHMMSS.f 223855.0
End Time	HHMMSS.f 224805.0
Increment	HHMMSS.f 000005
Altitude	10668 meters
<input type="checkbox"/> Read Data File	
<input type="button" value="CANCEL"/> <input type="button" value="OK"/>	

Figure 5 - Totality Run Confirmation Dialog.

Note: **EFLIGHT 2003X v2.0.0** is "pre-loaded" with ephemeris data specifically for the 23 November 2003 eclipse. The data file from which these data were pre-imported in **EFLIGHT 2003X v2.0.0** is included with the **EFLIGHT S/W**. Ephemeris data for other solar eclipses may be imported by checking Read Data File in the flight definition confirmation dialog. Ephemeris data is imported from ASCII files of specific format and content and are of the same form used for the **UMBRAPHILE** camera controller software. Please contact Glenn Schneider for additional information on data files other eclipses. If Read Data File is checked a file requester dialog will be presented, and after importation of ephemeris data, the data values read from the file will be displayed in the main text output window.

EFLIGHT then pre-computes all of the eclipse circumstances and aircraft related information before anything is display or tabulated. Generation of eclipse circumstances and navigation data proceeds in temporally increasing order for the totality run and is a computationally extensive task. While these data are being computed, a status message, indicating the instantaneous U.T. of the computation in progress, will be displayed in the title bar of the main window. During the computation some diagnostic information may be presented in the main window. This information can generally be ignored and will be cleared from the display when the computation completes. A message informing of the completion of the **COMPUTE TOTALITY RUN** task will be presented when the computation has finished.

When the pre-computations are completed, if the Display Graphics box was checked in the Flight Definition dialog, a graphics output window will be built (if it hadn't been from a previous Totality Run).

2) TABULATE TOTALITY RUN

The results of the totality run computation may be tabulated in a scrollable text window (and exported to an ASCII file). The format of the tabular display is shown in Figure 6.

The screenshot shows a window titled "EFLIGHT03:TABULATE TOTALITY RUN" with the following content:

```

U.T. Intercept: 22:44:00 | TOTALITY DURATION = 2m 34.7s
Flight Altitude: 35000ft |
Heading: 198.80° |
Air Speed: 470.0nm/h | 2ND 22:42:43.1 +14.8 109.0 109.3 3RD 22:45:17.8 +15.0 108.6 289.7
Wind Speed: 0.0nm/h | LATITUDE: -069° 49' 24.2'' | LATITUDE: -070° 08' 32.0''
Wind Direction: 0.0° | LONGITUDE: +093° 09' 44.5'' | LONGITUDE: +092° 50' 52.3''
-----
HHMMSS  Umbra Long  Umbra Lat  WidKM  Uaz°  Ual°  AirCr Long  AirCr Lat  Mid°T  Mid°D  LOS  Bearing  ACaz  ACal
223200  9422.514E  6239.618S  535.1  111.9  11.8  9423.086E  6829.493S  -720s  -94.0nm  +0.3  197.52  108.5  14.7
223205  9423.657E  6243.010S  534.8  111.8  11.8  9422.551E  6830.114S  -715s  -93.3nm  +0.3  197.52  108.5  14.7
223210  9424.773E  6246.395S  534.6  111.8  11.8  9422.015E  6830.736S  -710s  -92.7nm  +0.3  197.53  108.5  14.7
223215  9425.863E  6249.772S  534.4  111.7  11.9  9421.479E  6831.357S  -705s  -92.0nm  +0.3  197.54  108.5  14.7
223220  9426.927E  6253.143S  534.2  111.7  11.9  9420.942E  6831.978S  -700s  -91.4nm  +0.3  197.55  108.5  14.7
223225  9427.964E  6256.506S  533.9  111.7  12.0  9420.405E  6832.599S  -695s  -90.7nm  +0.3  197.56  108.5  14.7

```

KB: Non-APL

Figure 6 - Totality Run Tabular Output Window

The text output is organized in two sections: a header and a table. The left side of the header region echoes back the input parameters from the Flight Definition dialog. The right section provides the duration of totality and information on second and third contact*. The U.T. of each contact, along with the solar altitude, azimuth, and contact position angle is given, as is the location (latitude and longitude) of the aircraft at the instants of the contacts. The tabular section is presented in time order at the temporal resolution specified in the Flight Definition Dialog.

NOTE: For very high precision contact determinations, a 1s temporal granularity should be used in computing the totality run.

The time-ordered table section is as follows:

```

HHMMSS = [ ] [ ] [ ] [ ] Universal Time (Hours, Minutes, Seconds)
UMbra Long = Longitude of the Center of the Umbra
UMbra Lat [ ] = Latitude of the Center of the Umbra
WidKM = [ ] [ ] [ ] [ ] Width of the Umbral Shadow Projection in KM
Uaz = [ ] [ ] [ ] [ ] [ ] Altitude of the Sun (degrees) from that point
Ual = [ ] [ ] [ ] [ ] [ ] Altitude of the Sun (degrees) from that point
AirCr Long = Longitude of the Aircraft at the corresponding time
AirCr Lat [ ] = Latitude of the Aircraft at the corresponding time
Mid [ ] T [ ] [ ] [ ] [ ] = Time in seconds until/since mid-eclipse
Mid [ ] D [ ] [ ] [ ] [ ] = Distance to be flown (in units requested) to/from mid-eclipse
LOS [ ] [ ] [ ] [ ] [ ] [ ] = LOS deviation angle to the Sun w.r.t. aircraft windows (degrees)
Bearing [ ] [ ] [ ] [ ] = Instantaneous Bearing of the Aircraft (degrees)
ACaz [ ] [ ] [ ] [ ] [ ] [ ] = The azimuth angle of the sun from the Aircraft (degrees)
ACal [ ] [ ] [ ] [ ] [ ] [ ] = The altitude of the Sun from the Aircraft (degrees)

```

The geographical co-ordinates for the instantaneous center of the umbra and position of the aircraft are formatted as specified in the Flight Definition Dialog.

3) SELECT WAYPOINTS

The totality run is defined by a series of time correlated waypoints to which the aircraft trajectory must conform both in position and time. COMPUTE TOTALITY RUN determines a set of target points with a temporal granularity that is generally much denser than is required for a flight path specification. The Totality Run may be very closely approximated by extracting a subset of waypoints from the more densely computed values. For nearly all eclipses (except for those with very narrow shadows or very close to the points of sunrise/set) waypoint densities on the order of several minutes in time will not limit the accuracy achieved in the actual targeting of the aircraft.

SELECT WAYPOINTS provides a simple mechanism for extracting target position waypoints from the computed totality run. The selected waypoints and associated local eclipse circumstances are displayed in a pop-up window (the Selected WAYPOINTS window) and are used for incremental relative position updates in the EFLIGHT graphical display of the totality run. The SELECT WAYPOINTS menu item should be used after COMPUTE TOTALITY RUN completes. Select Waypoints will allow you to extract a subset of waypoints from a time-ordered list with granularities of 5, 10, 30, or 60 seconds via the Waypoint Selection Time Granularity dialog (Figure 7)

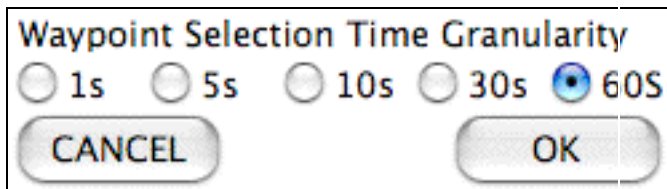


Figure 7 - Waypoint Selection Time Granularity dialog

After specifying the Selection Time Granularity, a Waypoint Extraction Dialog (Figure 8) will be presented. This dialog will contain a list of Universal Times corresponding to positions along the totality run within the computed time window at the selection granularity specified. The instant of mid-eclipse is pre-selected. Additional points (by time) along the totality run may be selected (or deselected) by checking (or unchecking) the boxes adjacent the list of Universal Times. After clicking [OK] the extracted waypoints will be displayed in a Selected WAYPOINTS window (Figure 9).

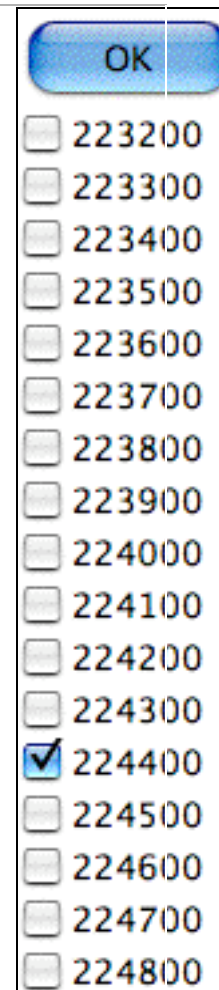


Figure 8 – Way Point Extraction Dialog

Selected WAYPOINTS																		
#	HHMMSS	UMbra	Long	UMbra	Lat	WidKM	Uaz°	Ual°	AirCr	Long	AirCr	Lat	MidAT	MidAD	LOS	Bearng	ACaz	ACal
A	223200	9422.514E	6239.618S	535.1	111.9	11.8	9423.086E	6829.493S	-720s	-94.0nm	+0.3	197.52	108.5	14.7				
B	223600	9449.442E	6515.523S	523.8	110.1	13.3	9356.833E	6859.287S	-480s	-62.7nm	+0.2	197.92	108.6	14.8				
C	224000	9422.996E	6740.906S	512.7	109.0	14.3	9329.370E	6929.011S	-240s	-31.3nm	+0.1	198.35	108.7	14.9				
D	224400	9300.609E	6958.660S	502.7	108.8	14.9	9300.609E	6958.663S	+0s	+0.0nm	-0.0	198.88	108.8	14.9				
E	224800	9030.598E	7209.511S	494.5	109.6	15.2	9231.848E	7028.309S	+240s	+31.3nm	-0.1	197.54	108.9	15.0				

Figure 9 - Selected WAYPOINTS Window

4) DISPLAY TOTALITY RUN

Selecting **DISPLAY TOTALITY RUN** from the EFLIGHT menu creates a graphical output window, which provides a continually updating display showing the topocentric geographical circumstances of the total phase of the eclipse, and the computed track of the aircraft throughout the duration of the totality run.

TIME SYNCHRONIZATION

The totality run graphics display will update in one of three ways.

1. If **RT SIMULATION** was *NOT* selected in the **COMPUTE TOTALITY RUN** Flight Definition dialog, then the graphical output will update asynchronously with respect to the computer's clock. In that case, each successive graphic frame will be displayed with an inter-frame cadence specified by Flight Definition dialog's **Display Frame Delay** without regard to the system clock time.

If **RT SIMULATION** was selected, then a Clock Synchronization Dialog (Figure 10) will be presented before the totality run graphic output begins.

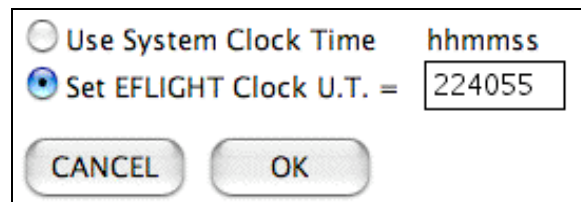


Figure 10 - EFLIGHT Clock Synchronization Dialog

2. If **Use System Clock Time** is selected the Totality Run display will commence when the System Clock reaches the Universal Time of the first point computed for the totality run. After clicking [**OK**], the subsequent graphic output of the totality run will then be synchronized to the computer's system clock time.

In flight, it is imperative that the computer's internal clock has been accurately set and synchronized to a Coordinated Universal Time (e.g., through a network time server or GPS time reference).

3. You may set an "EFLIGHT U.T. Clock", independent of the computer's system clock but running at a real-time cadence, to which the graphical output can be synchronized by selecting **Set EFLIGHT Clock U.T.** The "EFLIGHT Clock" will be set to the U.T. as specified (in HHMMSS format) in the Clock Synchronization Dialog. This time will automatically be pre-set to one graphics frame delay period (as specified through the Flight Definition Dialog) before the U.T. of the first point computed for the totality run, but may be over-ridden to any legal value by user input. After clicking [**OK**], the subsequent graphic output of the totality run will then be synchronized to the "EFLIGHT Clock". This is particularly useful for simulating a real-time

lapse-rate totality run, without the necessity of adjusting the computer's system clock to achieve synchronization with a "simulated" Universal Time.

DISPLAY GRAPHIC OUTPUT FORMAT

The **EFLIGHT** graphical output window is divided into a Map region (left) and a Text region (right). Five clocks in the title bar provide absolute and relative time references. A sample "snapshot", frozen from the graphical output window, is shown in Figure 11 one instant of time.

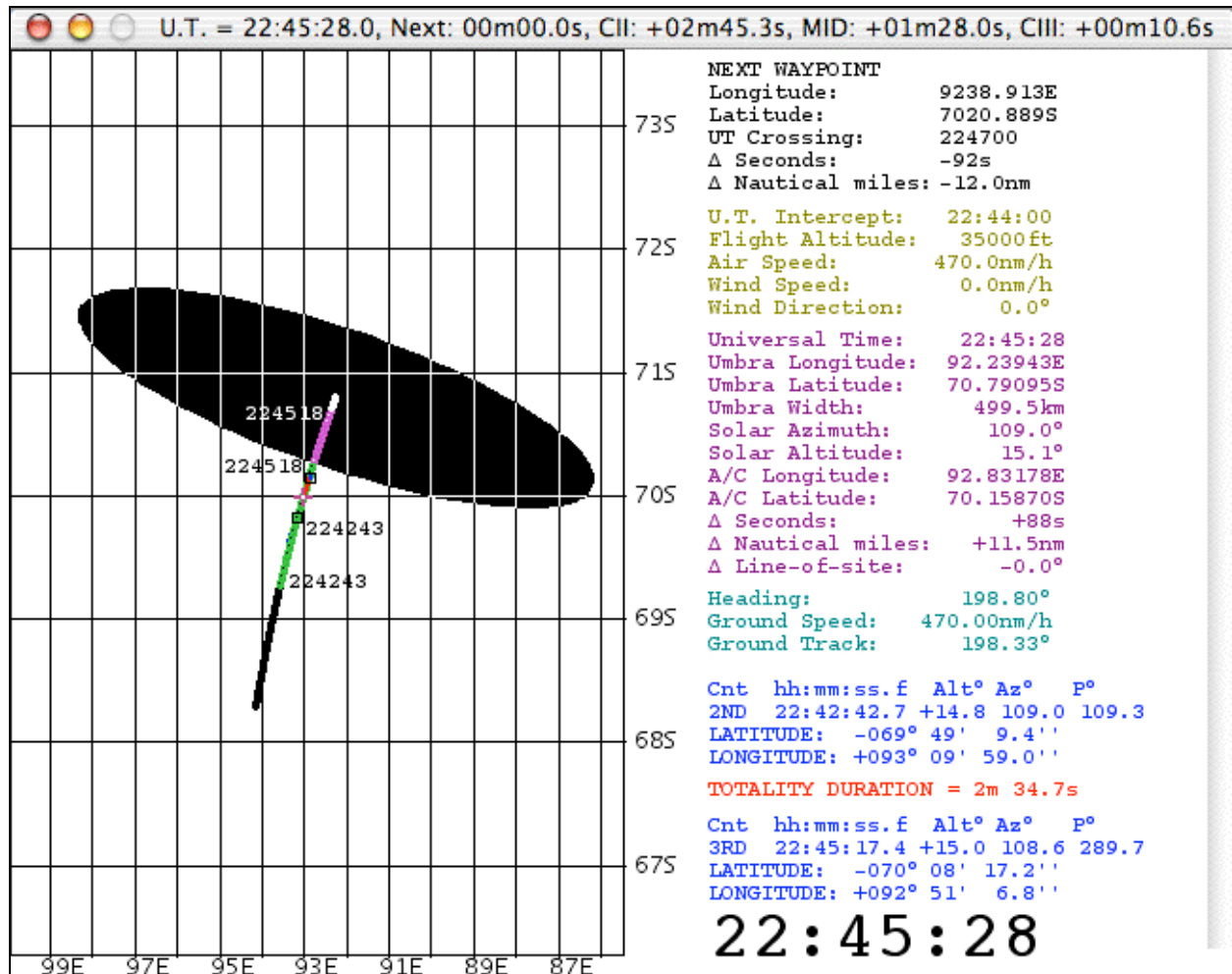


Figure 11. EFLIGHT totality run graphical output window

This particular example, corresponds a Universal Time of 22:45:27 UT (as indicated both by the large UT clock at the bottom right of the text region, and at the left of the graphics window title bar. In the title bar are four other incrementing clocks which indicate:

- Ⓜ1) Next how long until the next graphics display update
- Ⓜ2) CII how long until (or since) Contact II
- Ⓜ3) MID how long until (or since) mid-eclipse
- Ⓜ4) CIII how long until (or since) Contact III

Map Region (Left):

The intersection of the shadow center with the geoidal surface (see [note on geodetic reference](#)) at the altitude of the aircraft (i.e., the path of centerline at flight-altitude) is shown along with the path of the aircraft, and an approximate representation umbral shadow on a Mercator projection.

Umbral Shadow: The projection of the umbral shadow, showing the instantaneous region on the at-altitude geoidal surface in totality, sweeps across the map region over the duration of the totality run. As a visualization tool, and for display purposes only, the shadow boundary is approximated as an ellipsoid. Shadow axis (and aircraft) positions, contact times, and other numerical quantities are derived with high precision independent of this approximation. The shadow boundary display approximation loses high fidelity at very low solar elevations (e.g., near sunrise or sunset), but this does not affect the efficacy of any of the more rigorously computed quantities which are displayed and tabulated. The umbral shadow projection is not shown for instants of time (also near sunrise and sunset) when the eclipse is non-central (i.e., when the apex of the shadow cone does not reach the flight-level elevated geoidal surface).

Mid-Eclipse Intercept Point: The location of the point of mid-eclipse intercept, where the aircraft is instantaneously co-axially located in the umbral shadow (on centerline), is marked by a [purple cross +](#).

Centerline: The instantaneous positions of the center of the lunar umbra (defined by the lunar center of figure, not the dynamical center of mass) are shown for each instant of time throughout the totality run. As time progresses the locus of these points discretely maps out the centerline of the path of totality. At any instant of time each point (retained in sequential frames) is displayed as a black dot (inverted as white when a point is immersed in the umbra). Points along the centerline through which the umbra passes while totality is visible from the aircraft as it moves along its track are circumscribed in green (or purple when within the umbra). In the example above, which is for a time very soon after sunrise, the non-linearity of the point spacing due to the deceleration of the shadow in projection on the geoidal surface is readily apparent.

Aircraft Ground Track: The ground track of the aircraft is shown throughout the totality run. Before the aircraft enters the umbra (or, more generally as the umbra overtakes the aircraft [except in some circumstances for supersonic flight]) these positions are marked in dark blue (inverted to yellow as the umbra later passes over). Points along the ground track corresponding to times when the aircraft is flying through the umbral shadow are marked in light blue (inverted to red when those points are outside of the umbra).

Contact Times: The instants and locations of second and third contact, marking the start and end of totality as seen from the moving aircraft, are annotated along the aircraft ground track as the aircraft passes those points. The locations are marked by small black squares (inverted to yellow with the passage of the umbra over those positions) along with the Universal Times at which the contacts occur. In addition, the points along the centerline corresponding to the instants when the aircraft enters and exits the umbra are also annotated with the Universal Times of those instants.

Notes on Contact Times:

- 1) Due to the approximate nature of the representation of the shadow ellipsoid, the shadow boundary, at the instants of contact may not appear exactly at the aircraft location by may be discrepant by a few kilometers.
- 2) Contact times and circumstances are determined by interpolative fitting of discrete values associated with the temporal spacing (intervals) selected. When the Display Time Resolution is set to 1s, the internal uncertainty (not including the limb profile, changes in delta-T, etc.) in the times of contact on the order of a few tenths of a second seconds, but takes longer to compute. If a large area is mapped at low temporal resolution (e.g., 30 seconds), contact times (and totality duration) will not be as accurately computed. Such coarse temporal granularities are useful for evaluating centerline flight options over large positions of the path of totality, but must be re-evaluated with a finer time resolution after selection.
- 3) For a moving platform, times of contacts are estimated numerically (to the noted precision), not analytically, by computing the local circumstances for each discrete point along the (at-altitude) ground track. A determination is then made, for each instant of U.T., as to which side of the umbral boundary the aircraft is on. When two contiguous instantaneous positions straddle a boundary crossing the instant (and hence position) of the boundary crossing is estimated by interpolation, and local circumstances are then computed for those points.

Text Region (Right):

To the right of the map region, the circumstances of the eclipse and the aircraft flight parameters are updated at each incrementing time step, presented in five color coded sections:

1. (Black, Top). NEXT WAYPOINT.

Longitude of the next targeted waypoint
 Latitude of the next targeted waypoint
 UT Crossing = UT at which aircraft will reach next waypoint
 □ Seconds = Time in seconds until next waypoint crossing
 □ Nautical Miles = Distance in Nm to next waypoint crossing

2. (Light green). Static echo of input parameters.

Universal Time of Mid-Eclipse Intercept (HH:MM:SS).
 Flight Altitude (in feet) above MEan Sea Level
 True Air Speed in user-specified units
 Wind Speed in user-specified units specified

3. (Purple). Dynamic. Umbra Path Circumstances & AC Positions.

Current Universal Time
 Longitude of the center of the umbra at flight altitude
 Latitude of the center of the umbra at flight altitude
 Umbral shadow width in km (see UMBRAPHILE for definition)
 Solar Azimuth (degrees E of N) on centerline at current UT
 Solar Altitude (degrees) on centerline wrt astronomical horizon
 Aircraft Longitude
 Aircraft Latitude
 Time in seconds to/from mid-eclipse intercept
 Flight distance (ground track) in Nm to mid-eclipse intercept
 Deviation of LOS angle to sun orthogonal to flight direction

4 (Light Blue). Dynamic/Static. Instantaneous Flight Vector.

Aircraft Heading

Aircraft Ground Speed in units specified for Air/Wind Speed

Ground Track Direction

5. (Dark Blue/Red). Static. Contact Information.

U.T. of second and third contacts

Solar Altitude {elevation} (degrees) above the astronomical horizon at contacts

Position angles of contacts (east from north) along solar limb

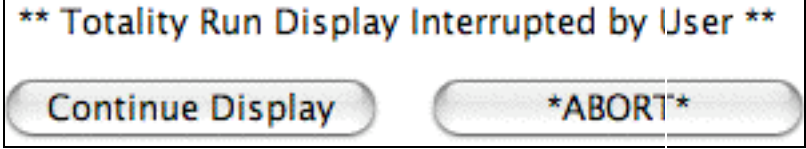
Aircraft Position (Latitude/Longitude) at contact times

Duration of Totality (minutes and seconds)

5) INTERRUPT(ing a Totality Run Graphic Display)

To interrupt a **TOTALITY RUN** in progress, select the **INTERRUPT** item from the **EFLIGHT03** menu.

Accidentally interrupting a totality run would be very undesirable in flight! Therefore, after an INTERRUPT is requested a confirmatory dialog (Figure 11) will be presented which must be positively acknowledged before the temporally incrementing graphical display is terminated. Clicking [**Continue Display**] will resume the graphical output. If **RT SIMULATION** was selected in the Flight Definition dialog, the display will advance (to compensate for the time lapse during the temporary suspension) to time re-synchronize the graphical output).



11. INTERRUPT Confirmation Dialog

Clicking [***ABORT***] will terminate the graphical display at the current time step. The graphical display window will remain opened (but can be closed if desired), and the clocks in the title bar will freeze at the moment of the interrupt request.

Sample Dynamic Graphical Display

The **EFLIGHT** dynamic graphic display for a 40,000 ft., 22h23m15s UT intercept of the 23 November 2003 total eclipse may be viewed, as an example, to gain a better understanding of the graphical output format. This "movie" was actually generated with an earlier version of **EFLIGHT** (and thus the graphics display is somewhat different) but is shown to illustrate the concept.

[View/Download the sample EFLIGHT Display as a QuickTime Movie \(4.2Mbytes\)](#)

[View/Download the sample EFLIGHT Display as an animated .gif file \(4.0 Mbytes\)](#)

This example is "played" at 4-times the real-time rate at four one-second updates per second of elapsed time.

In this example an intercept profile spanning (-1.5, +2) minutes centered on 22:23:15s U.T, (shortly after sunrise) is developed to fly a course of constant heading over those three minutes to have the sun "straight out" the aircraft sun-side windows at mid-eclipse. As the animation/movie opens at 22:21:45 U.T. the center of umbra has not yet "touched down" 40,000 ft. above the surface of the Earth. Hence, as the first time steps are displayed only the changing location of the aircraft (and the intercept point) is annotated in the map region, and parametric values associated with the umbra in the text region are blanked out. Eight seconds later at 22:21:53 U.T. the umbra-center reaches 40,000 feet above the surface of the Earth, and that location is marked inside the approximate projection of the shadow which then appears. At that point the aircraft is 10.7 nautical miles from mid-eclipse intercept which it will reach in 82 seconds by flying a true heading of 209.6° at a ground speed of 470 nM/hr (with no wind). Second contact has been computed to occur 17 seconds later at 22:22:10 U.T. Over those 17 seconds, as the shadow moves to the south east, the umbral projection on the geoidal surface decelerates as can be seen by the decreasing point spacing along the developing centerline. At 22:22:10 U.T. the position of the aircraft is annotated (as is the corresponding point along the centerline) as totality begins for in situ observers. The evolving path of the eclipse, and flight of the aircraft can then be followed through mid-eclipse, to third contact, and beyond to the end of the requested time window.

6) COMPUTE COURSE

For developing a time constrained pre-totally run intercept flight plan, **EFLIGHT** provides a facility for easy producing the time-critical routing to approach the first point on the **TOTALITY RUN** from some pre-run location. This is done through the **COMPUTE COURSE** menu item and dialog as shown in Figure 12.

<input checked="" type="radio"/> DECIMAL DEGREES	<input type="radio"/> km
<input type="radio"/> DDMSS	<input type="radio"/> mi
	<input checked="" type="radio"/> nm
	LATITUDE LONGITUDE
P1:	<input type="text" value="-37.7"/> <input type="text" value="+144.95"/>
P2:	<input type="text" value="-69.60717"/> <input type="text" value="+93.37175"/>
COURSE= +204.4075	
DISTANCE= 2505.798 nm	
Number of Points	<input type="text" value="10"/>
U.T. of Last	<input type="text" value="224100.0"/>
Ground Speed (/hr)	<input type="text" value="470.0"/>
<input type="checkbox"/> Export Table	
Click [ENTER] Before Generating Table	
<input type="button" value="ENTER"/>	<input type="button" value="CANCEL"/> <input type="button" value="TABLE"/>

Figure 12. COMPUTE COURSE dialog.

COMPUTE COURSE will produce a set of time-ordered way points to be followed to get from point 1 (P1) to point 2 (P2). As a matter of convenience, after generating a **TOTALITY RUN**, the aircraft coordinates of the first point for the run is transferred to P2 in the **COMPUTE COURSE** dialog. The time at which the aircraft *must* be at P2 is the time corresponding to the first point in the totality run, and is the U.T. for the last point (U.T. of Last) in the **COMPUTE COURSE** waypoint table. This time is also automatically transferred to the **COMPUTE COURSE** dialog after generating a **TOTALITY RUN**. It is likely desirable to approach this point sometime prior to the critical "must be at" time, to allow for any unanticipated delays in route, and to execute a hold pattern at that position until the requisite release time. The U.T. Last field may be entered manually, to build in as long a hold time as desired. These co-ordinate fields, as well, may be manually over-written by entering whatever coordinates are desired. Coordinates may be entered in decimal degrees or DDMSS format as specified.

After the coordinates are entered *first* click the [ENTER] button. This will update the **COURSE =** and **DISTANCE =** values shown in the dialog. The course is the great circle heading in degrees from P1 to P2 (flown from P1), and the distance is in the units that were selected (upper right). To generate a table of intermediate way points (e.g., figure 13), then click [TABLE].

Great Circle Track and Penumbra Crossing: 22:41:00

Mid-Eclipse Intercept: 224400 U.T., Totality Run Start at -3 minutes

U.T. Start = 171938.5 Course = +204.1381° Ground Speed = 470.0nm/hr
 U.T. End = 224100.0 Distance = 2517.302nm Number of Segments = 10

1ST Contact = 21:43:18 4TH Contact = xxxxxx.x

HMMSS	Latitude	Longitude	Latitude	Longitude	Course	NEXTnm	TOTALnm	Elapsed	Remaining
171938.5	37 42.0S	144 57.0E	37.7000S	144.9500E	204.14	249.52		000000.0	052121.5
175129.8	41 32.4S	142 53.3E	41.5402S	142.8889E	205.67	249.15	249.52	003151.2	044930.2
182318.1	45 20.5S	140 35.7E	45.3422S	140.5944E	207.54	248.68	498.67	010339.6	041741.9
185502.9	49 05.7S	138 00.0W	49.0952S	138.0006E	209.86	248.07	747.35	013524.4	034557.1
192643.0	52 47.0S	135 01.1E	52.7837S	135.0184E	212.78	247.27	995.42	020704.5	031417.0
195817.0	56 23.2S	131 31.4E	56.3862S	131.5239E	216.52	246.25	1242.69	023838.5	024243.0
202943.2	59 52.2S	127 20.4E	59.8704S	127.3397E	221.44	245.04	1488.94	031004.7	021116.8
210100.1	63 11.1S	122 12.1E	63.1857S	122.2015E	228.17	243.93	1733.98	034121.6	013959.9
213208.5	66 14.7S	115 41.7E	66.2455S	115.6952E	238.05	244.23	1977.92	041230.0	010851.5
220319.2	68 52.8S	107 06.3E	68.8797S	107.1058E	255.11	227.77	2222.14	044340.7	003740.8
223223.8	70 37.0S	94 48.5E	70.6162S	094.8086E	255.11	67.39	2449.91	051245.3	000836.2
224100.0	69 36.4S	93 22.3E	69.6072S	093.3718E			2517.30	052121.5	000000.0

KB: Non-APL

Figure 13. COMPUTE COURSE Text Window output.

The title bar of the text window containing the COMPUTE COURSE table indicates the Universal Time at the completion of the computed track from P1 to P2.

The first line of the table header gives the U.T. of mid-eclipse intercept, and the time before that intercept (in minutes) the Totality run begins.

The second line gives the U.T. the aircraft would have to leave P1 and the great circle heading to fly, given the ground speed (as computed based upon earlier airspeed and wind information entered in the **COMPUTE TOTALITY RUN** Flight Definition dialog).

The third line gives the arrival time at the end of the great circle track (and start of the totality run), and the total distance flown, as the number of segments in the table which then follows.

IF the aircraft crosses the penumbral shadow boundary along the track from P1 to P2 the estimated crossing time, which is the instant of 1st or 4th contact is indicated (as appropriate).

For each instant of Universal Time in the table, the Latitude and Longitude of the aircraft is given (in two formats as shown), as well as the course from that point (in degrees), and the distance to the next segment is indicated. Also shown is the running distance and time from start, and time remaining to the end of the course.

COMPUTE COURSE *critically* seams together the approach to the Totality Run and the start of the Totality Run. For the actual Croydon/QANTAS flight, the plans developed have the aircraft reaching a "hold" point ahead of the start of the totality run before the critical time (by nominally 15 - 20 minutes) to allow for any unforeseen in-flight delays.

7) QUIT

To terminate **EFLIGHT** select QUIT from the **EFLIGHT** menu.

Summary

This page is intended to briefly introduce you to **EFLIGHT**, and to give you an idea as to how it was used to develop baseline flight scenarios for the Croydon/QANTAS and TravelQuest(Sky & Telescope)/LanChile Antarctic eclipse overflights. This is not intended to be a fully comprehensive user's guide, since I suspect the number of potential users (other than myself) are rather small. However, if you consider yourself a smitten umbraphile, I suspect the **EFLIGHT** concept might be of interest to you (particularly if you have read this far down the page). So... now you know.

What's next? **EFLIGHT** continues to evolve to support the 23 Nov 2003 eclipse flight planning and execution. Indeed, baseline test scenarios developed with EFLIGHT were recently tested in a three-hour session in the QANTAS B747-400 simulator in Sydney by QANTAS Senior Check Captain John Dennis (who will be the pilot in command for the Croydon/QANTAS flight) as he dry ran the eclipse flight. As a result of that simulator session, a few "tweaks" were made to the user and display interfaces (which are now as documented here), to make its real-time use in conjunction with the requirements of the 747 Flight Management System more seamless.

If you are seriously contemplating an airborne observation of this, or of a future eclipse and would like to take advantage of **EFLIGHT** as a planning and in situ execution tool then [contact me](#). Unlike [UMBRAPHILE](#), however, I am not freely giving **EFLIGHT** away, primarily because to use it properly requires a fair amount of detailed familiarity. I would, however, be very happy to work with like-minded eclipse chasers in defining and planning future airborne eclipse observations using **EFLIGHT** - maybe in exchange for an opportunity observe and fly with you into the bottom of the lunar umbral cone.

Glenn Schneider

Initially posted: 15 February 2002

Updated: 26 July 2003

APPENDIX C

Baseline Totality Run Waypoint Tables for QANTAS/Croydon Eclipse Flight

*Note: The tables contained in Appendix C are formatted for broadside (landscape) printing and display. They are NOT included in this MS Word source document, but may be found in the accompanying documents: **QANTAS_APPENDIX_C.{doc/pdf}**. The content of those tables is discussed here.*

The baseline waypoint tables detail a two parameter (aircraft altitude and *ground* speed) family of possible "Totality Runs", for a mid-eclipse intercept of 22:44:00 U.T. only. The intended use of these tables is for pre-eclipse planning and evaluation by QANTAS flight operations. The tables assume NO variations in family parameters for a given scenario and, thus, are non-optimal for direct implementation flight.

Flight altitudes from 32,000 ft to 38,000 ft above MSL in increments of 1,000 ft, and ground speeds of 420 nM/hr to 520 nM/hr in increments of 10 nM/hr are considered.

The totality run is flown as 4 discrete but contiguous flight segments defined by five waypoints to be loaded into the Boeing 747-400 FMS.

Each possible totality run spans 20 minutes in time, beginning 15 minutes before mid-eclipse (waypoint A), and ending 5 minutes after mid-eclipse (waypoint B). Alternatively, using the same tables, one could begin the totality run 10 minutes before mid-eclipse (waypoint B), though this leave less time and margin for initial on-track course corrections.

The waypoints along the totality run very closely *approximate* a linear track, but in detail deviate from a true geodesic curve by a very small amount. (necessarily to optimize the line-of-site angle to the Sun at mid-eclipse and throughout the totality run)

The waypoints are uniformly spaced in time with a temporal spacing of 5 minutes (300 seconds). Hence, for a fixed ground speed, the distance between successive waypoints is constant (e.g., 39.2 nM @ 470 nM/hour).

The five waypoints are defined (and were chosen) as follows:

A: Totality Run Track Insertion Point. Mid-eclipse minus 15 minutes (22:29:00 UT). The aircraft should complete any heading alignment maneuvers prior to intercepting this point as close to 22:29:00 UT as possible. Any residual errors from initial approach in both heading and position should be nulled out (or minimized) in segment AB.

B: Totality Run Critical Start Point. Mid-eclipse minus 10 minutes (22:34:00 UT). Aircraft flight vector, as defined by waypoints, should be stable at and after crossing this point. Necessary Course and speed corrections due to windage only during segment BC.

C: Final Ingress Target Point. Mid-eclipse minus 5 minutes (22:39:00 UT). Last waypoint before lunar shadow overtakes aircraft. Contact II ~ 3m 43s after crossing waypoint C. Differential course and speed corrections due to windage only during segment CD.

D: Mid-Eclipse. (22:44:00 UT) Aircraft coincident with the instantaneous position of the center of the lunar shadow. Heading = instantaneous solar azimuth + 90 degrees. Contact III ~ 1m 17s after crossing waypoint D.

E: Totality Run Termination. Mid-eclipse plus 5 minutes (22:49:00 UT). Contact III plus 3m 43s.

Following crossing of waypoint E, at the discretion of the pilot in command, the aircraft may continue on a heading of 197° to allow additional viewing of the early phases of egress, the recession of the umbral shadow, and atmospheric color/brightness gradient effects.

This discrete parametric grid of waypoint tables were generated with EFLIGHT 2003 X version 2.0.0*, and is expected to sufficiently tile the parameter space in flight altitude and ground speed required for evaluation purposes of a 22:44 U.T. intercept as baselined for the QANTAS/Croydon eclipse flight. Other tables can (and will) be generated as needed in future planning, or in situ during the flight.

* See Appendix A

APPENDIX D: Glenn Schneider - Curriculum Vita / Resume

Contact:

Steward Observatory	Home:	7742 E. Oakwood Circle
933 N. Cherry Avenue		Tucson, AZ 85750 USA
University of Arizona	Phone:	1-520-296-5296
Tucson, Arizona 85721 USA	Fax:	1-775-924-5422
Phone: 1-520-621-5865	e-mail:	gschneid@mac.com
Fax: 1-520-621-1891		
e-mail: gschneider@as.arizona.edu		
URL: http://nicmosis.as.arizona.edu:8000/		

Education:

Ph.D. in astronomy, August 1985, University of Florida.

B.S. in physics (cum laude), June 1976, New York Institute of Technology.

Employment History (Chronology):

1994-Present: Steward Observatory, University of Arizona
Associate Astronomer &
NICMOS Project Instrument Scientist

1985-1994: Computer Sciences Corporation
Space Telescope Science Institute
Operations Astronomer
Staff Scientist (1992-1994)
Senior Member of the Technical Staff (1988-1992)
Member Technical Staff-A (1985-1988)

1987-1989: Catonsville Community College
Adjunct faculty

1984-1985: Department of Astronomy, University of Florida
Research assistant

1982-1984: Space Astronomy Laboratory, University of Florida
Research assistant

1978-1982: Department of Astronomy, University of Florida
Teaching/Research assistant

1977-1980: Warner Computer Systems, Inc.
APL technical consultant

1976-1977: Warner Computer Systems, Inc.
APL technical analyst

Present Position: Steward Observatory, University of Arizona**Associate Astronomer & Instrument Scientist for the Near Infrared Camera and Multi-Object Spectrometer Project at the University of Arizona**

SYNOPSIS. For nine years, as the NICMOS Project Instrument Scientist at Steward Observatory, I have seen the instrument through its final design, implementation, integration and test, on-orbit calibration, science/operational, and post-mission recommissioning phases while taking on a number of pivotal leading and supervisory responsibilities. The compression of our guaranteed time observing (GTO) program into a single HST observing cycle posed many unanticipated challenges in maintaining coherence in data calibration and analysis, as well as in reformulating many aspects of our investigations. In accomplishing the completion of those programs I worked with and for the NICMOS science team in many diverse aspects of planning (and replanning) our GTO observations while continuing to serve as the project's primary technical interface to the Space Telescope Science Institute, Goddard Space Flight Center's (GSFC) codes 440, 441 and 512. During the pre-launch and commissioning phases of the NICMOS mission I worked closely with Ball Aerospace's integrated product teams leading to the successful emergence of NICMOS as a facilities class instrument in the Hubble Space Telescope. My responsibilities have included frequent interaction with the aforementioned agencies in the development and implementation of ground and flight systems, procedures, software, interfaces, calibration methodologies and data, on-orbit test procedures and detailed observing proposals to assure that the primary goals of NICMOS science programs were carried to successful conclusion. Concomitant with these activities were my daily interactions with our software and technical support staff lending guidance and supervision on a diverse variety of team-support tasks. With the advent and rapid acquisition of NICMOS data, particularly in the coronagraphic programs which were enabled in the later phases of HST Cycle 7, my labors were successfully divided between science and functional support (see publication list).

With the successful completion of the GTO observations, I have continued in collaboration with many of the NICMOS science team members in the reduction, calibration, analysis, and interpretation of data amassed during our accelerated observing program. I have actively lead, participated in, and contributed to a significant number of scientific investigations in collaboration with other team members and "outside" investigators, including follow-up programs to our NICMOS projects utilizing resources and facilities at Keck, Palomar, IRTF, Lick, here at Steward Observatory, and other HST instruments. On the research front, I also have served in a de facto leading role for the NICMOS Environments of Nearby Stars Group (and advocate for the continuance of NICMOS coronagraphic and high-contrast imaging and spectrophotometric science).

With the cessation of on-orbit operations, since the instruments' early cryogen depletion, a significant portion of my efforts have been devoted not only to post-mission calibration, characterization, and performance evaluation while supporting a large integrated systems engineering effort readying NICMOS for "resurrection" with the installation of an active cooling system (recently successfully installed on HST servicing mission 3B). In that regard, I lead test teams both at the NICMOS detector laboratory at Steward Observatory and at the EMI/EMC facility at GSFC in conducting comprehensive experiments with a flight spare array replicating

the on-orbit performance of the NICMOS detectors replicating on-orbit thermal conditions and integrated with the to-be-flown NICMOS cooling system. During this era my responsibilities extended to detailed end-to-end instrumental systems evaluations, in collaboration with GSFC and STScI personnel, in preparation for both serving mission (SM)3B and the Cycle 11 SM observatory verification (SMOV) program to follow, including leading the planning and analyses of key elements of the NICMOS recommissioning activities (e.g., detector performance, optical alignment and focus, target acquisition reactivation, etc.), which have recently been completed successfully as a precursor to re-enabling Cycle 11 near-IR science on HST.

Science Team Support. The complex (and often confusing) process of developing viable observational strategies for carrying out astronomical investigations with HST did not relax as the mission evolved. Indeed, the rapid acceleration of the program demanded a closer and more detailed level of involvement in the monitoring, execution, and evaluation of our observations than if our programs were played out over three cycles as originally envisioned. This was exacerbated with a new instrument whose characteristics were changing on short time scales. Dealing with this required vigilance in shepherding many of our needs through the "system", which I had attacked with success. I attribute this to the fact that I have worked closely with numerous aspects of HST operations and planning for fourteen years and, through trial-by-fire, have gained first-hand intimate knowledge of NICMOS. Together these have afforded me the ability to assist team members in dealing with unrelenting minutiae associated with the implementation of their scientific programs. I have seen this as a pivotal aspect of this position, and accordingly such activities have occupied much of my attention. Thus, I have directed my efforts toward making NICMOS as scientifically a productive instrument as possible (often, in the face of seemingly adversarial external forces to be overcome). The emergence of the continuing stream of NICMOS GTO and follow-on science, is demonstrative of the success in working toward that goal.

Instrument Operations, Data Reduction, Processing and Analysis. I continue to work on a daily basis as the UofA/IDT technical interface with STScI's PRESTO, CMD/ESB, Systems Engineering and NICMOS Instrument support groups. In addition to identifying and resolving proposal planning, execution, and instrument operations problems, I have recommended specific strategies to improve on-orbit efficiency, and instrument stability and calibratability to expand the scope of NICMOS capabilities both in cycle 7, and now through Cycle 11 and beyond. Such recommendations resulted from an expenditure of a considerable effort to understanding the on-orbit characteristics of NICMOS (as interfaced with HST) enabling the extraction of photometric and astrometric data from NICMOS images unbiased of systematic effects to the greatest extent possible. In doing so I have iterated many times with both STScI's NICMOS support group, and our own software and database personnel, in improving calibration reference files as well as reduction and analysis software. I have also worked with STScI in planning for, and analyzing the results of the NICMOS warm-up in light of the concerns of an independent science review committee established by NASA, and for post SM-3B science operations. I have taken an active role in coordinating the "warm up anomaly" testing in our detector lab based upon test goals discussed with STScI and have assumed the responsibility for supervising our test team and laboratory personnel.

NICMOS Environments of Nearby Stars (EONS) Programs. A significant portion of the NICMOS GTO time was dedicated to obtaining observations leading to a better understanding the physical processes inherent in the formation of stellar systems possibly harboring substellar components. Is there a continuity of companion objects across the sub-stellar mass-spectrum bridging the stellar main-sequence into the planetary domain? In what sort of local environments will such objects form, and at what distances will they be found from their primaries? How is this biased by the characteristics of the primary and companion objects and those of the circumstellar regions? What implications will the discovery and characterization of such objects have for our understanding of formation mechanisms? These fundamental questions embody the goals of the EONS investigations. In seeking to shed light on these, and related questions I had assumed a de facto leading role in overseeing and organizing the implementation of those programs. I have played a pivotal part in development the NICMOS coronagraphic capability, which is essential to the success of these programs. After overcoming initial hardware and software difficulties, the NICMOS coronagraph has been proven itself as a unique instrumental and scientific resource by enabling the imaging of faint spatially unresolved objects, and diffuse extended features in the close proximity to very bright sources. Post-calibration image processing and reconstruction methodologies, which I have developed, uniquely suited to NICMOS coronagraphic data, are being used by the EONS team in the analysis and interpretation of our observations and are bearing exceptional fruit. Our recent discoveries of sculpted debris disks around young stars (seen in reflected light) may be explained by the dynamical influences exerted by unseen planetary-mass companions. A significant number of candidate objects, seen in our coronagraphic images, may indeed provide a stepping-stone to answer the questions already posited. Multi-wavelength follow-up observations to our NICMOS EONS programs have been approved and carried out as HST/ GO programs and, where applicable, using ground-based facilities.

Pre-launch Instrument Calibration (SLTV, RAS/HOMS, EMI/EMC testing). To explore and evaluate the operating characteristics of NICMOS, I took a leading role in the definition, execution and analysis of the NICMOS pre-launch calibration programs at BATC. Working closely during round-the-clock shifts with BATC project management, hardware, S/W, and test team personnel I investigated anomalous behaviors which led to both a better understanding of the instrument, and changes in the methods and philosophy of instrument operation.

HST Systems Level Integration, Test, and Verification (VEST, STOCC), SOGS/SPSS. The exercise of pre-deployment validation of a new HST science instrument required extensive sub-system and integrated tests to be run with both ground and flight hardware and software. I supported these efforts by defining, contributing to, and participating in numerous ground system and functional tests (unit and end-to-end) and simulations. To validate the command generation capability of the HST ground system for NICMOS, and the response to those command requests by the instrument, I worked with STScI ESB/Commanding personnel in creating test proposals, calendars, and SMS's used in these series of tests and subsequently analyzed resulting image data and engineering telemetry. I worked with BATC I&T and MOSES SI/SE personnel in reviewing Real-Time command and operations procedures required for these tests. In addition, I monitored and evaluated the ground system and instrument behavior during test execution, and participated in real-time hardware and software anomaly analysis and resolution.

SM-2 and SM-3B On-Orbit Instrument Checkout (AT/FT Planning and Execution). I was an active member of the SM-2 and 3B flight preparation and operations teams to define and improve procedures used during the NICMOS on-orbit installation and checkout. I participated in the requirements definition and detailed implementation of the NICMOS portions of the Servicing Mission Integrated Timeline, Command Plan, and on-orbit Aliveness and Functional tests, and developed evaluation/acceptance criteria and real-time analysis S/W for the latter. This included on-console at the STOCC for all SMGTs, JISs, and during the mission as the IDT science support representative.

SM OV 2 and 3B Program Planning, Implementation, and Analysis. I served (and continue to serve) as the UofA/IDT representative and technical lead for the NICMOS Servicing Mission Observatory Verification program. This engendered defining the NICMOS SMOV plan and requirements in concert with HST and STScI project management. As Principle Investigator for many of the SMOV programs (and co-I on most others), I developed and implemented on-orbit check-out, engineering, and calibration proposals, operations procedures and analysis plans in consultation and association with STScI and the BATC I&T teams. Post-launch I worked extensively at STScI to support near-RT analysis and a dynamically evolving and changing SMOV program in light of unexpected instrumental problems and anomalies.

Research Activities - Hubble Space Telescope Science Programs

AWARD/FUNDING SUMMARY AS P.I. AT STEWARD OBSERVATORY

Title: A Search for Stellar Duplicity and Variability
from FGS Guide Star Acquisitions and Guiding Data
Program: HST-AR-05811
Start Date: 04/01/1995 Closeout Date: 10/15/1999
Funds Awarded: \$37,346

Title: Direct Imaging of a Circumstellar Disk: Beta
Pictoris, a Case Study
Program: HST-GO-06058
Start Date: 09/01/1995 Closeout Date: 09/30/1999
Funds Awarded: \$9,921

Title: Near-IR Photometry of a Candidate companion to
Proxima Centauri
Program: HST-GO-07847
Start Date: 11/01/1998 Closeout Date: 06/25/2001
Funds Awarded: \$11,296

Title: Confirmation and Characterization of Brown Dwarfs
and Giant Planets from NICMOS 7226/7667
Program: HST-GO-08176
Start Date: 09/01/1999 Closeout Date: 08/31/2003 (active)
Funds Awarded: \$69,092

Title: Duplicity and Variability in HST Guide Stars –
An FGS Serendipitous Survey
Program: HST-AR-08730
Start Date: 02/01/1999 Closeout Date: 07/18/2002
Funds Awarded: \$39,615

Title: Imaging and Spectroscopy of Dusty Circumstellar
Disks
Program: HST-GO-08624
Start Date: 11/01/2000 Closeout Date: 10/31/2003 (active)
Funds Awarded: \$32,2738

Title: Enabling Coronagraphic Polarimetry with NICMOS
Program: HST-GO-09768
Start Date: 09/01/2003 (observations pending HST Schedule)
Closeout Date: 08/31/2004
Funds Awarded: Program Approved, \$32,375 requested

ON-GOING/ACTIVE HST PROGRAM SUMMARIES (GO, GTO, AR)

Imaging and Spectroscopy of Dusty Circumstellar Disks, co-I/GO (8624): Understanding the properties and evolution of dusty disks in the circumstellar environments of young stars is a key element in furthering our concepts of the formation mechanisms of extra-solar planetary systems. In the past year, the advent of NICMOS and STIS coronagraphy has given rise to the first reflected light imaging, other than for β Pictoris, of dusty circumstellar disks with spatially resolved morphological structures. NICMOS has taken a first step in imaging these new disks, elucidating their geometries, morphologies, and bulk photometric properties, while increasing the number of such known systems from one to half a dozen. These dusty disks vary in physical size by over two orders of magnitude and exhibit radial anisotropies in their brightness distributions which may be indicative of dynamical confinement or sculpting of the disk particles by unseen planetary bodies. STIS follow-on imaging and spectroscopy are needed to provide further insight into the nature of the disk particles. With spectra, we will measure the albedo of the disk dust and search for complex molecules and water ice. With coronagraphic images, we are investigating the scattering phase function and hence the composition of the disk dust as well as measuring the disk sizes and shapes with high precision. Such observations are of fundamental importance in establishing the physical basis for emergent theories of disk evolution and planet-building.

Imaging the Dust Disk around Epsilon Eridani, co-I/GO (9037): Epsilon Eridani is the closest star to the Sun, around which a planet has been discovered. An asymmetric dust disk around the star has been detected in sub-millimeter observations. The clumps in the disk have been interpreted as resulting from resonant interaction, and the pattern has been predicted to revolve around star at a rate of $\sim 0.7^\circ$ per year. Our first epoch observations of the dust disk with STIS will be followed up in subsequent cycles. These observations will not only reveal what may be the first extra-solar Kuiper belt, but will also provide a crucial step in the development of observational techniques that can determine the presence and properties of planets, from the visible morphology of the disks around the parent stars.

Confirmation and Characterization of Brown Dwarfs and Giant Planets from NICMOS 7226/7227, P.I./GO (8176): A selected candidate list of 74 stars was observed using the NICMOS coronagraph at 1.6 microns. We have found eight objects as faint as $H = 20$, up to 13 magnitudes fainter than their primaries with separations less than 5", which have very high probabilities of being true substellar companions. For the stars in our sample this covers minimum physical separations of 1.2-50 AU at the inner spatial detection limit. The lower mass limit depends on age, distance, and spectral type, but is as low as $3-5 M_{\text{Jupiter}}$ for many of our targets. Spectrographic observations are essential to characterize the physical nature of the putative companions we have discovered. Our observations address fundamental questions such as: Is there a continuity of objects across the substellar mass spectrum bridging the main sequence to planetary objects? What is their frequency of occurrence? At what distances are they found from their primaries? And, what implications will these discoveries have for our understanding of stellar/planetary formation mechanisms?

A Search for Low Mass/Sub-Luminous Companions to M-Stars, P.I./GTO (7227): Knowledge of stellar and sub-stellar masses and luminosities at and below the $\sim 0.08 M_{\text{sun}}$

Hydrogen burning limit is of fundamental importance in many inter-related areas such as probing the end of the stellar mass function, the theory of stellar evolution, the end of the main sequence, the galactic missing mass, age and evolution. Yet, this transition region in the mass spectrum of objects between low-mass stars and giant planets is poorly understood and ill-observed. Until very recently, with the discovery of the Brown Dwarf companion to GL 229, the very existence of such objects remained in the conjectural realm. To make further progress in low end of the mass distribution function, additional objects first must be found. Potentially fruitful hunting-grounds to search for such transitional objects using NICMOS, in parameter spaces which do not overlap with ground-based capabilities, are as companions to M-dwarfs which are: Nearby ($d < 6$ pc) and spectral types later than $\sim M3.5$; Young ($\leq 10^8$ years) and at $d \leq 25$ pc.; and Spectrally the latest known ($> M8.5$). This investigation carries out a coronagraphic imaging program aimed at discovering such objects. Once located one may address such fundamental questions such as: Is there a continuity of objects across the sub-stellar mass spectrum bridging the main sequence to planetary objects? At what frequency will they be found? At what distances will they be found from their primaries? And, what implications will this have for our understanding of stellar/planetary formation mechanisms?

A Search for Massive Jupiters. Co-I/GTO (7226): We use NICMOS to search for massive planets around nearby, young main sequence stars. We use Camera 2 and the coronagraph to search from 0.3" to 3" at the wavelength band of 1.4–1.8 μm (F160W) which corresponds to strong emission in the brown dwarf candidates GL 229B and GD 165B as well as to strong reflections in Jupiter and Titan. Because of the extreme youth of these objects, any low-mass brown dwarf and planetary companions will still be in a higher luminosity phase and thus easily detectable. The lower mass limit depends on age, distance, and spectral type, but can be as low as 3–5 M_{Jupiter} for targets in our sample. Follow-up observations of candidate companions will provide proof of true physical association with the primary. The typical separations observable with NICMOS are near the empirical maximum in the binary distribution of stars (~ 20 –40 AU), which also corresponds to the mean distance of the giant planets in our own solar system.

Dust Disks Around Main Sequence Stars. Co-I/GTO (7233): We observe a selection of mostly main sequence stars which have (a) $\tau_{\text{dust}} > 10^{-3}$ or (b) other characteristics that suggest the presence of circumstellar dust disks. The observations will be made with the coronagraph to minimize the effects of glare from the bright central star. Our primary filter is the F160W, although the science does not depend critically on the choice of filter. We dither the pointing by means of a spacecraft roll for best background subtraction. As a primary objective, all images will be examined for the presence of dust disks. An important secondary objective is a search of all images for possible brown dwarfs or high-mass planets. If detections are made, additional observations will be attempted to characterize the physical properties of those objects found.

(Spectroscopy and) Polarimetry of the β Pictoris Disk, Co-I/GTO (7248): Little is known about the β Pictoris disk within 50 AU of the central star. No near-infrared spectrophotometry or polarimetry exists within this dynamically interesting region, which is about the same size as our own solar system and which appears to be relatively depleted of disk material. We do grism spectroscopy and polarimetry of the disk from within 5 AU of the star to the outer limits of the disk as determined by the total integration time. Such observations will help to characterize the chemical and physical properties of the disk particles as a function of their distance from the star.

By moving the star close to the edge of the coronagraphic hole, we will probe the disk as close as 2 AU from the star.

Near-IR Photometry of Candidate Companion to Proxima Centauri, Co-Investigator/GO (7847): We have identified what may be a low luminosity companion to the closest star to the Sun, Proxima Centauri (dist. ~ 1.3 pc). The candidate companion was discovered during Cycle 6 using the FOS as a coronagraphic camera (Program ID: 6059). The candidate companion is within $\sim 0.4''$ of Proxima Cen, too close to be detected with WFPC2. It's apparent motion on the sky is similar to the parallactic motion of Proxima Cen, which makes its effect upon Proxima Cen difficult to detect with FGS astrometry. If the candidate companion is in orbit about Proxima Cen, modeling indicates the orbital period would be ~ 1 year. The ideal time to image the companion is during the latter half of the year (September-December) when it is farthest from Proxima Cen. We use HST NICMOS camera 1 observations to confirm the companion, determine IR magnitudes, and to constrain orbital elements. Due to the small spatial separation and large magnitude differences, direct image detection of the companion cannot be done from the ground.

Recently Completed / Published Investigations

(Spectrophotometry and) High Resolution Imaging of HD 98800, Co-I/GTO (7232): HD98800, located nearby at a probable distance of 20 pc, is a unique stellar system consisting of two K7-V stars separated by 0.8 arcsec. Composite optical spectra show Li absorption, indicating pre-main sequence age, and IRAS found extraordinarily large amounts 165 K dust emission, suggesting the presence of a possible "zodiacal dust cloud in the making". NICMOS Camera 1 was used in five bands from 0.9 to 2.0 μm to make fully saturated MULTIACCUM images that can be deconvolved to separate the two well resolved bright stars from light scattered by the dust. If the dust cloud is sustained by a recently "failed planet" it should also be resolved at about 0.2" diameter. Comparisons of dust properties such as (a) scattered to emitted light, (b) color of scattered light and (c) size of the dust cloud can then be made with corresponding data for the solar system. Repeated observations enabled the dynamics of the systems to be established.

Spectrophotometry and Imaging of Pluto and Charon, Co-Investigator/GTO (7223): Detailed spectra of the individual members of the Pluto-Charon system are not known. Different surface compositions are suggested by some evidence obtained when the two were undergoing mutual eclipses. Grism spectrophotometry will provide a direct comparison of the surface materials of each member of the double planet. Dispersion should be approximately normal to a line joining Pluto and Charon, and observations should be made in four separate orbital positions in order to differentiate surface variations on the two objects. Charon's leading (in Charon's orbital direction) trailing, Pluto-facing and non-Pluto-facing hemispheres will be observed. **A Search for Stellar**

Duplicity and Variability from FGS Guide Star Acquisition and Guiding Data, P.I./AR (5811): The HST Fine Guidance Sensors (FGS) have the unique astrometric capabilities of revealing faint companions in close binary systems. They can measure their position angles and component separations, with a precision which exceeds that which is possible using any ground

based techniques for primary components in the magnitude range $V = 9$ to 14. In addition, the intensity data which are produced by the FGS PMTs provide high precision relative photometry on rapid time scales. In mid Cycle 4 a new telemetry format was adopted for all normal operations which serendipitously provide these astrometric and photometric data at 40 Hz for all guide star acquisitions and periods of active guiding. This program is conducting a systematic examination of these data, obtained from the HST engineering telemetry, to perform a search for stellar duplicity to determine the incidence of doubles in the Guide Star Catalog as well as the separations, position angles, and relative brightnesses of the individual stellar components in such binaries. The light curves and power spectra of the photometric data are also being reduced and analyzed in an effort to perform an astroseismological survey of these stars, as well as look for and characterize variations due to other intrinsic mechanisms.

Duplicity and Variability in HST Guide Stars - An FGS Serendipitous Survey, P.I./AR (8370) - A continuation of 5811.

High Spatial Resolution Imaging of Comet Hale-Bopp (C/1995 O1), Co-Investigator/GTO (7240): Comet Hale-Bopp provides an excellent opportunity for high-resolution imaging of the nuclear and inner coma regions of a bright comet. Observations in the near- infrared offer high contrast between the coma and nucleus since reflected sunlight/fluorescence are at a minimum and thermal emission from coma dust is important only at longer wavelengths. The primary scientific objective is to probe the production of gas and dust in the inner coma very near the nucleus and to monitor the emergence and activity of jet structures. Images obtained in/out of known spectral features due to water ice (2.04 μm), gaseous water (1.9 microns), and C2 (1.9–2.0 μm). If a nuclear rotation period has been determined prior to the time of the observations, this will be used to devise an optimal strategy for measuring the nuclear brightness as a function of rotational phase. There also exists the possibility that the nucleus will fragment or undergo enormous flaring, in which cases it will be important to have repeated observations. Unfortunately, the comet's solar elongation angle was below HST limits in March '97 when it is closest to earth. Observations were obtained as soon as possible after the comet emerged from solar avoidance between 25–27 August. Parallel imaging with STIS required the maximum allowable roll angle of $+5^\circ$.

Pyramid Imaging of Circumstellar Material About Nearby Stars, Co-I/GO (6469): Observations obtained with the Infrared Astronomical Satellite (IRAS) have indicated that many of the nearby, bright stars have an infrared excess from a comparable sample of stars of similar spectral types. This IR excess has been attributed to emission from heated dust. Despite the definite presence of circumstellar dust for approximately one third of the nearby A-F stars, attempts at imaging candidates (other than β Pictoris) have yielded null results. Failure to detect these disks likely stemmed from the extreme differences in surface brightness between the central star and any surrounding disk material, as well as the evolution of such disks over time. The WFPC-2 pyramid edge will be used in a pseudo-coronagraphic manner in an attempt to detect and characterize circumstellar material about seven nearby stars which may have β Pic like disks as inferred from their IR excesses. Theories of planet formation based on nebular cosmogonies postulate that planets form during the contraction of a rotating gas cloud. Accretion of dust particles and volatile ices form planetesimals, the larger of which sweep up material from the nebula and grow into proto-planets. If disks are normal by-products during contraction of a

nebular cloud and are common place, then what are their compositions, grain size, and how do they evolve with time? If disks exist about other stars, where are they? One would expect the inner regions of a disk close to the central star to experience rapid evolution through sublimation of ices and clearing of the disk through collisions with bigger bodies or particles falling into the central star, while the evolution of the outer disk regions will proceed at a much slower rate. The scenario involving infall and evaporation of comet-like bodies has been used to explain the presence of circumstellar dust about β Pic. If this model for processing of the disk material is valid, this process could be expected to occur about other stars, which in turn could explain the reported large infrared excesses for many of the nearby stars.

Direct Imaging of the Circumstellar Disk of β Pictoris, Co-Investigator/GO (6058): The unique imaging capabilities of WFPC2 onboard HST have been used to obtain psuedo-coronagraphic high resolution images of the dust disk ($V = 16$ mag/arcsec²) about β Pictoris ($V=3.9$). With these, more accurate photometry of the disk may be obtained, the reported morphology (gaps) and variable disk thickness may be investigated along with the optical properties and size distribution of the circumstellar dust in detail. The β Pic circumstellar disk currently represents the best candidate for an extrasolar proto-planetary system or possibly a massive Kuiper belt. It is the only circumstellar disk that has been detected with ground-based coronagraphy. Accurate photometry is essential to determine the properties of the disk. Smith and Terrile reported an $r^{4.3}$ power law for the light distribution within the disk, while Artymowicz, Burrows, and Paresce reported a slightly less steep distribution of $r^{3.6}$. Their disk model suggested an upper limit for the tilt between the plane of the disk and the line of sight of 14° , with a mixture of grain sizes (radii between 1 and 20 μ m) to explain the light scattering in the visible and IR images. Telesco et al. suggest the inner disk extends 50 AU (3 arcsec) from β Pictoris based on 10 and 20 μ m observations, while Backman, Gillett, and Witteborn suggest the disk reaches inward to between 1 and 30 AU from IRTF observations. R-band images obtained with the Johns Hopkins University Adaptive Optics Coronagraph indicate an inverted asymmetry in the light distribution within 100 AU and imply a change in the scattering properties of the grains or a lower grain density in this region of the disk. There are possibly three processes involved in moving grains about in the disk: radiation pressure blowing small grains away from the vicinity of β Pictoris, Poynting-Roberston drag causing small grains to spiral into β Pictoris, and hidden planetary bodies perturbing the dust disk. Backman and Paresce suggest that planetary-like bodies orbiting at the inner boundaries of infrared-emitting regions could explain the central voids in circumstellar disks, while the outer disk could represent a Kuiper belt, a remnant of planetary formation. This program will shed some light on whether this model is correct and will help to answer the question "Do disks represent success or failure modes in planet building?"

HST/NICMOS Early Release Observation Programs

See Publication List for: NGC 2264 IRS [ref 10R], Orion 114-426 Silhouette Disk, [ref 11R], Nuclei of ARP 220, [ref 12R] Nucleus of IC 5063, [ref 13R], OMC-1, [ref 14R], and CRL 2688, [ref 15R].

HST/NICMOS Instrument Calibration and Engineering Programs

GO/CAL (CYCLE 12):

Enabling Coronagraphic Polarimetry with NICMOS, co-Investigator, 9768

SMOV3B (CYCLE 11):

NICMOS Filter Wheel/Mechanisms Functional Test, Principal Investigator, 8944

NICMOS SMOV3B Transfer Function Verification Test,
Principal Investigator, 8976

NICMOS Optimum Coronagraphic Focus Determination,
Principal Investigator, 8979

NICMOS Mode-2 Target Acquisition Test, Principal Investigator, 8983

NICMOS Coronagraphic Performance Assessment, Principal Investigator, 8984

NICMOS Coronagraphic Performance Assessment Part 1
Principal Investigator, 8984

NICMOS Coronagraphic Performance Assessment 1, Principal Investigator, 9693

NICMOS Filter Wheel/Mechanisms Functional Test,
Principal Investigator, 8944

SMOV2 (CYCLE 7):

NICMOS Internal Parallel (Electrical Cross Talk) Test,
Principal Investigator, 7032 & 7136

NICMOS Field Offset Mirror Operations Test, co-Investigator, 8973

NICMOS Pupil Alignment ("Tilt") Test, co-Investigator, 9645

NICMOS Transfer Function Verification Test, Principal Investigator, 7037

NICMOS Target Acquisition Test Principal Investigator, 7038

NICMOS Coarse Optical Alignment, Principal Investigator, 7041 & 7150

NICMOS Fine Optical Alignment, Principal Investigator, 7042

NICMOS Focus Monitor, Principal Investigator, 7043

NICMOS Coronagraphic Performance Verification, Principal Investigator, 7052

NICMOS Pre-Alignment Check-out, Principal Investigator, 7134

NICMOS Intermediate Focus/Alignment, Principal Investigator, 7135

NICMOS Coronagraphic Hole Monitor, Principal Investigator, 7154

NICMOS Revised Field Offset Mechanism Test, Principal Investigator, 7156

NICMOS Optimum Coronagraphic Focus Determination,
Principal Investigator, 7157

NICMOS Coronagraphic Hole Location Test, Principal Investigator, 7808 & 7924

Previous Employment/Positions

Computer Sciences Corporation - Space Telescope Science Institute

Served for nine years as an Operations Astronomer in the Operations, and Science and Engineering Support Divisions of the Space Telescope Science Institute (STScI).

General Responsibilities: Appointed as a member of the Instruction Management (Science Instrument Commanding) Task Group. Designed, implemented, and tested science commanding instructions (for the Science Planning and Scheduling System (SPSS) /Science Commanding Subsystem of the Hubble Space Telescope (HST) Science Operations Ground System (SOGS)). Developed operational procedures, science instrument command groups and supportive file structures for inclusion in the HST Project Data Base (PDB) for operating the Wide Field/Planetary Camera (WFPC), Fine Guidance Sensors (for astrometric science), Wide Field/Planetary Camera-2 (WFPC-2), as well as other Science Instruments and spacecraft subsystems. Participated in the validation of low-level and atomic command constructs tested during Assembly and Verification for all HST Science Instruments. Adapted these for use in the SOGS and Payload Operations Control Center/Applications Support Software (PASS) ground systems. Designed and built higher-level logic to control the use of these command structures. Developed requirements and software interfaces for driving flow-down control logic from a structured Proposal Management Data Base (PMDB) and calendars of time-ordered events. Developed and implemented reconfiguration instructions and associated table driven logic to allow for automatic setup and transitioning of the science instruments to/from various defined operational states. Generated detailed requirements for the proposal Transformation software. Contributed to the Proposal Instructions and Instrument Handbooks.

WFPC-2: In preparation for the on-orbit installation of WFPC-2 I was responsible for working with the WFPC-2 Science, Instrument Development, and Integration & Test teams in both pre-launch testing of the hardware and ground system software. This effort engendered my gaining specific first-hand knowledge of the workings of the instrument by participating a series of ground system, thermal vacuum, hardware, and system functional tests. This also encompassed my participation in the SMOV Proposal Implementation Team, where I assisted in defining the overall implementation requirements for WFPC-2 SMOV and performed detailed reviews of those proposals, implementation plans, calendars and SMSs. I supported the HST servicing mission by first participating in a number of pre-launch simulation and training exercises, and later performing real-time monitoring, data collection and evaluation during the servicing mission itself.

* **Command Development:** Developed ground system command constructs which were required for testing and operating the WFPC-2, both pre-launch and on-orbit. The scope of this activity was sufficiently broad so my involvement went beyond just creating executable procedures and software, but lent itself to my active participation in and contributing to development efforts across many groups at STScI, MOSES, JPL and the WFPC-2 Science team. The need to be responsive to ever changing demands and requirements were met as the operational methodologies and instrument characteristics evolved and/or solidified during the long series of ground tests which occurred during this period.

* **SLTV:** Actively participated in the WFPC-2 System Level Thermal Vacuum Test and Instrument Calibration as the STScI/Science Commanding on-site representative at JPL. Worked closely during round-the-clock shifts with JPL hardware, S/W, instrument and science team personnel. Defined, modified, executed and analyzed real-time tests designed to explore and evaluate the operating characteristics of the WFPC-2. Investigated anomalous behaviors which led to both a better understanding of the instrument, and to changes in the methods of operating and commanding it. Information and knowledge which was acquired during SLTV was transferred to other STScI and WFPC-2 project personnel and incorporated in the implementation of the WFPC-2 stored command instructions. Worked with the ESB WFPC-2 engineer on obtaining the SLTV engineering data in a timely manner from JPL and porting it to a data archive at STScI.

* **Tests and Simulations:** The exercise of pre-deployment validation of a new science instrument required extensive sub-system and integrated tests to be run both ground and flight hardware and software. Supported this effort by contributing to, and participating in the various ground system and functional tests, discrete simulations, and joint integrated simulations. In particular, to validate the command generation capability of the ground system for the WFPC-2, and the response to those command requests by the instrument, I created test proposals, calendars, and SMS's used in these series of tests. Worked with the MOSES SI personnel in reviewing new Real-Time command procedures which were needed in support of these tests, and the servicing mission. Monitored the ground system and instrument behavior during execution, and participated in real-time hardware and software anomaly analysis and resolution. Worked with other members of flight team, through the real-time simulations, to define and improve procedures to be used during the servicing mission.

* **Servicing Mission:** Assisted in preparing and configuring the ESB/commanding work site at the OSS facility by setting up the hardware and S/W interfaces to permit real-time analysis on the engineering data. Developed adjunct data collection and analysis tools, and set up automated data reduction and network transfer processes. During the Servicing mission participated in the 24-hour commanding shift coverage - monitoring instrument and spacecraft sub-system changeouts. Key subsystem parameters were watched and trended and, for the WFPC-1 and 2 in particular, thermal considerations were constantly addressed and discussed with other project elements - as were contaminant and other issues of real-time concern.

* **Servicing Mission Observatory Verification:** Served as a member of the SMOV Proposal Implementation Team. Worked on the development and implementation of engineering, calibration, and ERO proposals for the SMOV program in consultation and association with the WFPC-2 IDT and I&T teams. Identified the need for special commanding and/or structuring of the PMDB through a series of proposal implementation meetings and reviews. Built, tested, and delivered non-standard commanding for early operations of the WFPC-2. Test, and later flight, calendars and SMS's were microscopically reviewed for any deficiencies - and proposals reworked as needed when problems were found. During execution monitored all first-time operations, and was prepared to respond to unanticipated anomalies. Throughout this era worked with the WFPC-2 engineering and science teams (JPL and SIB) to evaluate the instrument's performance and provided information on commanding related activities to these

groups through regular calibration and team meetings. Worked with the with the WFPC-2 science team to develop a coherent transition plan to the Cycle 4 calibration program. Currently working with both the IDT and STSci/SIB on defining additional on-orbit and laboratory tests to better characterize and calibrate the photometric performance of the instrument, based upon on-orbit data.

WFPC-1: Participated in the planning and implementation of all ground system simulation, throughput, and vehicle tests. Prepared special commanding instructions and structured inputs for the WFPC-1. Worked on the production, and reviewed the content, of the WFPC-1 commanding on Calendars, Science Mission Specifications (SMS's) and command loads used in all Ground System Tests (GST's). Supported real-time monitoring of the use of the WFPC-1 during integrated system GST's. Participated in the development and implementation of many special WFPC engineering operations, procedures, and instructions including the implementation and redefinition of the UV Flood, CCD decontamination procedures, integration of the NASA Standard Spacecraft Computer-1 (NSSC-1) soft safing capability and Real Time safing recovery plans. Worked with GSFC Flight Software Group (Code 512) in defining special executive flight software requirements, and WFPC/NSSC-1 command interfaces for special operations. Provided "emergency" support for unplanned safing events, WFPC instrument anomalies and unforeseen Target of Opportunity observations. Worked with WFPC engineers (both contractor and in-house) and representatives of the Telescope Instrument Branch in assessing general post-launch instrument performance, operational use trending, and in response to directed technical inquiries. Worked with the WFPC on-site Instrument Development Team (IDT) representative to help assure that new WFPC command capabilities (not originally specified by the IDT) were implemented and assimilated into the ground systems in a faithful and efficient manner. Created new instructions, data base definitions, and supported ground testing and validation of these capabilities, which included: the on-board WFPC Idle checking (and bay 5 temperature regulation) software; suppression of CCD erasure following preflashes; issuance of autoerase commands following pyramid rotations; allowing Kspot, Bias, Dark and exposures to be preflashed and CR-Splitting of the latter two; and permitting subsetted CCD reads with efficient use of the onboard tape recorder and/or communications downlink.

Observatory Verification: Member of the Orbital Verification (OV) Planning/Implementation Team. Reviewed and identified technical problems in OV proposals. Developed solutions to these problems and worked with the IDTs to reach closure on those items. Wrote detailed implementation plans used by personnel involved in defining science and engineering objectives, planning and scheduling of activities, developing, testing, and implementing special science instrument and spacecraft subsystem commanding, identifying required real-time support, and supplying specific database constructs and entries needed to carry out these proposals.

FGS/Astrometry: Served, for two years, as the STSci Operation Division's technical representative to the Space Telescope Astrometry Team. Worked with the team on defining baseline functional astrometric requirements. Developed command constructs and procedural logic for using the HST Fine Guidance Sensors (FGS's) to carry out astrometric science observations, and special Orbital Verification focus and alignment tests. Oversaw the creation of test calendars, and SMS's used to validate FGS commanding. Participated in ground-system simulation, unit level hardware, and vehicle testing of Fine Guidance Electronics/FGS

commanding. Developed and provided software to assist in the Real-Time analysis of FGS, Pointing Control System and Optical Telescope Assembly telemetry during early on-orbit operations.

Operations Support: Reviewed proposals scheduled for execution and resulting commanding on flight SMS's. Participated in iterative SMS analysis/rerun cycling during the OV, SMOV, Science Verification epochs, and Science Assessment and Early Return Observations. Uncovered and reported numerous problems, developed and offered solutions to SPSS, User Support and Science Planning Branches (SPB) as appropriate. Worked with SPSS personnel on fixing many problems related to improper PMDB population or proposal structure, and interpreting PASS mission scheduler and command loader products. Often consulted with the proposer (directly or through SPB) to recommend proposal changes to enable his/her scientific or engineering goals to be accomplished when the proposal itself was improperly or incompletely specified. Developed many software tools which were provided to various branches of the Operations and Systems Engineering divisions to assist in validating the integrity of transformation products, the PMDB, and flight SMS's and to facilitate engineering data analysis.

HST/WFPC (1 & 2) Instrument Calibration and Engineering Programs

WFPC-2 SOFA Partial Stepping Test, Co-Investigator

WFPC K-Spot Reflectivity Test, Principle Investigator

WFPC Calibration: UV Flood Test, Co-Investigator

WFPC Calibration: UV Grism Test, Co-Investigator

WFPC Light-Pipe Throughput Test, Co-Investigator

Department of Astronomy - University of Florida

South Pole Telescope: Designed, implemented and tested the firmware program for the automated operation of the University of Florida's multi-color photometric South Pole Telescope. Developed process control, data acquisition and calibration management software. Assisted in telescope, photometer, and control system mechanical and electronic design, fabrication, and telescope calibration. Performed instrument installation, photometric calibration and operational field check at the Amundsen-Scott South Pole Station. Performed instrument anomaly analysis during observing season. Returned to the South Pole for post-season instrument performance evaluation and engineering diagnostics. Reduced and analyzed photometric data as part of a quantitative site survey program, as well as astronomical studies of \square Velorum and HR 2554. This work was supported by National Science Foundation grants DPP 82-17830 and DPP 84-14128.

Additional Instrumental Work: Designed, fabricated, and installed a new Cassagrain light baffle and offset guiding systems for the RHO 76 cm. telescope. Designed and built a multi-channel digital data acquisition system to be used by several photometric instruments. Redesigned and put into working service a 3-color flare star photometer. Designed and constructed coelostat fed flash spectrograph employing a U.T.-synchronous high speed camera

used for obtaining time resolved spectra of the solar chromosphere and inner corona during the inner tangential contacts of solar eclipses. Interfaced an Ebert-Faste scanning spectrograph to a new microprocessor based control system, and used this system to determine the size of the H-Alpha emission region of several B-emission (shell) stars, including Zeta Tauri. Performed maintenance and repairs on Alvin Clark 20 cm. refractor and Celestron telescopes.

Space Astronomy Laboratory - University of Florida

Giotto/Halley Optical Probe Experiment: Ground System data acquisition and real-time analysis S/W lead for (multi-channel photo-polarimeter employing a MAMA detector) flown on the European Space Agency's Giotto Mission to Halley's Comet. Designed, developed and programmed ground support equipment and real-time spacecraft simulator. Assisted in optical calibration, electronic circuit board design, fabrication, and calibration of engineering and flight model units. Performed flight unit engineering checkout during spacecraft/payload Assembly & Verification at British Aerospace. Worked with project mission planners and scientists at the European Space Agency (Noordwijk, Netherlands) and Service d'Aeronomie-Centre National de la Recherche Scientifique (Paris, France) on many payload interface and operational issues.

Additional Instrumental Work: Specified, designed, and programmed a microcomputer interface for an optical vignetting table constructed to perform photometric and radiometric calibration of spacecraft instrumentation as part of a collaborative project between the Space Astronomy Laboratory and Ruhr-Universitat, Bereich Extraterrestrische Physik (Bochum, W. Germany).

Warner Computer Systems, Inc.

APL Technical Consultant: Maintained public and development system workspace libraries. Wrote system specific application functions and integrated them into the libraries. Developed plotting/graphics display software for Tektronix, Versatek, and Diablo/Spintronic devices. Supervised creation of documentation of APL software libraries by technical writing staff.

APL Technical Analyst: Developed turn-key end-user directed software systems. Products created included software for econometrics forecasting, statistical analysis, laser/resonant-cavity design, message and packet switching, and inventory and process control. Conducted APL programming classes and handled technical inquires from time-sharing clients.

Other Research Activities - (Completed)

Dissertation Research, Department of Astronomy, University of Florida: The observation and analysis of lunar occultations. A systematic program of fast photometric observations of lunar occultations was carried out to measure stellar diameters, obtain better astrometric positions of stars, search for previously unsuspected stellar duplicity and provide fundamental data for the determination of time based on corrections and checks to the lunar theory. Fast

photometric data acquisition instrumentation was designed and developed to carry out a systematic study of selected stellar targets which were occulted by the moon. New numerical techniques for data reduction and analysis, including the introduction of probabilistic constraints into a non-linear least-squares differential-correction model fitting process, were investigated and implemented. Physical parameters (including diameters) for many stars and stellar systems were successfully determined. Chairman: Dr. John P. Oliver. (e.g., see: Dissertation Abstract [ref 7R] or Program Summary [ref 8R])

Asteroidal Photometry: Initiated a collaborative program of multi-color asteroidal photometry and fast photometric observations of asteroidal occultations of stars to determine the size, shape and density of selected minor planets, and to search for asteroidal duplicity. Designed and constructed portable photoelectric photometers, electrometer amplifiers, time-code converters and digital data acquisition electronics for remote-site observations. Deployable field stations were used for independent observations, and in conjunction with observations made at Rosemary Hill Observatory (RHO) and other fixed observatory sites. Profiles, diameters, and densities, as well as other physical and photometric properties of many asteroids were determined, including Nemausa, Pallas, and Ceres. This program was conducted under a grant from the University of Florida's Division of Sponsored Research. (e.g., see work on: (51) Nemausa [ref 3R] Ceres, [ref 4R], and Pallas [ref 7R])

Numerical Modeling of White Dwarf Stars: Developed a computational model for investigating dynamical instabilities in the structure of white dwarf stars of varying chemical compositions, ionic partitions and central densities, applicable over a wide range of partial and total degeneracy regimes. The model included such effects as Coulomb interactions between electrons and nucleons, inverse beta decays, the effects of the general theory of relativity on the condition on hydrostatic equilibrium (local and global), stellar rotation, mass accretion in binary systems and interactions with external magnetic fields. This work was supported by a grant from Warner Computer Systems, Inc. (e.g., see: "Astrophysical APL - Diamonds in the Sky" [ref 2P])

Polar Atmospheric / Climatological Research: The integrity of the synoptic meteorological record of the South Pole is important both to the continuing effort to understand the climatology of the Antarctic Plateau, and to a number of interdisciplinary studies aimed at discovering the details of the mechanism responsible for the depletion of upper atmospheric ozone. An analysis of the nighttime synoptic meteorological record from the South Pole station was undertaken, and a systematic error in the sky cover observations was discovered. As a result it was determined that the seasonal variations in sky cover, as inferred from these observations, are not nearly as significant as previously believed. This project was partially supported under National Science Foundation grant DPP 86-14550. Grant funds are currently being sought from NSF/DPP and NOAA to deploy an automated instrument at the South Pole to measure variations in the nighttime atmospheric turbidity to detect the conditions which are a precursor to the formation of polar stratospheric clouds, which can lead to the onset of ozone reduction. (e.g., see: "Systematic Error in the Synoptic Sky Cover Record of the South Pole" [ref 6R]).

See Publication List for [ref]erences.

Teaching Experience

Taught laboratory and lecture sections of introductory astronomy (at U.F. and CCC); general astronomy for astronomy majors, astronomical techniques, digital electronics (at U.F.); computer programming with APL (at WCS); and a seminar series on APL programming for physical sciences (at U.F.). Planned, supervised and evaluated exercises in astronomy, data manipulation and analysis, instrumentation, and photographic and photoelectric photometry.

Observing Experience

Hubble Space Telescope:

Near Infrared Camera & Multi-Object Spectrometer

Wide Field/Planetary Camera (1 & 2)

Fine Guidance Sensors

Space Telescope Imaging Spectrograph

Heinrick Hertz Sub-Millimeter Telescope

Palomar/PHARO Adaptive Optics System

Data Analysis/Reduction from Keck-II and Lick {NGS+LGS} AO Systems and IRTF

76, 45, and 40 cm. reflecting telescopes

A wide range of small fixed, and portable optical telescopes

Multi-color differential photometry of eclipsing and intrinsic variables

Fast photometry of lunar and asteroidal occultations

Photography with hypersensitized plates

Plate reduction with iris photometer and microdensitometer

Solar chromospheric/inner coronal spectroscopy and polarimetry

Computer Experience

Hardware, Mainframes/WorkStations Operating Systems: VAX 11/750, 11/780, 8600, 8800, Alphas (VMS); Sun SparcStations (Solaris 2.4+); Xerox 6/7/9 and 560 systems (CP-V, UTS, BPM); IBM 360, 370, 3033N, 3081, 3094 and 4341 (OS/VS, MVS); DEC 20 (TOPS); Ahmdal 470/V6; Harris 500; PDP-11/34; Data General Nova

Hardware, Micros/PC's: Rockwell AIM-65 and RM-65 systems; Apple Macintosh (MacOS, all flavors 6.0—10.2.6); Apple II, II+, IIe; HP-85a; MCM 700; Commodore Pet, SX-64, and SP-9000; IBM 5100, 5110, and Pc

Software: APL, IDL, FORTH, BASIC, 6502, 6800 and RCA 1802 machine and assembly languages, many special purpose application programs, data analysis packages, graphics and plotting software (e.g. TRANSFORM, KALEIDAGRAPH, PHOTOSHOP), Systems utility functions and development software.

Professional Society Membership

International Astronomical Union

American Astronomical Society

SPIE (International Society for Optical Engineering)

American Association for the Advancement of Science

Association for Computing Machinery (SIGAPL)

International Occultation Timers Association

Honors and Awards

ASTRONOMICAL SOCIETY OF THE PACIFIC - Maria and Eric Muhlmann Award for 2003
(NICMOS IDT)

NASA/GSFC - Science Leadership Award

SPACE TELESCOPE SCIENCE INSTITUTE - Individual Achievement Award

NASA - Public Service Achievement Award (HST Orbital Verification)

NASA - Achievement Award (WFPC-2 Science Team)

NASA - Project Award (HST Program)

NASA - Project Award (HST 1st Servicing Mission)

JET PROPULSION LABORATORY - Wide Field/Planetary Camera II Project Award (SLTV
and Calibration)

NASA/GSFC - Achievement Award (HST 1st Servicing Mission WFPC-2 Development and
Delivery)

NASA/GSFC - Achievement Award (HST 1st Servicing Mission Integration & Test)

NASA/GSFC - Achievement Award (HST 1st Servicing Mission Observatory Verification)

NASA/GSFC - Achievement Award (HST NSSC-1 FSW, Mission Ops, Engineering Support,
IDT)

NASA/GSFC - "Special Act" Award (HST Continuous Process Improvement Team)

NASA/GSFC - Certificate of Recognition (HST Program)

NYIT - Physics Research Award

NYIT - Silver Medal for Physics Research

Member: Sigma Pi Sigma (National Physics Honor Society)

Recent Public/Community Service

Hubble Space Telescope Post-SM4 Scientific Review Panel
STScI “White Paper” on Ground vs. Space Domains of Observability
NICMOS Dewar Anomaly Review Board

Publications

Refereed Publications (42), Conference Proceedings (32), Meeting Abstracts/Presentations (66), Others (5). See separate Publication List (*Appendix E*).

Additional information: <http://nicmosis.as.arizona.edu:8000/>

APPENDIX E: Glenn Schneider - Publication List

(Chronological order. Links to cited papers on:
<http://nicmosis.as.arizona.edu:8000/Publications.html>)

- [Refereed Journals](#)
- [Conference Proceedings](#)
- [Meeting Abstracts/Presentations](#)
- [Selected NASA/STScI Solicited Reports](#)
- [Other Publications](#)
- [Posters/Display Presentations](#)

Refereed Journals

- 1R. **Schneider, G.**, 1982, "[Fourier Transformation by Harmonic Analysis](#)", *APL Quote Quad*, **11-2**, 19.
- 2R. **Schneider, G.**, 1982, "[Inverse Fourier Transformation](#)", *APL Quote Quad*, **11-2**, 21.
- 3R. Dunham, E. W., Baron, R. L., Conner, S., Dunham, D. W., Dunham, J. B., **Schneider, G.**, Cohen, H. L., Helms, V. T. III, Croom, M., and Safko, J., 1984, "[Results from the Occultation of 14 Piscium by \(51\) Nemausa](#)", *Astronomical Journal*, **89**, 1755.
- 4R. Millis, R. L., Wasserman, L. H., Franz, O. G., Nye, R. A., Oliver, R. C., Kreidl, T. J., Jones, S. E., Hubbard, W., Lebofsky, L., Goff, R., Marcialis, R., Sykes, M., Fecker, J., Hunten, D., Zellner, B., Reitsema, H., **Schneider, G.**, Dunham, E., Klavetter, J., Meech, K., Oswalt, T., Rayfert, J., Strothers, E., Smith, J., Povenmire, H., Jones, B., Kornbluh, D., Reed, L., Izon, K., A'Hearn, M. F., Schnurr, R., Osborn, W., Klemola, A., Rios, M., Sanchez, A., Pirronen, J., Mooney, M., Ireland, S., Parker, D., Douglas, W. T., Beish, J. D., and Leibow, D., 1987, "[The Size, Shape, Density, and Albedo of Ceres from Its Occultation of BD+08 471](#)", *Icarus*, **72**, 507.
- 5R. **Schneider, G.**, 1989, "[The Jurkevich Periodogram](#)", *APL Quote Quad*, **19-2**, 23.
- 6R. **Schneider, G.**, Paluzzi, P., and Oliver, J. P., 1989, "[Systematic Error in the Synoptic Sky Cover Record of the South Pole](#)", *Journal Of Climate*, **2**, 295.
- 7R. Dunham, D. W., Dunham, J. B., A'Hearn, M. F., Schnurr, R., Binzel, R. P., Henry, G., Frueh, M., Evans, D. S., Bowell, E., Wasserman, L. H., Nye, R., Chapman, C. R., Dietz, R. D., Moncivais, C., Douglas, W. T., Parker, D. C., Beish, J. D., Martin, J. O., Monger, D. R., Hubbard, W. B., Reitsema, H. J., Klemola, A. R., Lee, P. D., McNamara, B., Maley, P. D., Manly, P., Markworth, N. L., Nolthenius, R., Povenmire, H., Purrington, R. D., Durham, F. E., Trenary, C., Jenevin, W., Dauns, J., **Schneider, G.**, Schuster, W. J., Moreno, M.A., Guichard, J., Sanchez, G. R., Strothers, E., Taylor, G. E., and Usgren, A., 1989, "[The Size and Shape of \(2\) Pallas from the 1983 Occultation of 1 Vulpeculae](#)", *Publication of the Astronomical Society of the Pacific*, **99**, 1663.
- 8R. **Schneider, G.** and Anderson, C., 1993, "[Rosemary Hill Observatory Lunar Occultation Summary for 1983-1984](#)", *Publication of the Astronomical Society of the Pacific*, **105**, 367.
- 9R. McCarthy, D., Stolovy, S., Kern, S., **Schneider, G.**, Ferro, A., Spinrad, H., Black, J., and Smith, B., 1997, "[NICMOS/HST Post-Perihelion Images of Comet Hale-Bopp in Outburst](#)", *Earth, Moon and Planets*, **78**, 243.
- 10R. Thompson, R.I., Rieke, M., **Schneider, G.**, Hines, D.C., Corbin, M., 1998, "[Initial On-Orbit Performance of NICMOS](#)", *Astrophysical Journal*, **492**, L95.

- 11R. Thompson, R. I., Corbin, M., Young, E., **Schneider, G.**, Rieke, M., 1998, "[NGC 2264 IRS Evidence for Triggered Star Formation](#)", *Astrophysical Journal*, **492**, L177.
- 12R. McCaughrean, M. E., Chen, H., Bally, J., Erickson, E., Rieke M., **Schneider, G.**, Stolovy, S., Thompson, R., Young, E., 1998, "[High-Resolution Near-Infrared Imaging of the Orion 114-426 Silhouette Disk](#)", *Astrophysical Journal*, **492**, L157.
- 13R. Scoville, N. Z., Evans, A. S., Dinshaw, R., Thompson, R., Rieke, M., **Schneider, G.**, Low, F. J., Hines, D., Stobie, B., Becklin, E., and Epps, H., 1998, "[NICMOS Imaging of the Nuclei of ARP 220](#)", *Astrophysical Journal*, **492**, L107.
- 14R. Kulkarni, V. P., Calzetti, L., Bergeron, L., Rieke, M., Axon, D., Skinner, C., Colina, L., Sparks, W., Daou, D., Gilmore, D., Holfeltz, S., MacKenty, J., Noll, K., Ritchie, C., **Schneider, G.**, Schultz, A., Storrs, A., Suchkov, A., and Thompson, R., 1998, "[Unveiling the Hidden Nucleus of IC 5063 with NICMOS](#)", *Astrophysical Journal*, **492**, L121.
- 15R. Stolovy, S. R., Burton, M. G., Erickson, E. F., Kaufman, M. J., Chrysostomou, Young, E. T., Colgan, S., Axon, D.J., Thompson, R.I., Rieke, M.J., and **Schneider, G.**, 1998, "[NICMOS 2 Micron Continuum and H2 Images of OMC-1](#)", *Astrophysical Journal*, **492**, L151.
- 16R. Sahai, R., Hines, D., Kastner, J., Weintraub, D., Trauger, J., Rieke, M., Thompson, R., and **Schneider, G.**, 1998, "[The Structure of the Prototype Bipolar Protoplanetary Nebula CRL 2688 \(Egg Nebula\): Broadband, Polarimetric, and H2 Line Imaging with NICMOS on the Hubble Space Telescope](#)", *Astrophysical Journal*, **492**, L163.
- 17R. Chen, Hua, Bally, J., O'Dell, R.C., McCaughrean, J., Thompson, R., Rieke, M., **Schneider, G.**, and Young, E. T., 1998, "[2.12 Micron Molecular Hydrogen Emission from Circumstellar Disks Embedded in the Orion Nebula](#)", *Astrophysical Journal*, **492**, L173.
- 18R. **Schneider, G.**, Hershey, J. L., Wenz, M. T., 1998, "[Duplicity in HST Guide Stars - FGS Serendipitous Survey Results](#)", *Publication of the Astronomical Society of the Pacific*, **110**, 1012.
- 19R. Thompson, R. I., Storrie-Lombardi, L. J., Weymann, R. J., Rieke, M. J., **Schneider, G.**, Stobie, E., and Lytle, D., 1999, "[NICMOS Observations of the Hubble Deep Field: Observations, Data Reduction, and Galaxy Photometry](#)", *Astronomical Journal*, **117**, 17.
- 20R. Lowrance, P., McCarthy, C., Becklin, E., Zuckerman, B., **Schneider, G.**, Webb, R., Hines, D., Kirkpatrick, J., Koerner, D., Low, F., Meier, R., Rieke, M., Smith, B., Terrile, R., and Thompson, R., 1999, "[A Candidate Substellar Companion to CoD -33°7795 \(TWA5\)](#)", *Astrophysical Journal*, **512**, L69.
- 21R. **Schneider, G.**, Smith, B.A., Becklin, E.E., Koerner, D.W., Meier, R., Hines, D.C., Lowrance, P.J., Terrile, R.J., Thompson, R.I., and Rieke, M., 1999, "[NICMOS Imaging of the HR 4796A Circumstellar Disk](#)", *Astrophysical Journal*, **513**, L127.
- 22R. Dumas, C., Terrile, R. J., Smith, B. A., **Schneider, G.**, Becklin, E., 1999, "[Stability of Neptune's Ring-Arcs In Question](#)", *Nature*, **400**, 733.
- 23R. Low, F. J., Hines, D. C., and **Schneider, G.**, 1999, "[NICMOS Observations of the Pre-Main-Sequence Planetary Debris System HD 98800](#)", *Astrophysical Journal*, **520**, L45.
- 24R. Weinberger, A. J., Becklin, E. E., **Schneider, G.**, Smith, B.A., Lowrance, P. J., Silverstone, M. D., and Zuckerman, B., 1999, "[The Circumstellar Disk of HD 141569 Imaged with NICMOS](#)", *Astrophysical Journal*, **522**, L53.

- 25R. Kulkarni, V. P., Hill, J. M., **Schneider, G.**, Weymann, R. J., Storrie-Lombardi, L. J., Rieke, M. J., Thompson, R. I., and Jannuzi, B., 2000, "[NICMOS Imaging of the Damped Ly- \$\alpha\$ Absorber at \$z = 1.89\$ toward LBQS 1210+1731: Constraints on Size and Star Formation Rate](#)", *Astrophysical Journal*, **536**, 36.
- 26R. Corbin, M. R., Vacca, W. D., O'Neil, E., Thompson, R. I., Rieke, M., and **Schneider, G.**, 2000, "[Photometric Redshifts and Morphologies of Galaxies in the NICMOS Parallel Fields](#)", *Astronomical Journal*, **119**, 1062.
- 27R. Hines, D. C., Schmidt, G. D., and **Schneider, G.**, 2000, "[Analysis of Polarized Light with NICMOS](#)", *Publication of the Astronomical Society of the Pacific*, **112**, 983.
- 28R. Luhman, K. L., Rieke, G. H., Young, E. T., Cotera, Angela, S., Chen, H., Rieke, M. J., **Schneider, G.**, and Thompson, R.I., 1999, "[The Initial Mass Function of Low-Mass Stars and Brown Dwarfs in Young Clusters](#)", *Astronomical Journal*, **540**, 1016.
- 29R. Lowrance, P. J., **Schneider, G.**, Kirkpatrick, J. D., Becklin, E. E., Weinberger, A. J., Zuckerman, B., Plait, P., Malimuth, E. M., Heap, S. R., Schultz, A., Smith, B. A., Terrile, R. J., and Hines, D.C., 2000, "[A Candidate Substellar Companion to HR 7329](#)", *Astrophysical Journal*, **541**, L390.
- 30R. Corbin, M.R., O'Neil, E., Thompson, R.I., Rieke, M.J., and **Schneider, G.**, 2000, "[A Color Analysis of the NICMOS Parallel Image Archive](#)", *Astronomical Journal*, **120**, 1209.
- 31R. **Schneider, G.**, Becklin, E. E., Smith, B. A., Hines, D., Weinberger, A. J., and Silverstone, M., 2001, "[NICMOS Coronagraphic Observations of 55 Cancri](#)", *Astronomical Journal*, **121**, 525.
- 32R. Corbin, M.A., Urban, A., Stobie, E., Thompson, R. I., and **Schneider, G.**, 2001, "[A Multivariate Analysis of Galaxies in the Hubble Deep Field](#)", *Astronomical Journal*, **551**, 23.
- 33R. Dumas, C., Terrile, R. J., Brown, R. H., **Schneider, G.**, and Smith, B. A., 2001, "[HST/NICMOS Spectroscopy of Charon's Leading and Trailing Hemispheres](#)", *Astrophysical Journal*, **121**, 1163.
- 34R. Kulkarni, V. P., Hill, J. M., **Schneider, G.**, Weymann, R. J., Storrie-Lombardi, L. J., Rieke, M. J., Thompson, R.I., and Jannuzi, B., 2001, "[A Search for the Damped Ly- \$\alpha\$ Absorber at \$z= 1.86\$ toward QSO 1244+3443 with NICMOS](#)", *Astrophysical Journal*, **551**, 37.
- 35R. Cotera, A. S., Whitney, B. A., Young, E., Wolff, M. J., Wood, K., Povich, M., **Schneider, G.**, Rieke, M., and Thompson, R., 2001, "[High-resolution Near-Infrared Images and Models of the Circumstellar Disk in HH 30](#)", *Astrophysical Journal*, **556**, 958.
- 36R. Boeker, T., Bacinski, J., Bergeron, L., Calzetti, D., Jones, M., Gilmore, D., Holfeltz, S., Monroe, B., Nota, A., Sosey, M., **Schneider, G.**, O'Neil, E., Hubbard, P., Ferro, A., Barg, I., and Stobie, E., 2001, "[Properties of PACE-I HgCdTe Detectors in Space - the NICMOS Warm-up Monitoring Program](#)", *Publication of the Astronomical Society of the Pacific*, **113**, 859.
- 37R. Weinberger, A.J., Becklin, E. E., **Schneider, G.**, Chaing, E. I., Lowrance, P. J., Silverstone, M., Zuckerman, B., Hines, D. C., and Smith, B. A., 2002, "[Infrared Views of the TW Hya Disk](#)", *Astrophysical Journal*, **566**, 409.
- 38R. Dumas, C., Terrile, R. J., Smith, B. A., and **Schneider, G.**, 2002, "[Astrometry and Near-Infrared Photometry of Neptune's Inner Satellites and Ring-Arcs](#)", *Astronomical Journal*, **123**, 1776.
- 39R. **Schneider, G.**, Wood, K., Silverstone, M., Hines, D.C., Koerner, D. W., Whitney, B. A., Bjorkman, J. E., and Lowrance, P.J., 2002, "[NICMOS Coronagraphic Observations of the GM Aurigae Circumstellar Disk](#)", *Astronomical Journal*, **125**, 1467.

40R. **Schneider, G.**, Pasachoff, J. M., and Golb, L., 2003, "[TRACE Observations of the 15 November 1999 Transit of Mercury and the Black Drop Effect for the 2004 Transit of Venus](#)", *Icarus*, submitted.

41R. **Schneider, G.**, Smith, B. A., Becklin, E. E., Weinberger, A. J., Silverstone, M. J., Hines, D. C., and Lowrance, P. J., 2002, "[STIS Imaging of the HR 4796A Circumstellar Debris Ring](#)", *Astronomical Journal*, in preparation.□

42R. Low, F., **Schneider, G.**, Neugebauer, G., "[NICMOS Imaging of the ULIRG MRK 231](#)", *Astrophysical Journal*, in preparation.

Conference Proceedings

1P. Chen, K-Y, Esper, J., McNeill, J. D., Oliver, J. P., **Schneider, G.**, and Wood, F. B., 1986, "[An Automated South Pole Stellar Telescope](#)", *Conference Proceedings: Instrumentation and Research Programmes for Small Telescopes*, ed. J. B. Hearnshaw & P. L. Cottrell, (Dordrecht:Reidel), *International Astronomical Union Symposium*, **118**, 83.

2P.□**Schneider, G.**, Paluzzi, P., and Webb, J., 1989, "[Astrophysical APL - Diamonds in the Sky](#)", in [APL89 Conference Proceedings: APL as a Tool of Thought](#), ACM Press, New York, (*APL Quote Quad*), **19-4**, 308.

3P. MacKenty, J. W., **Schneider, G.**, 1993, "[On-orbit Management of Contaminants within the HST Wide Field Planetary Camera and Their Effect on Instrument Performance](#)", *Conference Proceedings: Space Astronomical Telescopes and Instrumentation II*, eds. P. Y. Bely & J. B. Breckinridge, *SPIE Proceedings Series*, **1945**, 340.

4P. Fitch, J. and **Schneider, G.**, 1993, "[Serendipitous Background Monitoring of the Hubble Space Telescope's Faint Object Spectrograph](#)", *Space Astronomical Telescopes and Instrumentation II*, eds. P. Y. Bely & J. B. Breckinridge, *SPIE Proceedings Series*, **1945**, 214.

5P. Stobie, B., **Schneider G.**, and Bushouse, H., 1995, "[NICMOS Calibration Pipeline](#)", *Calibrating Hubble Space Telescope: Post Servicing Mission*, (STScI: Baltimore), 416.

6P. Bushouse, H., Mackenty, J., Skinner, C., Axon, D., Stobie, E., and **Schneider G.**, 1996, "[NICMOS Calibration Pipeline - A Collaborative Project Between IDT and STScI](#)", in *Astronomical Data Analysis Software and Systems V: A.S.P. Conference Series*, **101**, 281.

7P. **Schneider, G.**, Thompson, R. I., Smith, B. A., Terrile, R. J., 1998, "[Exploration of the environments of nearby stars with the NICMOS coronagraph: instrumental performance considerations](#)", *Conference Proceedings: Space Telescopes and Instrumentation V.*, at *Astronomical Telescopes and Instrumentation*, eds. P. Y. Bely & J. B. Breckinridge, *SPIE Proceedings Series*, **3356**, 222.

8P. Thompson, R. I., and **Schneider, G.**, 1998, "[NICMOS performance on the Hubble Space Telescope](#)", *Space Telescopes and Instrumentation V.*, at *Astronomical Telescopes and Instrumentation*, eds. P. Y. & Bely, J. B. Breckinridge, *SPIE Proceedings Series*, **3356**, 215.

9P. **Schneider, G.**, 1998, "[NICMOS Coronagraphic Surveys. Preliminary Results](#)", *Conference Proceedings: NICMOS and the VLT: A New Era of High Resolution Near Infrared Imaging and Spectroscopy*, eds. W. Freudling & R. Hook, *ESO Workshop and Conference Proceedings*, **55**, 88.

10P. Lowrance, P. J., Becklin, E. E., **Schneider, G.**, Hines, D., Kirkpatrick, D., Koerner, D., Low, F., McCarthy, D., Meier, R., Reike, M., Smith, B.A., Terrile, R., Thompson, R., Zuckerman, B., 1998, "[A Coronagraphic Search for Substellar Companions to Young Stars](#)", *NICMOS and the VLT: A New Era of High Resolution Near Infrared Imaging and Spectroscopy*, eds. W. Freudling & R. Hook, *ESO Workshop and Conference Proceedings*, **55**, 96.

- 11P. Corbin, M.R., Thompson, R.I, O'Neil, E., Rieke, M., and **Schneider, G.**, 1999, "[High Redshift Galaxies and QSOs in the NICMOS Parallel Fields, Conference Proceedings: Photometric Redshifts and the Detection of High Redshift Galaxies](#)", eds. R. Weymann, L. Storrie-Lombardi, M. Sawicki, & R. Brunner. *ASP Conference Series*, **191**, 247.
- 12P. Kulkarni, V. P., Hill, J. M., **Schneider, G.**, Weymann, R. J., Storrie-Lombardi, L. J., Rieke, M. J., Thompson, R.I., and Jannuzi, B., 1999, "[NICMOS Imaging of Damped Ly- \$\alpha\$ Absorber at z=2](#)". *The Hy-Redshift Universe: Galaxy Formation and Evolution at High Redshift*, eds. A. J. Bunker and W. J. M. van Breugel, *ASP Conference Series*, **193**, 603.
- 13P. Kulkarni, V. P., Hill, J. M., Weymann, R. J., Storrie-Lombardi, L. J., Rieke, M. J., **Schneider, G.**, Thompson, R. I.; Jannuzi, B., 1999, "[Search for a High-Redshift Damped Lyman-Alpha Absorber with NICMOS](#)", eds. J. R. Walsh, M. R. Rosa, *Chemical Evolution from Zero to High Redshift*, (Berlin: Springer-Verlag), 62.
- 14P. **Schneider, G.**, Becklin E. E., Lowrance, P. J., and Smith, B. A., and the NICMOS IDT/EONS & HST GO/8176 Teams, 2000, "[Substellar Companions to Nearby Stars from NICMOS Surveys](#)", *Conference Proceedings: Disks, Planets and Planetesimals*, eds. F. Garzon, E. D. de Winter, & T. J. Mahoney, *ASP Conference Series*, **219**, 499.
- 15P. Weinberger, A. J., Becklin E. E., and **Schneider, G.**, 2000, "[NICMOS Imaging of Dusty Circumstellar Disks](#)", *Conference Proceedings: Disks, Planets and Planetesimals*, eds. F. Garzon, E. D. de Winter, & T. J. Mahoney, *ASP Conference Series*, **219**, 329.
- 16P. **Schneider, G.**, and the NICMOS IDT/EONS Teams, 2000, "[NICMOS Imaging of Candidate Extra-Solar Planetary Systems](#)", *A Decade of HST Science*, (STScI: Baltimore), 81.
- 17P. Schultz, A. B., Hart, H. M., Kochte, M., Bruhweilwe, G. F., Di Sanit, M. A., Miskey, C., Cheng, K. P., Reinhard, K, **Schneider, G.**, Taylor, D.C., 2000, "[Pyramid Imaging with WFPC2: the Beta Pictoris Disk and Other Circumstellar Disks](#)", *A Decade of HST Science*, (STScI: Baltimore), 85.
- 18P. **Schneider, G.**, Lowrance, P. J., Becklin, E. E., Kirkpatrick, J. D., Plait, P., Heap, S. R., Malumuth, E., Dumas, C., Schultz, A. B., Smith, B. A., Weinberger, A. J., and D. C. Hines, 2001, "[Imaging and Spectroscopy of Hot \(Young\) 'Ultracool' Companions](#)", *Ultracool Dwarfs - New Spectral Types L and T*, eds., H.R.A. Jones & I.A. Steele, (Springer-Verlag: Berlin), 56.
- 19P. **Schneider, G.**, Hines, D.C., Silverstone, M., Weinberger, A.J., "[A Comparative Anatomy of Dusty Disks Imaged by NICMOS](#)", 2000, *Planetary Systems in the Universe: Formation and Evolution*, eds. A.J. Penny, P. Artimowics, & A.M. Lagrange, *ASP Conference Series*, in press.
- 20P. **Schneider, G.**, Hines, D.C., Silverstone, M., Weinberger, A.J., Becklin, E.E., Smith, B.A., 2000, "[Dust to Dust: Evidence for Planet Formation?](#)", *Astrophysical Ages and Time Scales*, eds. T. von Hippel, N. Manset, & C. Simpson, *ASP Conference Series*, **245**, 121.
- 21 P. **Schneider, G.**, NICMOS/EONS & GTO/8624 Teams, 2001, "[HST Observations of Dusty Disks in the TW Hydra Association](#)", *Young Stars Near Earth: Progress and Prospects*, eds. R. Jayawardhana & T., Green, *ASP Conference Series*, **244**, 203.
- 22P. Weinberger, A. J., Becklin, E. E., Zuckerman, B., Schneider, G., and Silverstone, M. D., 2001, "[A Stellar Association Near HD 141569?](#)", *Young Stars Near Earth: Progress and Prospects*, eds. R. Jayawardhana & T. Green, *ASP Conference Series*, **244**, 203.

- 23P. Lowrance, P. J., Becklin, E. E., **Schneider, G.**, & the NICMOS IDT/EONS and STIS 8176 Teams, 2001, "[Finding Brown Dwarf Companions with HST/NICMOS](#)", *Young stars Near Earth: Progress and Prospects*, eds. R. Jayawardhana & T. Green, *ASP Conference Series*, **244**, 289.
- 24P. Macintosh, B., Max, C., Zuckerman, B., Becklin, E. E., Kaisler, D., Lowrance, P., Weinberger, A., Christou, J., **Schneider, G.**, Acton, S., 2001, "[Keck adaptive optics observations of TW Hydrae Association Members](#)", *Young stars Near Earth: Progress and Prospects*, eds. R. Jayawardhana & T. Green, *ASP Conference Series*, **244**, 309.
- 25P. **Schneider, G.**, & Stobie, E., 2002, "[Pushing the Envelope: Unleashing the Potential of High Contrast Imaging with HST](#)", *ADASS XI*, eds. D. A. Bohlender, D. Durand & T. H. Handleys, *ASP Conference Series*, **281**, 381.
- 26P. **Schneider, G.**, 2003, "[Coronagraphy with NICMOS](#)", *The 2002 HST Calibration Workshop*, S. Arribas, A. Koekemoer & B. Whitmore, (STScI: Baltimore), 249.
- 27P. **Schneider, G.**, and Silverstone, M., 2003, "[Coronagraphy with HST/NICMOS: detectability is a sensitive issue](#)", *High-Contrast Imaging for Exo-Planet Detection*, eds. A. B. Schultz & R. G. Lyon, *SPIE Proceedings Series*, **4860**, 1.
- 28P. **Schneider, G.**, 2003, "[High Contrast Imaging and the Disk/Planet Connection](#)", *Hubble's Science Legacy: Future Optical-UV Astronomy From Space*, ed. C. Blades, *ASP Conference Series*, **291**, 69.
- 29P. Grady, C. A., Woodgate, B., Bowers, C., and **Schneider, G.**, 2003, "[The HST Legacy and Future for High Contrast Imaging of Disks and Outflows from Young Stars](#)", 2003, *Hubble's Science Legacy: Future Optical-UV Astronomy From Space*, ed. C. Blades, *ASP Conference Series*, **291**, 375.
- 30P. **Schneider, G.**, Weinberger, A. J., Silverstone, M. D. Cotera, A. S., 2003, "[HST Imaging of Circumstellar Disks](#)", *Conference Proceedings: Debris Disks and the Formation of Planets*, ed. D. Bachman, *ASP Conference Series*, in press.
- 31P. Weinberger, A. J., Becklin, E. E., **Schneider, G.**, 2003, "[Young Stellar Disks as the Sites of Planetary Evolution](#)", *Conference Proceedings: Scientific Frontiers in Extrasolar Planets*, ed. D. Deming & S. Seager, *ASP Conference Series*, in press.
- 32P. **Schneider, G.**, 2003, "[Highlights from HST-NICMOS](#)", *Conference Proceedings: Committee on Space Research, Astronomy at IR/Submm and the Microwave Background*, ed. P.R. Wesselius & H. Olthof, in press.

Meeting Abstracts/Presentations

- 1M. Millis, R., Wasserman, L., Franz, O., Hubbard, W., Lebofsky, L., Goff, R., Marcialis, R., Sykes, M., Fecker, J., Hunten, D., Reitsema, H., Zellner, B., **Schneider, G.**, Rios, M., Dunham, E., Klavetter, J., Meech, K., Oswald, T., Rayfert, J., A'Hearn, M., Osborn, W., Parker, D., Klemola, A., and Pirronen, J., 1985, "[The Occultation Diameter of Ceres](#)", *Bulletin of the American Astronomical Society*, **17**, 729.
- 2M. **Schneider, G.**, Wood, F. B., Chen, K-Y, Giovane, F., and Oliver, J. P. ,1984, "[Automated Photometry of Selected Stars at the South Pole](#)", *Bulletin of the American Astronomical Society*, **16**, 497.
- 3M. **Schneider, G.**, 1990, "[A Cautionary Note on the Use of Synoptic Climatological Observations for Observatory Site Selection](#)", *Bulletin of the American Astronomical Society*, **21**, 1067 .

- 4M. Ritchie, C. E., MacKenty, J. W., Baggett, S. M., Ewald, S. P., Griffiths, R. E., Horne, K., **Schneider, G.**, Walters, L., 1991, "[Calibration Stability, QE, and Contamination in the HST Wide Field Planetary Camera](#)", *Bulletin of the American Astronomical Society*, **23**, 1361.
- 5M. Wenz, M., **Schneider, G.**, and Hershey, J., 1995, "[A Search for Stellar Duplicity and Variability from FGS Guide Star Acquisitions and Guiding Data](#)", *Bulletin of the American Astronomical Society*, **187**, #43.01.
- 6M. **Schneider, G.**, Thompson, R., Rieke, M., Mentzell, E., Koromos, K., Stobie, B., 1995, "[The Near Infrared Camera and Multi-Object Spectrometer. A Status Report](#)", *Bulletin of the American Astronomical Society*, **187**, #04.06.
- 7M. Hershey, J., **Schneider, G.**, and Wenz, M., 1996, "[A Search for Stellar Duplicity and Variability from FGS Guide Star Acquisitions and Guiding Data - Project Status](#)", *Bulletin of the American Astronomical Society*, **189**, #77.08.
- 8M. **Schneider, G.**, Thompson, R., Rieke, M., Mentzell, 1996, "[The Near Infrared Camera and Multi-Object Spectrometer. Ready for Launch](#)", *Bulletin of the American Astronomical Society*, **189**, #43.07.
- 9M. **Schneider, G.**, 1997, "[On-Orbit Performance of the NICMOS Coronagraph](#)", *Bulletin of the American Astronomical Society*, **25**, pp. 1225.
- 10M. S. R. Stolovy, E. T. Young, R. I. Thompson, M. J. Rieke, **G. Schneider**, M. G. Burton, E. F. Erickson, M. J. Kaufman, S. W. J. Colgan, A. Chrysostomou, D. J. Axon, 1997. "[NICMOS 2-micron Continuum and H 2 Images of the Core of OMC-1](#)", *Bulletin of the American Astronomical Society*, **25**, 1219.
- 11M. F. Bruhweiler, B. Smith, C. Miskey, J. Silvis, M. DiSanti, A. Schultz, H. Hart, **G. Schneider**, K. Reinhard, 1997, "[WFPC2/PC Imagery of the Extended Circumstellar Disk of Beta Pictoris](#)", *Bulletin of the American Astronomical Society*, **25**, 1285.
- 12M. D. McCarthy, S. Stolovy, S. Kern, **G. Schneider**, T. Ferro, H. Spinrad, J. Black, B. Smith, 1997, "[Diffraction-limited Imaging of Comet Hale-Bopp at 1.9-2.2 microns with NICMOS/HST](#)", *Bulletin of the American Astronomical Society*, **25**, 1320.
- 13M. Kulkarni, V. P., Calzetti, D., Bergeron, L., Rieke, M., Axon, D., Skinner, C., Colina, L., Sparks, W., Daou, D., Gilmore, D., Holfeltz, S., Mackenty, J., Noll, K., Ritchie, C., **Schneider, G.**, Schultz, A., Storrs, A., Suchkov, A., Thompson, R., 1997, "[NICMOS Continuum and Emission-line Imaging of the Seyfert Galaxy IC 5063](#)", *Bulletin of the American Astronomical Society*, 191, #130.10.
- 14M. **Schneider, G.**, Thompson, R., Becklin, E., Smith, B., Terrile, R., 1998, "[NICMOS Coronagraphic Observations of Circumstellar Environments - Preliminary Results](#)", *Bulletin of the American Astronomical Society*, AAS 192th Meeting, [67.17](#).(May, '98).
- 15M. Dumas, C.; Terrile, R. J.; Burgasser, A.; Brown, R.; Rieke, M.; **Schneider, G.**; Thompson, R.; Koerner, D., 1998, "[Reflectance Spectroscopy of the Individual Members of the Pluto/Charon System: HST/NICMOS Results](#)", American Astronomical Society, DPS meeting #30, #49.P08.
16. Kern, S., McCarthy, D.W., Stolovy, S., **Schneider, G.**, Ferro, A., Spinrad, H., 1998, "[NICMOS/HST Post-Perihelion Images of Comet Hale-Bopp in Outburst](#)", American Astronomical Society, DPS meeting #30, #29.P11.
- 17M. Terrile, R. J., Dumas, C., Smith, B. A., Rieke, M., **Schneider, G.**, Thompson, R., Becklin, E., Koerner, D., 1998, "[First Infrared Imaging of the Neptune Ring Arcs: HST/NICMOS Results](#)", American Astronomical Society, DPS meeting #30, #17.P06.

18M. Becklin, E. E., Smith, B. A., **Schneider, G.**, Lowrance, P. J., Hines, D. C., Low, F. J., McCarthy, D. W., Rieke, R. I., Thompson, R.I., Terrile, R. J., Kirkpatrick, J. D., Koerner, D. W., Meier, R., and Zuckerman, B., 1998, "[Coronagraphic Search for Substellar Companions to Young Stars with NICMOS on HST](#)", *Bulletin of the American Astronomical Society*, AAS 193th Meeting, [31.02](#). (December, '98).

19M. Smith, B. A., **Schneider, G.**, Becklin, E. E., Koerner, D. W., Meier, R., Terrile, R. J., Hines, D. C., Lowrance, P.J., and Thompson, R.I., 1998, "[NIR Imaging of the HR4796A Circumstellar Disk](#)", *Bulletin of the American Astronomical Society*, AAS 193th Meeting, [89.05](#). (December, '98).

20M. **Schneider, G.**, Becklin, E. E., Smith, B. A., Terrile, R. J., Lowrance, P. J., Weinberger, A. J., Dumas, C., Koerner, D.W., Hines, D. C., Meier, R., Kirkpatrick, D., Thompson, R.I., Rieke, M., Low, F., 1998 "[Results from the NICMOS Environments of Nearby Stars Coronagraphic Imaging Programs](#)", *Bulletin of the American Astronomical Society*, AAS 193th Meeting, [73.13](#). (December, '98).

21M. Koerner, D.W., **Schneider, G.**, Smith, B.A., Becklin, E.E., Hines, D.C., Kirkpatrick, J.D., Lowrance, P.J., Meier, R., Rieke, M., Terrile, R.J., Thompson, I., 1998, "[NICMOS Imaging of a Circumstellar Disk around the T Tauri Star GM Aurigae](#)", *Bulletin of the American Astronomical Society*, AAS 193th Meeting, [89.05](#). (December, '98).

22M. Silverstone, M. D., Weinberger, A.J., Becklin, E. E., Lowrance, P. J., Zuckerman, B., Marsh, K.A., Koerner, D.W., Werner, M.W., Terrile, R.J., Smith, B.A., **Schneider, G.**, Rieke, M., Thompson, R.I., 1998, "[High-Resolution Infrared Imaging of Dust Disks Orbiting Main Sequence Stars](#)", *Bulletin of the American Astronomical Society*, AAS 193th Meeting, [73.16](#). (December, '98).

23M. Lowrance, P. J., McCarthy, C. M., Becklin, E. E., Zuckerman, B., **Schneider, G.**, Webb, R. A., Hines D. C., Low, F.J., Rieke, M., Thompson, R. I., Smith, B. A., Meier, R., Terrile, R. J., Kirkpatrick, J. D., Koerner, D. W., 1998, "[A Candidate Substellar Companion to CD-33° 7795 \(TWA5\)](#)", *Bulletin of the American Astronomical Society*, AAS 193th Meeting, [73.15](#). (December, '98).

24M. Weinberger, A.J., **Schneider, G.**, Becklin, E. E., Smith, B. A., Hines, D. C., 1999, "[NICMOS Imaging of a Circumstellar Disk About TW Hydrae](#)", *Bulletin of the American Astronomical Society*, AAS 194th Meeting, [69.04](#). (May, '99).

25M. Hines, D. C., Low, F. J., and **Schneider, G.**, 1999, "[NICMOS Observations of the Pre-Main-Sequence Planetary Debris System HD 98800](#)", *Bulletin of the American Astronomical Society*, AAS 194th Meeting, [87.01](#). (May, '99).□

26M. Kulkarni, V. P., Hill, J. M., Weymann, R. J., Storrie-Lombardi, L. J., **Schneider, G.**, Rieke, M. J., Thompson, R. I., and Jannuzi, B., 1999, "[Staring Hard at a z~2 Damped Lyman-alpha Absorber with NICMOS](#)", 1999, *Bulletin of the American Astronomical Society* AAS 194th Meeting, [87.01](#). (May, '99).

27M. **Schneider, G.**, and Smith, B. A., 1999, "[A Snapshot of Results from NICMOS/GTO Environments of Nearby Stars Surveys](#)", *Gordon Research Conference on the Origin of Solar Systems*.

28M. Smith, B. A., **Schneider, G.**, Becklin, E., Weinberger, A., Lowrance, P., Hines, D., and Terrile, R., 1999, "[The Environments of Nearby Stars as Observed with NICMOS](#)", *Bioastronomy 99: A New Era in Bioastronomy*

29M. Hines, D. C., Low, F. J., and **Schneider, G.**, 1999, "[The Planetary Debris System in HD98800](#)", *The Solar System and Circumstellar Dust Disks: Prospects for SIRTf*

30M. Weinberger, A.J., Becklin, E.E.,□Lowrance, P.J., Silverstone, M.D., **Schneider, G.**, Hines, D.C., Smith B., and Terrile, R., 1999, "[Combining NICMOS and Mid/Far-Infrared Measurements of Circumstellar Disks](#)", *The Solar System and Circumstellar Dust Disks: Prospects for SIRTf*

- 31M. **Schneider, G.**, Hershey, J. L., and Nelan, E., 1999, "[Duplicity and Variability in HST Guide Stars - An FGS Serendipitous Survey](#)", *Bulletin of the American Astronomical Society*, AAS 195th Meeting, [75.16](#). (December, '99).
- 32M. V.P. Kulkarni, V. P., Hill, J.M., **Schneider, G.**, Weymann, R. J., Storrie-Lombardi, L. J., Rieke, M. J., Thompson R. I. and Jannuzi, B., 1999, "[NICMOS Observations of the Damped Ly-alpha Absorber toward QSO1244+3443](#)", *Bulletin of the American Astronomical Society*, 195th Meeting, [52.06](#). (December, '99).
- 33M. Low, F. J., Hines, D. C. and **Schneider, G.**, 1999, "[The Planetary Debris System in TWA 4 \(HD98800\)](#)", *Bulletin of the American Astronomical Society*, AAS 195th Meeting, [78.35](#). (December, '99).
- 34M. Schultz, A.B., Hart, H.M., Bruhweiler, F. C., DiSanti, M. A., Miskey, C. L., Cheng, K. P., Reinhard, K., **G. Schneider**, Taylor, D. C., 1999, "[Searching infrared excess stars for disks and substellar companions using HST/WFPC-2](#)", *Bulletin of the American Astronomical Society*, AAS 195th Meeting, [45.04](#). (December, '99).
- 35M. **Schneider, G.** and the NICMOS/IDT EONS Team, 2000, "[NICMOS Imaging of Candidate Extra-Solar Planetary Systems](#)", *A Decade of HST Science*, (STScI: Baltimore).
- 36M. Schultz, A. B., Hart, H.M., Kochte, M., Bruhweilwer, G. F., Di Sanit, M. A., Miskey, C., Cheng, K. P., Reinhard, K, **Schneider, G.**, Taylor, D. C., 2000, [Pyramid Imaging with WFPC2: the Beta Pictoris Disk and Other Circumstellar Disks](#), *A Decade of HST Science*, (STScI: Baltimore).
- 37M. **Schneider, G.**, NICMOS IDT/EONS Team, STIS/8176 Team, 2000, "[STIS Spectroscopy of Candidate Substellar Companions Imaged by NICMOS](#)", *Bulletin of the American Astronomical Society*, AAS 196th Meeting, [3.04](#). (May, 2000).
- 38M. Vener, P. C., Brown, J., Bennum, D., Rothstein, D. , Gurwell, M., Ho, P., **Schneider, G.**, Schultz, A., Backman, D., 2000, "[NICMOS Search for Circumstellar Dust and Substellar Companions around Six Nearby Main Sequence Stars](#)", *Bulletin of the American Astronomical Society*, AAS 196th Meeting, [2.05](#). (May, 2000)
- 39M. **Schneider, G.**, and the NICMOS EONS Team, 2000, "[A Comparative Anatomy of Dusty Disks Imaged by NICMOS](#)", *IAU Symposium 202 on Extrasolar Planetary Systems*" (Manchester, UK)
- 40M. **Schneider, G.**, 2000 "[Imaging and Spectroscopy of Hot \(Young\) 'Ultracool' Companions](#)", 2000, *IAU Commission 45/29 Joint Discussion on Ultracool Stars* (Manchester, UK)
- 41M. Dumas, C., Terrile, R. J., Smith, B. A., **Schneider, G.**, Becklin, E.E., 2000, "[Near-Infrared Photometry and Astrometry of Neptune's Inner Satellites and Ring-Arcs](#)", *Bulletin of the American Astronomical Society*, DPS 32nd Meeting, 42.02.
- 42M. **Schneider, G.**, Becklin, E. E., Smith, B. A., Weinberger, A. J., Silverstone, M., Hines, D. C., 2000, "[NICMOS Coronagraphic Observations of 55 Cancri](#)", *Bulletin of the American Astronomical Society*, AAS 197th Meeting, 60.03.
- 43M. Lowrance, P. J., Becklin, E. E., **Schneider, G.**, NICMOS IDT/EONS Team, STIS/8176 Team, 2000, "[Resolving Low-Mass Companions to G-type stars - Two Stars and a Binary Brown Dwarf](#)", *Bulletin of the American Astronomical Society*, AAS 197th Meeting, 52.03.
- 44M. Hines, D. C., Schmidt, G. D., **Schneider, G.**, 2000, "[Analysis of Polarized Light with NICMOS](#)", *Bulletin of the American Astronomical Society*, AAS 197th Meeting, 12.10.
- 45M. O'Neil, E. J., **Schneider, G.**, Ferro, A. J., Hubbard, W. P., Barg, M. I., Stobie, E. B., Thompson, R. I., Boeker, Torsten, Holfeltz, S. T., Petro, L. D., 2000, "[NICMOS in the Cryo-Cooler Era: Expectations for On-Orbit Performance](#)", *Bulletin of the American Astronomical Society*, AAS 197th Meeting, 12.05.

- 46M. Brown, J., Bennum, D., Rodrigue, M., Schultz, A. B., Backman, D., Vener, P., Rosenthal, E., Perriello, B., Chen, H., Ho, P. T. P., Burrows, A., **Schneider, G.**, Lisse, C., Christian, D., Gorjian, V., 2000, "[Photometric Examination of Possible Sub-Stellar Companions of HD155826 and HD68456](#)", *Bulletin of the American Astronomical Society*, AAS 197th Meeting, 11.03.
- 47M. Weinberger, A. J., Becklin, E. E., **Schneider, G.**, Silverstone, M. D., Zuckerman, B., Webb, R.; Smith, B., 2000, "[Combining NICMOS Imaging and Mid-infrared Measurements of Circumstellar Disks](#)", *Bulletin of the American Astronomical Society*, AAS 197th Meeting, 8.20.
- 48M. **Schneider, G.**, Hines, D. C., Silverstone, M., Weinberger, A. J., Becklin, E. E., Smith, B. A., 2000, "[Dust to Dust: Evidence for Planet Formation?](#)", Conference Proceedings: [Astrophysical Ages and Time Scales](#) (ASP Conf Series), eds. T. von Hippel, N. Manset, C. Simpson, in press.
- 49M. **Schneider, G.**, NICMOS/EONS & GTO/8624 Teams, 2001, "[HST Observations of Dusty Disks in the TW Hya Association](#)", *Conference Proceedings: Young Stars Near Earth: Progress and Prospects* (ASP Conference Series), eds. R. Jayawardhana & T. Green, in press.
- 50M. **Schneider, G.**, 2001, "[HST/STIS Imaging of the HR 4796A Debris Ring](#)", *Bulletin of the American Astronomical Society*, AAS 198th Meeting, 83.01
- 51M. Silverstone, M. D., **Schneider, G.**, Schultz, A.B., 2001, "[NICMOS Imaging Search for a Candidate Companion to Proxima Centauri](#)", *Bulletin of the American Astronomical Society*, AAS 198th Meeting, 77.18.
- 52M. **Schneider, G.**, Becklin, E. E., Smith, B.A., Lowrance, P. J., Silverstone, M., NICMOS IDT/EONS Team, 2001, "[A Coronagraphic Companion Survey of Nearby M-Dwarf Stars with HST/NICMOS](#)", *Bulletin of the American Astronomical Society*, AAS 198th Meeting, 77.17.
- 53M. Schultz, A.B., Hart, H. M., Kochte, M., Bruhweiler, G.F., DiSanti, M.A., Miskey, C., Cheng, K-P, Reinhard, K., **Schneider, G.**, 2001, "[WFPC2 Pyramid Imaging: A Novel Technique to Image Circumstellar Disks](#)", *Bulletin of the American Astronomical Society*, AAS 198th Meeting, 77.07.
- 54M. **Schneider, G.**, 2001, "[Automated Eclipse Photography with Umbraphile](#)", *Totality Day 2001 Conference* (Open University, Milton Keynes, England).
- 55M. **Schneider, G.** & Stobie, E., 2001, "[Pushing the Envelope: Unleashing the Potential of High Contrast Imaging with HST](#)", *Conference Proceedings: ADASS XI*, (ASP Conference Series), in press.
- 56M. **Schneider, G.**, Pasachoff, J. Golub, L., 2001, "[TRACE Observations of the 15 November 1999 Transit of Mercury](#)", *Bulletin of the American Astronomical Society*, DPS 33nd Meeting, 10.02.
- 57M. Dumas, C., Terrile, R., Smith, B., **Schneider, G.**, 2001. "[HST-NICMOS Spectrophotometry of Small, Inner Satellites of the Outer-Planets](#)", *Bulletin of the American Astronomical Society*, [DPS 33nd Meeting](#), 37.10.
- 58M. **Schneider, G.**, 2002, "[High Contrast Imaging and the Disk/Planet Connection](#)" *Conference Proceedings: Hubble's Science Legacy: Future Optical-UV Astronomy From Space*, ed. C. Blades, (ASP Conf Series), in press.
- 59M. **Schneider, G.**, Weinberger, A.J., Silverstone, M.D. Cotera, A.S., 2002, "[HST Imaging of Circumstellar Disks](#)", *Conference Proceedings: Debris Disks and the Formation of Planets*, ed. D. Backman, (ASP Conf Series), in press.

60M. Wood, K., Koerner, D., Whitney, B., **Schneider, G.**, Stassun, K., Bjorkman, J., 2002, "[GM Auriagae's Circumstellar Disk: Multiwavelength Observations and Radiation Transfer Models](#)", *Bulletin of the American Astronomical Society*, AAS 200th Meeting, 71.05.

61M. Silverstone, M., **Schneider, G.**, Smith, B. A., 2002, "[NICMOS Observations of Vega: Upper Limits to the Detection of the Debris System](#)", *Bulletin of the American Astronomical Society*, AAS 200th Meeting, 74.07.

62M. Cheng, E. S., Zimbelman, D. F., Calzetti, D., Petro, L. D., Boeker, T., Jedritch, N., Swift, W., Thompson, R. I., **Schneider, G.**, NICMOS Cooling System Development Team, NICMOS Group at STScI Team, 2002, "[The NICMOS Cooling System: Technology in the Service of Science](#)", American Astronomical Society Meeting 200, #90.05, *Bulletin of the American Astronomical Society*, **34**, 953.

63M. **Schneider, G.**, 2002, "[Highlights from HST-NICMOS](#)", *Conference Proceedings: Committee on Space Research, Astronomy at IR/Submm and the Microwave Background*, ed. P.R. Wesselius and H. Olthof, in press.

64M. **Schneider, G.**, 2002, "[Coronagraphy with NICMOS](#)", *Conference Proceedings: The 2002 HST Calibration Workshop*, S. Arribas, A. Koekemoer, and B. Whitmore, submitted. □

65M. Pasachoff, J. M., **Schneider, G.**, Golub, L., 2003., "[Space Studies of the Black Drop Effect at a Mercury Transit](#)", IAU Commission 16/49 Joint Discussion on Mercury, (Sydney, UK)

66M. Cotera, A., **Schneider, G.**, 2003, "[The IMF of Newly Discovered Embedded Cluster](#)", IAU Symposium 221 on Star Formation at High Angular Resolution. (Sydney, UK)

Selected NASA/STScI Solicited Reports (inverse chronology)

1S. Black, D. C., Dressler, A., Kennicutt, R. C., Miley, G., Oegerly, W. R., **Schneider, G.**, Shull, J. M., 2003, "[Final Report of the Hubble Space Telescope Post-SM4 Scientific Review Panel](#)", a Requested Congressional Scientific Advisory Study Delivered to NASA Headquarters on 25 April 2003.

2S. **Schneider, G.**, and 13 contributors, 2002, "[Domains of Observability in the Near-InfraRed with HST/NICMOS and \(Adaptive Optics Augmented\) Large Ground-Based Telescopes](#)", a Summary Study Solicited by STScI in Preparation for HST Cycle 12 (31 December 2002).

3S. **Schultz, A. B.**, Schneider, G., Roye, E., Malhorta, S., 2002, "[SM3B NICMOS Focus Check](#)", NICMOS ISR 2002-002b (STScI).

4S. **Schneider, G.**, 2000, "[Results from the NCC/NICMOS Spare Detector June 2000 EMI Test](#)", NICMOS ISR 2000-006 (STScI).

5S. Boker, T., Ferro, A., Holfeltz, S. T., Hubbard, P., Jarrell, D., Monroe, B., Oneil, R. O., **Schneider, G.**, Sosey, M., 2000, "[NICMOS Dark Current Anomaly: Test Results](#)", NICMOS ISR 2000-002 (STScI).

6S. **Schneider, G.**, 1998, "EMI Noise Properties of the NICMOS Cooling System as Seen by a NICMOS-3 Flight Spare Detector", delivered to NASA Goddard Space Flight Center and STScI (1 May 1998)

7S. **Schultz, A. B.**, Noll, K., Storrs, A., Fraquelli, D., Ellis, T., Schneider, G., "[NICMOS Mode-1 Coronagraphic Acquisition](#)", 1999, NICMOS ISR 1998-019 (STScI).

8S. Morrow, G., **Schneider, G.**, and 15 additional board members, 1997, "[Final Report of the NICMOS Dewar Anomaly Review Board](#)" delivered to NASA Goddard Space Flight Center

Other Publications

10. Sterne, W.P., East, G., **Schneider, G.**, Treganowen, D., Arpin, P., Osman, J., Espenak, F., Buccini, J., Zoller, A., Peel, R., Gorski, A., Dunham, D., Chandler, D., Diego, F., 1980, "[The Maximum Eclipse - 1980Feb16](#)", *Sky and Telescope*, **59**, 383.

20. Wood, F. B., Chen, K-Y, **Schneider, G.**, and Giovani, F., 1984, "[South Pole Astronomy](#)", 1984, *Antarctic Journal of the United States*, **19**, 271.

30. **Schneider, G.**, 1985, [The Observation and Analysis of Lunar Occultations of Stars with an Emphasis on Improvements to Data Acquisition Instrumentation and Reduction Techniques](#), Ph.D. Dissertation, University of Florida.

40. Schneider, G., 1987, "[October's Remarkable 'Totality'](#)", *Sky and Telescope*, **73**, 222.

50. MacKenty, J. W., Griffiths, R. E., Sparks, W. B., Horne, K., Gilmozzi, R., Ewald, S. P., Ritchie, C. E., Baggett, S. M., Walter, L. E., **Schneider, G.**, 1992, [Hubble Space Telescope Wide Field and Planetary Camera Instrument Handbook](#), Space Telescope Science Institute.

Posters / Display Presentations*

A number of display presentations (posters) and PowerPoint annotated talks listed above are available for download in mixed formats (PostScript, PDF, jpeg, gif, or PowerPoint). Links are provided in the above references, and also tabulated by poster title below. Click on the reference number for the citation, or the title to display or download the presentation itself.

- [[6M](#)] [15JAN96](#) [ps] [The Near Infrared Camera and Multi-Object Spectrometer, A Status Report](#)
- [[8M](#)] [04JAN97](#) [ps] [The Near Infrared Camera and Multi-Object Spectrometer, Ready for Launch](#)
- [[9M](#)] [07JAN98](#) [jpg] [On-Orbit Performance of the NICMOS Coronagraph](#)
- [[12M](#)] [09JAN98](#) [pdf] [Diffraction-limited Imaging of Comet Hale-Bopp at 1.9-2.2 μm with NICMOS/HST](#)
- [[14M](#)] [11JUN98](#) [ps] [NICMOS Coronagraphic Observations of Circumstellar Environments – Preliminary Results](#)
- [[20M](#)] [08JAN99](#) [gif] [Results from the NICMOS Environments of Nearby Stars Coronagraphic Imaging Programs](#)
- [[22M](#)] [08JAN99](#) [ps] [High-Resolution Infrared Imaging of Dust Disks Orbiting Main Sequence Stars](#)
- [[24M](#)] [02JUN99](#) [jpg] [NICMOS Imaging of a Circumstellar Disk About TW Hydrae](#)
- [[25M](#)] [31MAY99](#) [jpg] [NICMOS Observations of the Pre-Main-Sequence Planetary Debris System HD 98800](#)
- [[26M](#)] [03JUN99](#) [jpg] [Staring Hard at a z~2 Damped Lyman-alpha Absorber with NICMOS](#)
- [[27M](#)] [13JUN99](#) [jpg] [A Snapshot of Results from NICMOS/GTO Environments of Nearby Stars Surveys](#)
- [[30M](#)] [18AUG99](#) [jpg] [Combining NICMOS and Mid/Far-Infrared Measurements of Circumstellar Disks](#)
- [[31M](#)] [14JAN00](#) [jpg] [Duplicity and Variability in HST Guide Stars - An FGS](#)

Serendipitous Survey

- [36M] 11APR00[]jpg[]NICMOS Imaging of Candidate Extra-Solar Planetary Systems
- [37M] 05JUN00[]jpg[]STIS Spectroscopy of Candidate Substellar Companions Image by NICMOS
- [39M] 12AUG00[]ppt[]A Comparative Anatomy of Dusty Disks Imaged by NICMOS
- [40M] 12AUG00[]ppt[]Imaging and Spectroscopy of Hot (Young) 'Ultracool' Companions
- [45M] 06JAN01[]ppt[]NICMOS in the Cryo-Cooler Era: Expectations for On-Orbit Performance
- [48M] 31JAN01[]ppt[]Dust to Dust: Evidence for Planet Formation?
- [49M] 26MAR01[]ppt[]HST Observations of Dusty Disks in the TW Hya Association
- [50M] 07JUN01[]ppt[]HST/STIS Imaging of the HR 4796A Debris Ring
- [51M] 07JUN01[]jpg[]NICMOS Imaging Search for a Candidate Companion to Proxima Centauri
- [52M] 07JUN01[]jpg[]A Coronagraphic Companion Survey of Nearby M-Dwarf Stars with HST/NICMOS
- [54M] 11AUG01[]jpg[]Automated Eclipse Photography with UMBRAPHILE
- [55M] 02OCT01[]ppt[]Pushing the Envelope: Unleashing the Potential of High Contrast Imaging with HST
- [56M] 27NOV01[]jpg[]TRACE Observations of the 15 November 1999 Transit of Mercury
- [57M] 03APR02[]ppt[]High Contrast Imaging and the Disk/Planet Connection
- [57M] 12APR02[]jpg[]HST Imaging of Circumstellar Disks
- [63M] 10OCT02[]ppt[]Highlights from HST/NICMOS
- [64M] 17OCT02[]ppt[]Coronagraphy with HST/NICMOS

*Posters and display presentations available at: @ <http://nicmosis.as.arizona.edu:8000/Publications.html#Posters>

Recent Invited Talks (Symposia, Colloquia, etc.)

- 15OCT99[] Exploring the Environments of Nearby Stars
at NASA/Goddard Space Flight Center Scientific Colloquium (Greenbelt, MD)
- 10OCT01[] Sub-Stellar Companions and Dusty Circumstellar Disks
at University of California, Berkeley, Center for Integrative Planetray Science
- 18DEC01[] Dust-Busters: when Wordletts Collide
at American Museum of Natural History, Rose Center (New York, NY)
- 02NOV02[] Stars, Galaxies, and HST/NICMOS: A Tale of Birth, Death and Resurrection
at Custer Institute Observatory, Annual F. Hess Lecture (Southold, NY)